Argonne National Laboratory

PHYSICS DIVISION SUMMARY REPORT

Annual Review

1 April 1967—31 March 1968

The facilities of Argonne National Laboratory are owned by the United States Government. Under the terms of a contract (W-31-109-Eng-38) between the U. S. Atomic Energy Commission, Argonne Universities Association and The University of Chicago, the University employs the staff and operates the Laboratory in accordance with policies and programs formulated, approved and reviewed by the Association.

MEMBERS OF ARGONNE UNIVERSITIES ASSOCIATION

The University of Arizona	Kansas State University	The Ohio State University
Carnegie-Mellon University	The University of Kansas	Ohio University
Case Western Reserve University	Loyola University	The Pennsylvania State University
The University of Chicago	Marquette University	Purdue University
University of Cincinnati	Michigan State University	Saint Louis University
Illinois Institute of Technology	The University of Michigan	Southern Illinois University
University of Illinois	University of Minnesota	University of Texas
Indiana University	University of Missouri	Washington University
Iowa State University	Northwestern University	Wayne State University
The University of Iowa	University of Notre Dame	The University of Wisconsin

Printed in the United States of America
Available from
Clearinghouse for Federal Scientific and Technical Information
National Bureau of Standards, U. S. Department of Commerce
Springfield, Virginia 22151
Price: Printed Copy $3.00; Microfiche $0.65

ANL-7481
Physics

ARGONNE NATIONAL LABORATORY
9700 South Cass Avenue
Argonne, Illinois 60439

PHYSICS DIVISION SUMMARY REPORT

Annual Review

1 April 1967—31 March 1968

Lowell M. Bollinger, Division Director

Preceding Summary Reports:

ANL-7384, July—September 1967
ANL-7405, October—December 1967
ANL-7436, January—March 1968

FOREWORD

This issue of the ANL Physics Division Summary Report presents a comprehensive picture of the work of the Division in the year ending in the spring of 1968. Instead of the usual small selection of relatively full accounts of individual researches reported at the random times at which they become available, this issue offers a complete and systematic overview of what is going on. Much of what is indicated briefly here has been described more fully in earlier issues of the Summary; most of the rest will appear in forthcoming issues.

In addition, the papers published in the 1-year period from 1 April 1967 through 31 March 1968 are listed immediately after the reports on the research. This list accounts for much the same effort but from a different point of view.

Still another picture of the relative emphases on the different programs of the Division is supplied by the roster of personnel, in which the staff members are grouped by program. (It must be understood, however, that staff members frequently do part of their work in another program.) This roster forms the last section of the report.

TABLE OF CONTENTS

I. EXPERIMENTAL NUCLEAR PHYSICS

INTRODUCTION

The over-all purpose of the program continues to be to obtain a much more complete understanding of the atomic nucleus. Consequently, most of the program consists of experimental and theoretical studies of the energies, quantum numbers, and lifetimes of nuclear energy levels and investigations of the mechanisms by which simple nuclear projectiles interact with nuclear targets. Experimenters and theorists work closely together so that new results in one area may suggest new approaches in another. An effort is made to stress work that can be done more advantageously at Argonne than elsewhere because of the special facilities available here. In view of the history and tradition of the Laboratory, it is natural that considerable emphasis is placed on studies of interactions between nuclei and neutrons; but this is balanced by a well diversified program of other nuclear investigations.

With a few exceptions, the program in experimental nuclear physics is most easily outlined by subdividing the work into various categories for which a major piece of equipment or an important experimental technique is the unifying factor. The current categories are:

(1) Studies of the neutron and of neutron-induced reactions at the reactor CP-5.

(2) Neutron and charged-particle-induced reactions at the 4-MeV Van de Graaff.

(3) Charged-particle reactions at the tandem Van de Graaff accelerator.

(4) Charged-particle reactions at the 60-in. cyclotron.

(5) Various other nuclear experiments, including the γ- and β-ray spectroscopy of radioactive sources.

Some physicists restrict their efforts to the use of a single machine or technique, whereas others investigate related problems with several systems of apparatus.

A. RESEARCH AT THE REACTOR CP-5

The program of the Physics Division at the reactor CP-5 is devoted entirely to nuclear physics. The experiments fall into three broad categories — experiments on the fundamental properties of the neutron, studies of neutron cross sections and resonances, and a variety of experiments with neutron-capture gamma rays.

Perhaps the most important recent development has been the start of a refined measurement of the angular asymmetries in the decay of polarized neutrons. This work is similar to the classic experiment (at Argonne) first carried out in 1958, but various improvements in the experimental system should result in much better accuracy. The measurement is expected to produce more precise values for the basic parameters of the weak interaction and possibly to give useful information about time reversal.

The various experiments on the neutron-capture gamma radiation have been unusually productive during the past year, partly because of the completion of technical developments started several years ago. Now four major experimental systems are available for capture γ-ray spectroscopy. These are a bent-crystal spectrometer, a Ge(Li)-detector coincidence system, an internal-target facility with a pair spectrometer, and a fast chopper. In addition, an internal-conversion spectrometer with a guide field supplied by a superconducting magnet has just been put in active use; and equipment for electron-gamma coincidence measurements is under construction. This large variety of highly developed experimental systems permits the experimenter to apply several complementary techniques to the unraveling of the complex decay schemes of heavy nuclides, with the result that temporarily (at least) the capture-γ-ray data are competitive with all other kinds of data for the study of many nuclides. The Argonne work on neutron-capture γ rays has the major advantage of being closely tied in with related charged-particle investigations in the same laboratory.

A highlight of the capture-γ-ray program during the past year has been the continuing demonstration of the power of average-resonance-capture spectra, which are obtained in a new kind of measurement developed at Argonne in late 1966. These measurements are now proving to be a good source of information on the spins and parities of low-energy nuclear states and are providing a systematic body of data on the radiative transitions from highly-excited nuclear states.

1. FUNDAMENTAL PROPERTIES OF THE NEUTRON

Measurements of the Symmetry Properties of the Decay of Polarized Neutrons

E. Bieber, C. J. Christensen, V. E. Krohn, and G. R. Ringo

The importance of these properties to the theory of weak interactions calls for substantially more accurate measurements than those done previously. During the past year an improved experimental arrangement was set up and the accumulation of data began. Improvements with respect to earlier experiments include better counting statistics, more precise measurements of the degree of neutron polarization, a more accurately aligned magnetic guide field, a demonstration that undesired asymmetries in the proton detector are not causing significant systematic errors, and an automatic arrangement to insert and remove a neutron-depolarizing shim at frequent intervals. To reduce statistical uncertainty by raising the neutron beam intensity, a new polarizing mirror was built. A Stern-Gerlach magnet is now used for routine measurements of the degree of neutron polarization. The proton detector being used for the present measurements is considerably better (more uniform in efficiency) than the one used in the earlier measurements.

An example of some recent data is shown in Fig. 1. The ratio of the intensities of the neutron peaks (after normalization to equal neutron monitor counts) provides a measurement of the degree of correlation between the direction of the neutron spin and the direction of emission of the

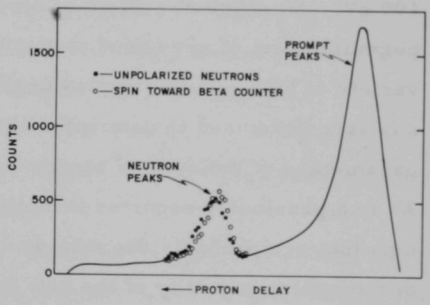

Fig. 1. Time distribution of coincidence data from the neutron-decay experiment. This plot was obtained from about 2 days of counting.

decay electron. The difference between the average proton delay times for the two peaks is a measure of the degree of correlation between the neutron-spin direction and the antineutrino direction. These data were taken with the neutron spin parallel to the center line of the electron and proton counters and with an electric field applied parallel to this center line.

2. SLOW-NEUTRON RESONANCES

a. Time-of-Flight Studies

During much of the past year the fast-chopper time-of-flight spectrometer was out of service because its electronic equipment was being modified to make it more effective for use with Ge-diode γ-ray detectors. These modifications have been completed, as described below.

(i) s- and p-Wave Resonances of ^{232}Th

Hla Shwe, G. E. Thomas, and L. M. Bollinger

The Argonne fast chopper has been used to measure the neutron total cross section of ^{232}Th for neutron energies less than about 100 eV. An efficient system of boron-loaded liquid scintillation detectors permitted data of very good statistical accuracy to be obtained for a variety of high-purity samples of thorium metal. Curve fitting and area analysis were used to determine exceptionally accurate values of the parameters of the s-wave resonances at 21.8, 23.5, 59.5, and 69.2 eV. As in a previously reported investigation, numerous tiny transmission dips that are probably due to p-wave resonances were detected. Because of the superior quality of the new data, it was possible to obtain accurate values of the total radiation widths of the p-wave resonances at 8.36 and 13.13 eV. These widths are not significantly different from those for s-wave resonances.

(ii) Determination of Spins of Neutron Resonances

K. J. Wetzel, G. E. Thomas, and L. M. Bollinger

Several techniques have been used to assign spins to the states formed in resonance-neutron capture. Besides lacking general applicability, no one of these methods presents the advantage of simplicity in measurement and analysis. The possibility of developing a more advantageous method is being investigated by studying the low-energy gamma-ray spectra following capture in individual resonances. This work was started in the spring of 1967 but progress was delayed until recently by major modifications of the electronic equipment.

Experimentally, the method consists in using a Ge(Li) spectrometer to observe the low-energy gamma-ray spectrum and its dependence on neutron energy with the aid of the chopper facility and the associated time-of-flight analyzer. The intensities of the gamma rays de-exciting the low-lying levels are proportional to the population of these states by direct and cascading transitions following capture.

If the population of the low-lying level is assumed to be dominated by a "statistical" gamma cascade of several E1 and/or M1 transitions, a simple model based on the number of "routes" by which a state of given spin may be populated will yield the relative probability for observing the de-exciting gamma ray for the two cases $J_{res} = I_{target} \pm \frac{1}{2}$. The known locations of low-lying 2^+, 4^+, and 6^+ states for many even-even nuclei would allow, in principle, the application of such a model to a wide range of nuclei.

The applicability of the model was tested by studying neutron capture in the resonances of several nuclei (^{105}Pd, ^{135}Ba, ^{167}Er, ^{177}Hf, ^{179}Hf, and ^{183}W). The relative population of pairs of low-lying states with known spins (2^+, 4^+ or 4^+, 6^+) in each of the resulting even-even nuclei shows a direct correlation with the previously known spins of the capturing state and is also in reasonable

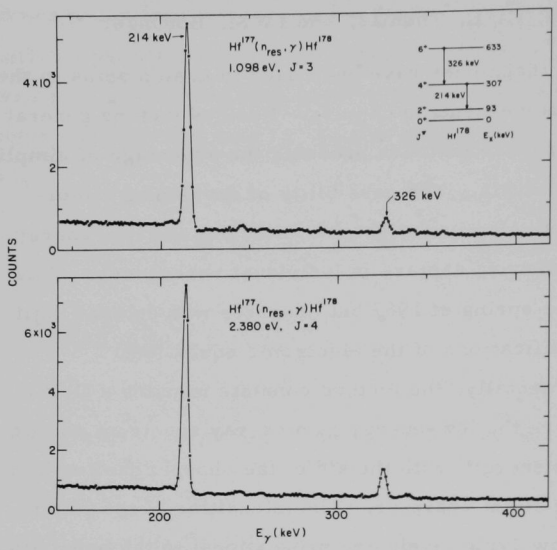

Fig. 2. A portion of the low-energy γ-ray spectrum of ^{178}Hf following neutron capture in resonances of ^{177}Hf.

quantitative agreement with the predictions of the model. In the case of ^{177}Hf (Fig. 2), for example, the ratios $I_\gamma(326)/I_\gamma(214)$ for the two resonances are seen to differ in agreement with the known difference in their spins.

This method has been successfully applied to a number of resonances in ^{187}Os and ^{189}Os, for which no prior spin assignments to any capture resonances exist. We are also studying ^{91}Zr, for which p-wave capture is important, to see if the method can be extended to such cases.

(iii) Study of the ^{93}Nb$(n_{res}, \gamma)^{94}$Nb Reaction

W. V. Prestwich, R. E. Coté, and Hla Shwe

The high-energy γ-ray spectra following capture in one s-wave and three p-wave resonances in Nb have been observed with a Ge(Li) detector. The low-lying ^{94}Nb energy levels inferred from the data are consistent with those previously reported on the basis of (d, p) and low-energy (n, γ) data. From the observed decay properties of the initial states, the spin assignments for the resonances are inferred to be $J_r^\pi = 5^-$ (35.8 eV), 4^+ (119.2 eV), 4^- or 5^- (42.3 eV), 3^- or 4^- (94.3 eV).

The distribution of partial radiative widths for the three p-wave resonances is consistent with that predicted by the statistical compound-nucleus model.

(iv) Modification of the Data-Acquisition System of the Fast Chopper

R. E. Coté,* W. V. Prestwich, M. G. Strauss,† and C. H. Freese†

In 1960 America's first multiparameter pulse analyzer[1] was put into service at the Argonne fast chopper, where it has been used in a series of investigations of the γ-ray spectra following neutron capture in resonances. The analyzer was built around a 25-track digital tape recorder and the control circuits were designed to permit the system to record events in which a neutron flight time was defined by 512 channels and each of two pulse heights is defined by 256 channels. The relatively small number of channels used for the pulse heights was chosen to be consistent with the poor energy resolution of NaI scintillators.

Recent experiments have shown the feasibility of resonance-capture studies with Ge(Li) detectors. In order to take full advantage of the high resolution of these detectors, it was desirable to be able to define the pulse height by a much larger number of channels than 256. Therefore, the analyzer system has been extensively modified. The most important change was the addition of control circuits that permit the system to be used as a two-parameter analyzer in which a pulse height is defined by up to 4096 channels and simultaneously the neutron flight time may be defined by up to 1024 channels. Also, to make it easier to use the system, the two-parameter analyzer was interfaced

---

*Deceased.

†Electronics Division.

[1] C. C. Rockwood and M. G. Strauss, Rev. Sci. Instr. 32, 1211 (1961).

to a 4096-channel time analyzer (normally used in neutron transmission measurements) in such a way as to monitor the spectrum of the full range of pulse heights stored in the two-parameter analyzer. The neutron-flight-time spectrum may still be monitored by the 256-channel memory that was built into the original multiparameter analyzer.

The detector part of the counting system has also been improved substantially by the addition of a low-noise preamplifier and by the electronic stabilization of the pulse height. These additions make it feasible to obtain high-resolution spectra in measurements that extend over a period of weeks.

b. Average-Resonance-Capture Measurements

The average γ-ray spectra from capture of neutrons in many resonances have been measured by the new experimental technique first described last year.[1] In this method, the capture γ-ray spectrum of a ^{10}B-surrounded sample is measured at the internal-target facility at CP-5.[2] The average spectrum of the captured neutrons is determined by the thickness of ^{10}B absorber. The significant feature of an average-capture spectrum is that the random fluctuations in γ-ray intensity characteristic of transitions from an individual initial state are averaged out, because the spectrum is formed by contributions from many initial states.

[1] L. M. Bollinger and G. E. Thomas, Phys. Rev. Letters 18, 1143 (1967).

[2] G. E. Thomas, D. E. Blatchley, and L. M. Bollinger, Nucl. Instr. Methods 56, 325 (1967).

(i) Improvements in the Internal-Target Facility

W. V. Prestwich and G. E. Thomas

The most important improvements were in the Ge(Li)-detector system. A large NaI annulus was added to permit the Ge(Li) detector to be used in either a pair-spectrometer or an anticoincidence-spectrometer mode. Also new electronic equipment was

added to permit the detector to be operated at very high counting rates. Inside the reactor, additional collimation was installed to reduce the intensity of background radiation issuing from the reactor.

(ii) Study of High-Energy γ-Ray Line Shape

K. J. Wetzel and G. E. Thomas

Measurements on thermal capture in light nuclei (B and N) have shown that, in favorable cases ($E_\gamma \approx 4$ to 8 MeV), the Doppler broadening of the secondary γ ray of a two-step cascade can be measured. This broadening, caused by decay while the nucleus still has an appreciable recoil velocity (but random direction) following emission of the primary quantum, typically adds about 0.7 keV to the resolution width of the system and can be measured with a high-resolution Ge(Li) spectrometer.

As more precise Ge(Li) detectors are developed, a knowledge of this effect becomes important in accurately evaluating high-energy γ-ray measurements, for which the line shape may be of importance—particularly if obtained from a reaction such as $^{14}N(n, \gamma)^{15}N$. Examples of this would be the average-resonance measurements discussed below, in which valuable information can be obtained from the deviation of experimental line shapes from the actual "system" line shape.

For the γ rays from the ground-state decay of the 5298- and 5270-keV levels in ^{15}N, both of which are long-lived ($\tau = 4.3 \times 10^{-14}$ sec and $\tau > 10^{-12}$ sec, respectively), the smaller observed broadening for a solid (melamine) sample, as compared with a gas sample, is consistent with the much shorter mean free path of the recoiling ^{15}N atom in the solid material.

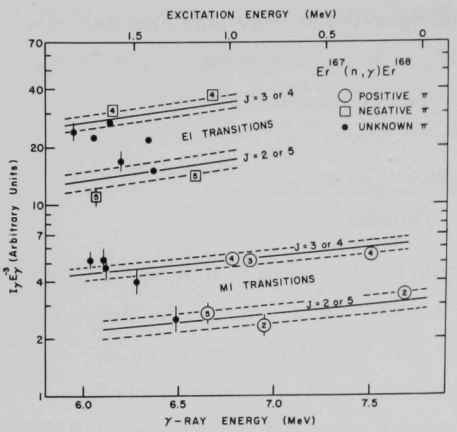

Fig. 3. The intensities I_γ of gamma-ray transitions in an average neutron resonance-capture spectrum from erbium. In this graph, the quotient I_γ/E_γ^3 is plotted against the gamma-ray energy E_γ (scale at bottom) and, equivalently, against the excitation energy of the low-energy final state (scale at top). The numbers within some of the data points give the previously known spins of the low-energy final state; their parities are shown by the shapes of the points. Since each point falls unambiguously along one or another of the four solid lines, the spin J of a state with unknown properties is determined within a choice between two values, and the parity π is uniquely established.

(iii) Nuclear Spectroscopy

L. M. Bollinger and G. E. Thomas

A systematic study of the value of the average-resonance-capture spectra for nuclear spectroscopy has been undertaken. Measurements on samples of neodymium, zirconium, molybdenum, palladium, tin, tellurium, erbium, and thulium have been completed. This study shows that two characteristics of the average spectra give useful information about low-energy nuclear states. The most useful characteristic is the intensity of the γ-ray lines, since for most nuclides it gives an unambiguous determination of the parity of the final state and sets limits on the spin. An example is shown in Fig. 3. For nuclides that have a relatively large p-wave strength function, the shape of the γ-ray line also gives the parity of the final state. The average-resonance-capture spectra are expected to be a major source of information about the parities of nuclear states during the next few years.

(iv) Search for Evidence of Direct Capture in $^{169}Tm(n,\gamma)^{170}Tm$

L. M. Bollinger and G. E. Thomas

A group working at the Brookhaven chopper[1] has reported that the widths of high-energy radiative transitions following neutron capture in resonances of ^{169}Tm are positively correlated with the neutron width, and has interpreted this correlation as evidence for the theoretically predicted direct capture. If this interpretation were correct, one would expect that the average width of radiative transitions from many initial states to an individual final state would depend on the single-particle character of the final state. We have looked for this effect by directly measuring the average spectrum formed by capture in many resonances of ^{169}Tm. The measured intensities do not depend on the character of the final state in a recognizable way, and they are quantitatively inconsistent with what would be expected on the basis of the direct-capture interpretation of the reported correlation between the radiation widths and neutron widths.

(v) M1 Radiation Widths

L. M. Bollinger and G. E. Thomas

Perhaps the most significant result being obtained from the average-resonance-capture spectra are reliable data concerning M1 transitions from highly excited states, since almost no accurate information of this kind has been reported previously. The behavior of average M1 transitions in ^{92}Zr, ^{96}Mo, ^{98}Mo, ^{106}Pd, ^{118}Sn, ^{120}Sn, ^{124}Te, ^{126}Te, ^{168}Er, and ^{170}Tm have been studied. Several interesting features of the behavior are (a) the ratio of E1 to M1 strength is not consistent with any of the published theoretical descriptions of the radiative process, (b) the ratio is much smaller than was expected for most nuclides, and (c) the reduced widths for M1 transitions in ^{118}Sn and ^{120}Sn appear to exhibit a giant-resonance-like structure at an energy of about 8.3 MeV. Neighboring nuclides are now being studied to determine whether they exhibit a similar structure.

[1] M. Beer, M. A. Lone, R. E. Chrien, O. A. Wasson, M. R. Bhat, and H. R. Muether, Phys. Rev. Letters 20, 340 (1968).

(vi) Average Radiation Widths from Neutron Capture in Manganese and Vanadium

K. J. Wetzel

As part of a program to study the average gamma-ray widths in the range of intermediate-mass nuclei ($50 < A < 60$), manganese and vanadium have been studied. For manganese, spectra have been obtained for capture in several broad ranges of neutron energies. Preliminary analysis of high-energy transitions ($5.0 \text{ MeV} < E_\gamma < 7.3$ MeV) shows much less fluctuation than in the thermal spectrum. Several transitions not appearing in thermal capture are observed in resonance capture, most notably a strong transition populating the excited level at 435 keV. In vanadium also, the fluctuations in the intensities of high-energy transitions are much smaller in the average resonance spectrum than in the thermal spectrum, where Porter-Thomas fluctuations are expected.

3. THERMAL-NEUTRON-CAPTURE GAMMA RAYS

a. Energy Levels and Decay Schemes of Odd-A and Odd-Odd Nuclides

This experimental program seeks to provide information concerning the energies and decay schemes of the low-lying excited states of selected odd-A and odd-odd nuclides populated in thermal-neutron-capture gamma-ray reactions. Two types of experimental systems are used to unravel these complex spectra. The high-energy gamma-ray transitions that populate the low-lying states of the product nucleus from direct decay of the capture state are observed with the high-sensitivity internal-target facility at the CP-5 reactor. These transitions establish the excitation energies of states up to $\sim 1-2$ MeV above the ground state. The low-energy gamma-ray transitions between these low-lying excited states are studied by means of singles and coincidence gamma-ray spectroscopic techniques in a new external-neutron-beam facility at CP-5. Here targets are placed in the external neutron beam (flux $\approx 10^7$ neutrons cm^{-2} sec^{-1}). Singles and coincidence spectra are obtained with the exclusive use of Ge(Li) detectors in conjunction with a two-parameter magnetic-tape recording system in a

pulse-height array of 1024 X 1024 channels. These two-parameter Ge(Li)-Ge(Li) coincidence studies of the gamma-ray transitions following thermal-neutron capture are the first known successful employment of this ultra-high-resolution technique in this field and are, to date, the sole reported examples of the use of this method in these types of investigations.

(i) Levels in ^{70}Ga and ^{72}Ga

H. H. Bolotin, J. Vervier, and J. L. Yntema

The excited states of the odd-odd ^{70}Ga and ^{72}Ga nuclides have been studied by the reactions ^{69,71}Ga(n, γ)^{70,72}Ga and ^{69,71}Ga(d, p)^{70,72}Ga with the aim of providing a complete and comprehensive description of the level structure of these nuclides. The combined information gleaned from these reactions has provided a detailed picture of many of these excited states. At present shell-model calculations are being performed and the results will be compared with the experimentally established properties of these states.

(ii) Excited States of ^{59}Ni and ^{63}Ni

H. H. Bolotin and D. A. McClure

The low-lying excited states of the odd-A ^{59}Ni and ^{63}Ni nuclides have been studied by use of the reactions ^{58,62}Ni(n, γ)^{59,63}Ni. The excited states of these Ni isotopes have received considerable attention in the form of detailed shell-model calculations appearing in the literature. The present investigations were initiated to provide additional information which, when combined with previously reported (d, p) studies, might more fully test these calculations and yield more complete specifications of these states. High-energy primary transitions were investigated at the high-sensitivity gamma-ray facility at the CP-5 reactor. The low-energy transitions were studied at the external-thermal-beam facility at the CP-5 reactor. Ge(Li) detectors were used exclusively. All samples were highly enriched in the isotope of interest.

These studies have provided the desired additional information on levels previously observed and have revealed several excited nuclear states not reported in other recent investigations which utilized other reactions. These findings are currently being compared with theoretical calculations.

(iii) Low-Lying Excited States of ^{122}Sb and ^{124}Sb

H. H. Bolotin

High-energy primary and low-energy secondary γ-ray transitions from the reactions ^{121,123}Sb(n, γ)^{122,124}Sb have been studied at the high-sensitivity gamma-ray and external-beam facilities at the CP-5 reactor. These investigations were initiated to examine the applicability of the pairing interaction in odd-odd spherical nuclei. The neighboring Sn isotopes have already been shown to be well described by this model. Final analysis of these experiments is in progress.

b. (n, γ) Studies with the Bent-Crystal Spectrometer and Ge-Diode Detector

The complex level structure of heavy nuclei produces correspondingly complex gamma-ray spectra following neutron capture. The bent-crystal gamma-ray spectrometer provides an effective means of studying such spectra, particularly at low energies where the average energy separation of gamma rays is comparatively small. The high resolution (resolution width = 45 eV at 100 keV, 12 eV at 50 keV) and energy precision (~ 1 part in 10 000) of this instrument enable the experimenter to construct largely unambiguous level schemes of these nuclei. Since the resolution obtained with the crystal diffraction process inherently falls off at higher energies, however, it is expedient to use the germanium-diode detector at energies above ~ 1 MeV. The comparatively high resolution (width ≈ 6 keV at E_γ = 5 MeV) of this device at high energies complements the superior characteristics of the bent-crystal spectrometer at low energies. Under certain conditions, it has proved advantageous to operate the Ge-diode detector in the diffracted gamma-ray beam of the bent-crystal spectrometer, thus combining the energy precision of the spectrometer with the high resolution of the Ge-diode detector.

(i) Modification of the Bent-Crystal Spectrometer

R. K. Smither, D. J. Buss, and D. Bushnell

Preliminary testing of a newly-bent 2-mm-thick quartz crystal (11 × 12 × 0.080 in.) has been completed. As predicted by theory, the energy resolution of the instrument was improved to twice what could be obtained with the previous crystal (4 mm thick) without any appreciable loss in efficiency (reflectivity of the crystal). At the same time, sensitivity has been increased as a result of a general reduction of background. The line width of the spectrometer has now been reduced to about 5 keV (FWHM) at 1 MeV and 50 eV at 100 keV. Plans to obtain a 1-mm-thick crystal and a further improvement in energy resolution are under consideration.

A new multislit collimator for the bent-crystal spectrometer has been constructed and installed. The three-tier design and elimination of support material between the plates has improved the transmission of the collimator and has quadrupled the efficiency of the bent-crystal spectrometer for 400-keV gamma rays, and has increased it by a factor of 190 for 30-keV gamma rays.

The drive mechanism for the rear collimator and shield was converted from a hydraulic to an electrical system in the fall of 1967. The higher effective feedback sensitivity of the new setup results in smoother operation and consequently in an improvement in spectrometer sensitivity at low energies.

A new multislit collimator (Fig. 4) has been placed in front of the diffracting crystal. This pre-diffraction collimator has produced a tenfold increase in signal-to-background ratio at high and low energies. The design includes provision to apply a tension to the vertical lead plates forming the slits. This increases the transmission factor of the device by counteracting the natural tendency of these thin plates to slowly sag and bow. Present measurements indicate that the average transmission is 60% of the theoretical design value.

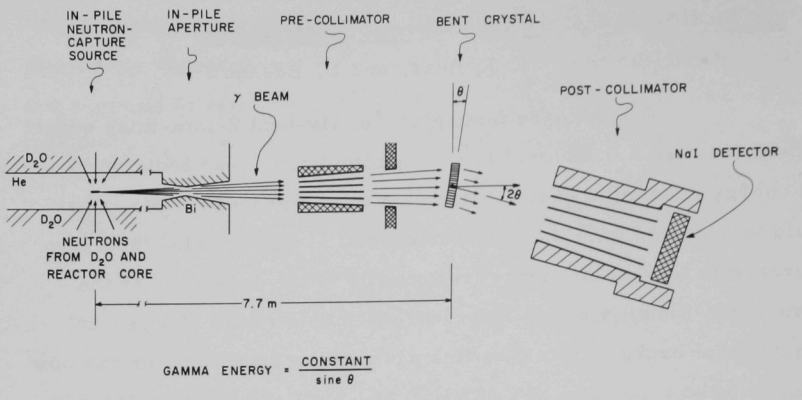

Fig. 4. Schematic drawing of the Argonne 7.7-m bent-crystal spectrometer with the new pre-collimator in place.

Modification of the remote-control source-changing apparatus was completed in June 1967. The changes have eliminated a number of weak points and have improved the general reliability of the system. Also, the addition of four more storage slots in the turret of the storage system has increased its capacity from three to seven very radioactive samples.

(ii) High-Energy K Conversion Coefficients

R. K. Smither, D. J. Buss, and E. Bieber

The K conversion coefficients for the 1—9-MeV region of the $^{113}Cd(n,\gamma)^{114}Cd$ γ-ray spectrum are obtained by combining the Ge-diode analysis of the (n, γ) spectrum with the conversion-electron intensities from the published work of von Egidy and Kaiser. The coefficient was found to depend on the γ-ray energy as $E_\gamma^{-1.96}$ for the E1 radiation and as $E_\gamma^{-2.18}$ for the M1. Contrary to the suggestion from extrapolating the theoretical calculation, the values of the E1 and M1 coefficients (Fig. 5) do not cross at high energies: at 9 MeV they still differ in the ratio of 1.7:1.0. A similar analysis of the $^{149}Sm(n,\gamma)^{150}Sm$ spectrum (Fig. 6), combined with the conversion-electron intensities of

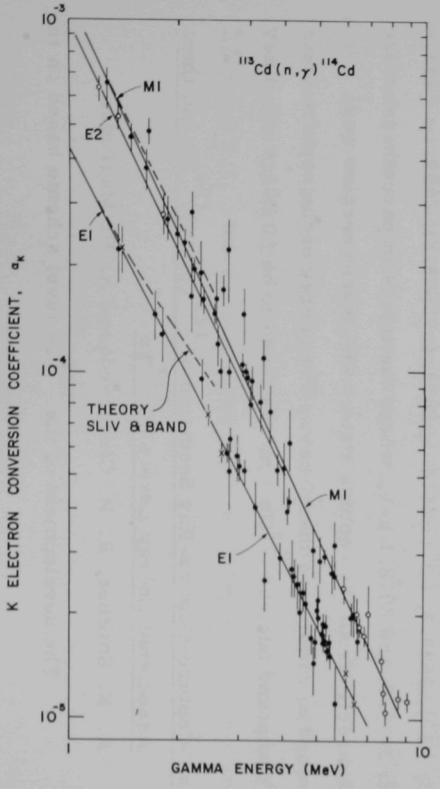

Fig. 5. Log-log plot of the K conversion coefficients of transitions in ^{114}Cd following thermal neutron capture. The coefficients remain split into two distinct groups (corresponding to E1 and M1 transitions) even at high energies. Open circles and crosses refer to known M1 (or E2) and E1 transitions, respectively.

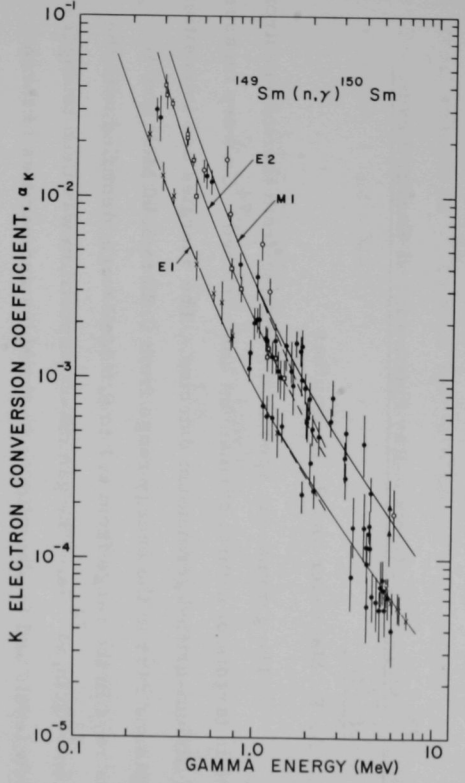

Fig. 6. Plot of K conversion coefficients of transitions in ^{150}Sm. The separation into E1 and M1 groups is still apparent at high energies. The dashed curves are theoretical values; the open circles and the crosses refer to known M1 (or E2) and E1 transitions, respectively.

Elze, showed that the α_K had a more nearly $E_\gamma^{-1.4}$ dependence at high energies. The ratio of $\alpha_K(M1)/\alpha_K(E1)$ was 2:1 at 7 MeV. Thus it is possible to distinguish between E1 and M1 transitions in the high-energy spectra of both ^{114}Cd and ^{150}Sm and to assign parities to many of the states in these nuclei.

(iii) ^{73}Ge(n, γ)^{74}Ge Gamma-Ray Spectrum and Energy Levels of ^{74}Ge

A. P. Magruder and R. K. Smither

The gamma-ray spectrum resulting from thermal-neutron capture in targets of natural germanium and enriched ^{74}Ge were measured with a lithium-drifted germanium detector. The energies and intensities of 85 gamma rays in the energy range from 0.20 to 3.00 MeV and 47 gamma rays in the range from 6.1 to 9.6 MeV were identified with the reaction ^{73}Ge(n, γ)^{74}Ge. The gamma-ray spectrum was used to suggest four new levels and to place limits on the spins and parities of three other levels. Errors in the gamma-ray energy values were reduced to less than 3 keV in all cases, and to less than 1 keV for many. On the basis of this experiment and other information, the energy levels identified below 3 MeV were: 0.0, [0^+]; 596.3, [2^+]; 1204.9, [2^+]; 1466.2, [4^+]; (1486, [0^+]); (1697.7); 1699.9 [$3^\pm$, 4^+]; 2168.3, [$3^\pm$, 4^+]; 2200.2, [2^+]; 2539.3, [3^-]; 2574.1; 2672.4; (2695.8); 2699.1; 2833.2; 2929.2; 2939.7; and 2978.1 keV, where the levels in parentheses were not fed directly from the capture state. The level energies were determined to within less than 1 keV. The energy of the capture state in the compound nucleus (^{73}Ge + n) was found to be 10 203.1 ± 0.9 keV.

(iv) Capture-Gamma-Ray Spectrum of ^{123}Te(n, γ)^{124}Te and the Associated Energy Levels in ^{124}Te

R. K. Smither, R. P. Chaturvedi, and A. P. Magruder

The development of the ^{124}Te level scheme based on the

$^{123}Te(n,\gamma)^{124}Te$ gamma-ray spectrum has been completed. New Ge-diode measurements were used to refine the gamma energies and intensities of the high-energy portion of the spectrum. The final level scheme consists of 42 levels below 3.1 MeV. A new value, $E_n = 9425.2 \pm 1.8$ keV, was obtained for the neutron binding energy of ^{124}Te. The level scheme of ^{124}Te is of special interest because the γ-ray branching ratios suggest a collective nature for many of the states between 1 and 2 MeV.

(v) Level Scheme of ^{138}Ba

D. J. Buss and R. K. Smither

The $^{137}Ba(n,\gamma)^{138}Ba$ spectrum has been studied with the Ge(Li) spectrometer. Seventy-eight of the 207 transitions observed in this spectrum have been placed in a tentative level scheme of ^{138}Ba. Primary transitions from the capture state $(1^+, 2^+)$ are expected to populate low-spin states. Negative-parity neutron-hole states have been identified in recent (p, p') and (d, p) experiments. Primary transitions to those states having spins of 0, 1, 2, or 3 have been observed in the present experiment at energies of 2881, 2895, 3505, 3646, 3923, 4079, 4167, 4280, 4325, 4446, 4517, 4536, 4564, 4647, 4745, 4799, and 4876 keV. A large number of transitions have also been placed in the level scheme as depopulating these states. In addition to the previously reported primary transitions to low-lying levels in ^{138}Ba, we have also observed six new transitions between these levels; and low-energy gamma rays have yielded more precise energy values for these low-lying levels. These are: 1435.6 ± 1.0, 1898.5 ± 1.5, 2218.1 ± 1.5, 2306.6 ± 1.5, 2445.9 ± 1.5, 2639.4 ± 1.5, and 2880.5 ± 1.5 keV.

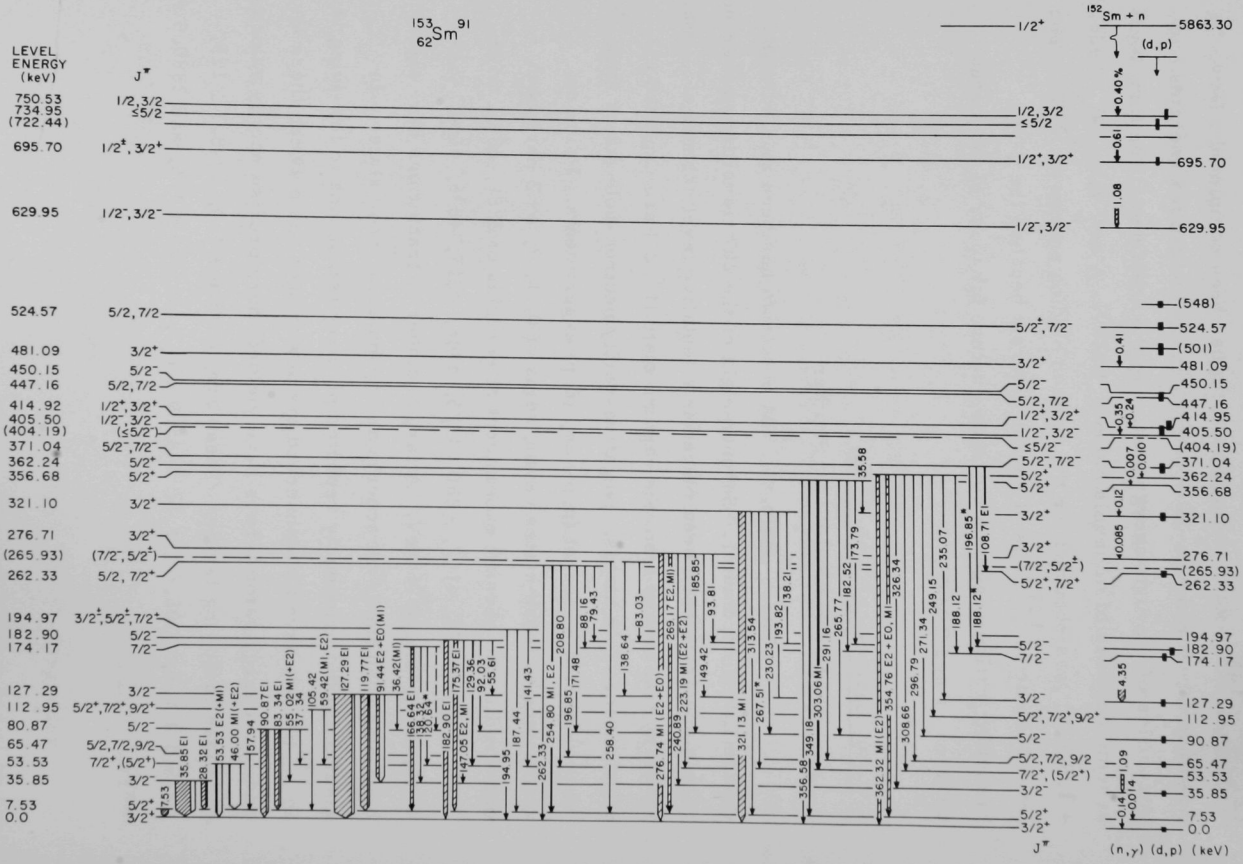
153Sm91
62
LEVEL ENERGY (keV)
Jπ
152Sm + n
5863.30
(d,p)
0.40%
695.70
629.95
1.08
(548)
524.57
(501)
481.09
450.15
447.16
414.95
405.50
(404.19)
371.04
362.24
356.68
321.10
276.71
(265.93)
262.33
194.97
182.90
174.17
127.29
112.95
80.87
65.47
53.53
35.85
7.53
0.0
(n,γ) (d,p) (keV)

Fig. 7. Level scheme of ^{153}Sm, showing details of the gamma decay of the low-lying levels following neutron capture in ^{152}Sm.

(vi) Level Schemes of ^{150}Sm and ^{151}Sm

R. K. Smither, E. Bieber, and A. P. Magruder

The high-energy portion of the ^{149}Sm(n, γ)^{150}Sm and ^{150}Sm(n, γ)^{151}Sm reactions were investigated with the new through-hole Ge-diode facility at the reactor CP-5. The results are now being combined with the bent-crystal data on the low-energy portion of the (n, γ) spectrum to extend the level schemes of ^{150}Sm and ^{151}Sm.

(vii) The Level Scheme of ^{153}Sm Based on (n, γ), (n, e$^-$), and (β, γ) Experiments

R. K. Smither, E. Bieber, T. v. Egidy,* W. Kaiser,* and K. Wein†

The ^{152}Sm(n, γ)^{153}Sm spectrum was measured with the Argonne bent-crystal spectrometer and with a Ge(Li) detector. The conversion-electron spectrum following neutron capture was studied with the β-ray spectrometer at the Munich research reactor. These data were combined to obtain the multipolarity of 28 low-energy transitions. The ^{153}Pm(β, γ)^{153}Sm gamma spectrum was studied with a Ge(Li) detector. The ^{153}Pm source was made with the electron linear accelerator at Darmstadt through the ^{154}Sm(γ, p)^{153}Pm reaction. These results were used to construct the level scheme of ^{153}Sm (Fig. 7) with 23 levels below 750 keV, the energy (keV) and J^π of the first 16 being: ground state, $\frac{3}{2}^+$; 7.53, $\frac{3}{2}^+$, $\frac{5}{2}^+$; 35.85, $\frac{1}{2}^-$, $\frac{3}{2}^-$; 53.56, $\frac{3}{2}^+$, $\frac{5}{2}^+$, $\frac{7}{2}^+$; 90.87, $\frac{5}{2}^-$; 127.29, $\frac{1}{2}^-$, $\frac{3}{2}^-$; 174.17, $\frac{5}{2}^-$; 182.90, $\leq \frac{5}{2}^-$; 262.37, $\frac{5}{2}^+$, $\frac{7}{2}^+$; 276.82, $\frac{1}{2}^+$, $\frac{3}{2}^+$; 321.10, $\frac{1}{2}^+$, $\frac{3}{2}^+$; 356.68, $\frac{3}{2}^+$, $\frac{5}{2}^+$; 362.29, $\frac{3}{2}^+$, $\frac{5}{2}^+$; 371.06, $\leq \frac{5}{2}^-$; 405.57, $\frac{1}{2}^-$, $\frac{3}{2}^-$; 414.95, $\frac{1}{2}^+$, $\frac{3}{2}^+$. The level

*Technischen Hochschule München.

†Technischen Hochschule Darmstadt.

energies are determined to ± 0.01 — 0.05 keV. Of special interest is the 7.53-keV state, which has a spin within one unit of that of the ground state and the same parity. Some evidence was found for low-lying rotational bands.

(viii) Level Scheme of ^{180}Hf

D. J. Buss and R. K. Smither

The gamma-ray spectrum following thermal neutron capture in ^{179}Hf has been obtained with the precision capture-gamma-ray spectrometer at the reactor CP-5. Primary interest has centered in the 1 — 2-MeV region of this spectrum in order to identify transitions between high-energy collective states and the ground-state rotational band. These data have led to the identification of about twelve levels between 1 and 2 MeV in ^{180}Hf, some of which have been tentatively identified as members of the beta and gamma vibrational bands. The average neutron resonance-capture spectrum of ^{180}Hf has also been obtained by the technique reported by Bollinger and Thomas. While these data have not yet been fully analyzed, they are expected to prove extremely useful in the verification of spins and in the determination of parities since the primary transitions to these levels seem to be quite insensitive to the collective nature of these states.

4. INTERNAL-CONVERSION-ELECTRON MEASUREMENTS

S. B. Burson and P. F. A. Goudsmit

The spectrum of gamma rays emitted by the nucleus as a result of thermal neutron capture has been studied in many laboratories with high-precision Compton and diffraction gamma-ray spectrometers and, more recently, with germanium-diode detectors.

There have also been a number of attempts to measure the internal-conversion coefficients of some of the transitions — but most of the successful experiments have been on nuclides with extremely high capture cross sections. The Argonne superconducting spectrometer was built to extend the measurements to other nuclides.

(i) Superconducting Internal-Conversion-Electron Spectrometer

The new conversion-electron spectrometer at Argonne uses an external beam from the reactor CP-5. A collimated beam of thermal neutrons from the reactor enters an evacuated target chamber and impinges upon a thin target located at the center of the chamber. The detectors are mounted on a vertical line through the intersection of the beam and the path along which the target can be moved. The gamma-ray detector, a 7-cm^3 Ge(Li) diode housed in an independent vacuum system, is inserted through an opening in the bottom of the chamber. The electron detector, a Si(Li) diode 0.75 in. in diameter and 2 mm thick, is mounted on the end of a cold finger suspended from the top of a through tube passing completely through the liquid helium cryostat in which the superconducting magnet is housed.

The magnet measures 2 in. inside diameter by 10 in. long and is situated immediately above the target chamber. Its central field is about 2×10^4 G. Conversion electrons having a velocity component upward along this field as they leave the target describe helical paths up the tube until they strike the detector approximately 10 in. above the target. This focusing action in effect enhances the solid angle of the electron detector approximately 50 fold, but the gamma-ray flux at the detector falls off in accordance with the inverse-square law. The electron spectrum obtained is thus virtually free of gamma-ray background from the sample. The Si(Li) detector has the advantage of making integral rather than differential measurements — i.e., all electrons striking the detector are analyzed for energy. The magnetic lens not only enhances the electron intensity relative to the gamma background but also affords an acceptance angle comparable to that of the best conventional spectrometers.

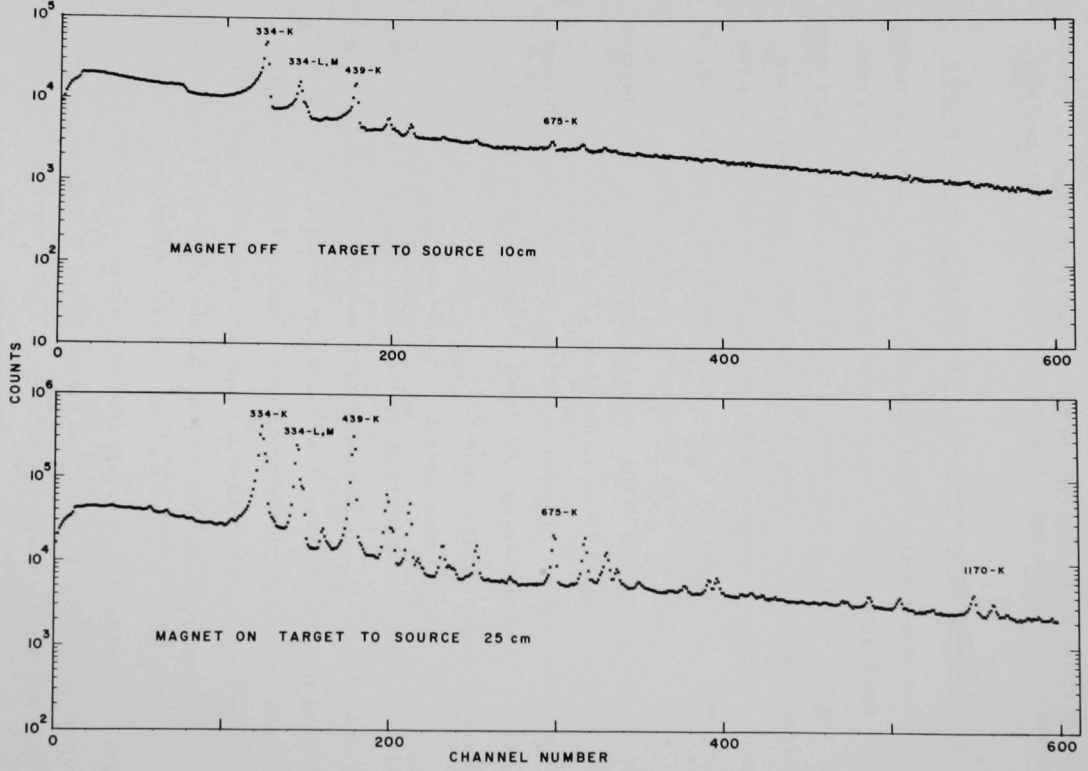

Fig. 8. Spectrum of conversion electrons following thermal-neutron capture in ^{149}Sm (σ = 41 500 b). The figure shows the depression of the gamma-ray background by the focusing effect of the magnetic field.

The suppression of the gamma-ray background is illustrated in Fig. 8. The figure shows the conversion-electron spectrum following capture of thermal neutrons in ^{149}Sm. The spectrum shown in the upper half of the figure was measured without the magnetic field. The reduced detection efficiency in the absence of the focusing magnetic field was partly compensated in this case by moving the detector closer to the target (10 cm instead of the normal 25 cm). The lower spectrum was measured with a magnetic field of approximately 1.5×10^4 G. The improvement in peak-to-background ratio is evident.

(ii) Studies of Electron Spectra of ^{182}Ta, ^{186}Re, and ^{188}Re

Spectra of conversion electrons following capture of thermal neutrons in ^{181}Ta, ^{185}Re, and ^{187}Re have been studied. The conversion-electron spectrum of ^{182}Ta is shown for illustration in Fig. 9. To obtain a favorable peak-to-background ratio in different energy regions, targets of different thicknesses have been used. The data are still being analyzed.

(iii) Measurements on Radioactive ^{181}Os (105 min) and ^{182}Os (22 h)

Data have also been obtained with radioactive samples. For example, one source was prepared by chemically extracting 105-min ^{181}Os produced by the (^{3}He, 4n) reaction on a tungsten target enriched in ^{182}W. The source undergoes orbital-electron capture to ^{181}Re, which in turn decays to ^{181}W with a 20-h period. Successive electron spectra were observed at 30-min intervals in order to distinguish the ^{181}Os spectrum from that of the daughter as the latter grew into the source. No internal-conversion coefficients for the transitions in ^{181}Re were previously available. More than 60 gamma transitions are observed, and of these we have determined conversion coefficients for 20.

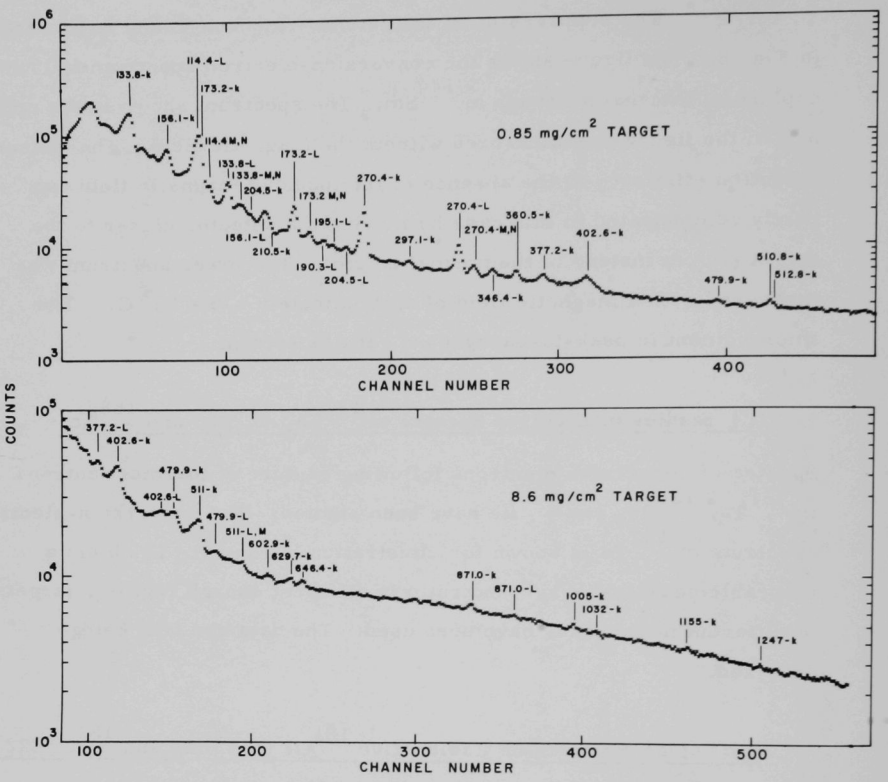

Fig. 9. Spectrum of conversion electrons following capture of thermal neutrons in ^{181}Ta (σ = 20 barns). The spectrum represents two measurements with targets of different thicknesses.

B. RESEARCH AT THE 4-MEV VAN DE GRAAFF ACCELERATOR

The experimental program with the 4-MeV Van de Graaff accelerator proceeded along much the same lines as in previous years. Experiments with fast neutrons were emphasized, especially measurements of the polarization of scattered neutrons. Recent interest in intermediate structure has prompted several investigations that have given convincing evidence of such structure and have stimulated related experiments with alpha particles. The 4-MeV machine has also been used to measure the lifetimes of nuclear states by a Doppler-shift method.

Because of the increasing need for a larger beam current than could be carried by the charging belt of the Van de Graaff, this machine is being replaced by a 4-MV Dynamitron capable of delivering a proton beam $\geq$ 1 mA. It will be installed during the summer and fall of 1968.

a. Operation and Improvement of the 4-MeV Van de Graaff Accelerator

(i) Operation of the Accelerator

Jack R. Wallace

The 4-MeV accelerator has operated 3573 hours in the period from 1 April 1967 to 31 March 1968. It is currently operating on a schedule of 80 hours per week.

The improvements include installation of a new energy-control system, the design and construction of a new shutter for higher beam currents, and improved vacuum pumping for target assemblies.

Much effort has been devoted to preparing for the new Dynamitron accelerator which will be installed late this summer. This accelerator will deliver much larger beams than our present accelerator, so many changes in the targetry will be required. A new design for the switching magnet has been worked out. New beam-transport tubes and other components are being designed and built. This work is intended to make the fullest possible use of the Dynamitron and to minimize the loss of time to the experimental program while the new accelerator is being installed.

(ii) Improvement of the Voltage Stability

A. Langsdorf, Jr., and W. K. Brookshier*

A new electronic circuit was built for the energy-control system of the 4-MV electrostatic accelerator. This circuit was tailored to provide a linearized control signal that could be modified by adjustments of a phase-advancing system within it, until the most stable voltage on the accelerator was empirically obtained. The system worked as well as was hoped for. Whereas before this circuit was used, the terminal voltage fluctuated rapidly (20 to 80 times per second) up and down about its set value with an amplitude of about 2000 V peak-to-peak, after it was put into use and adjusted properly, the fluctuations were considerably less than 200 V in the same region of operating voltage (near 2 MV). This system is quite simple in principle. It is capable of further development and is compatible with other more complex systems of voltage control. If used in conjunction, even much better stabilization of voltage might be achieved more economically than by another more complex and faster system alone.

The intention has been to provide higher precision of accelerator voltage control for any experimenter who has need for it.

No further work on this system is being contemplated in the immediate future. The important thing established by this development is that the well-known theory of linear control loops actually can be applied to improve the performance of this kind of accelerator. No unknown factors turned up that interfered seriously with carrying through to the immediate goal.

---

*Electronics Division.

b. Polarization and Differential Cross Sections for Neutron Scattering

(i) Scattering from Boron

R. O. Lane,* A. J. Elwyn, F. P. Mooring, and J. E. Monahan

Earlier measurements of the polarization and differential cross section for neutrons in the interval 0.075 MeV $\leq E_n \leq$ 2.24 MeV scattered from ^{11}B are being analyzed in terms of a 2-channel 3-level R-matrix formalism which allows the inclusion of the important s-wave bound states. The region 0.5 MeV $\leq E_n \leq$ 1.1 MeV probably contains two T = 1 s-wave scattering states: a broad one at $E_n \approx$ 1.05 MeV and a narrow one at nearly the same energy. Initial calculations indicate that these two have different J^π; one has 1^- (ℓ = 0) and the other 2^- (ℓ = 0). The assumption that both have the same J^π clearly disagrees with the data. The objective of this study is a more complete understanding of the structure of ^{12}B through a satisfactory simultaneous fitting of these data on the polarization and differential cross section. Similar data obtained for ^{10}B + n will be more difficult to interpret because of the larger number of reaction channels open in this case. However, little is known of the properties of states in ^{11}B in this region and the proper interpretation of these data should provide a better understanding of the structure of this nucleus.

(ii) Polarization and Differential Cross Section for Neutrons Scattered from ^{12}C

R. O. Lane,* R. D. Koshel,* A. J. Elwyn, F. P. Mooring, J. E. Monahan, and A. Langsdorf, Jr.

The polarization $P(\theta)$ and differential cross section $\sigma(\theta)$ for neutrons scattered from ^{12}C were measured at 5—9 angles at each

*Ohio University, Athens, Ohio.

of 38 neutron energies from 0.5 MeV to 2.0 MeV. The measured $P(\theta)$ is made up of a nearly constant term in $\sin\theta$ and a steadily increasing one in $-\sin 2\theta$ so that $P(120^{o}) \approx 0.4$ near $E_n \approx 1.9$ MeV. The term in $\sin\theta$ can be described by a pair of constant background R functions—one for $\frac{1}{2}^-$ and a different one for $\frac{3}{2}^-$. The term $-\sin 2\theta$ arises from interference between the $S_{1/2}$ phase shift (which has a large contribution from the $\frac{1}{2}^+$ state bound at 1.86 MeV in ^{13}C) and the relatively strong $D_{3/2}$ phase shift produced by the broad $\frac{3}{2}^+$ states in ^{13}C at $E_{ex} = 7.64$ MeV and 8.33 MeV. Rather good simultaneous fits to all the $\sigma(\theta)$ and $P(\theta)$ in this region have been obtained in terms of parameters of the R-function formalism for states in ^{13}C.

Because the cross section for energies less than 2.0 MeV appears to be dominated by a $2s_{1/2}$ single-particle state bound at 1.86 MeV, a potential model is being used to explain the differential cross section and polarization data for these energies. The parameters being used are those found in R-function fits.

c. Relation Between Fine and Intermediate Structure in the Scattering of Neutrons from Fe

A. J. Elwyn and J. E. Monahan

A structure with a width of about 150 keV has been observed in the energy dependence of the cross sections and polarizations for neutrons scattered from Fe at energies between 0.36 and 0.965 MeV. A phase-shift analysis of such data has been performed. The results are consistent with the existence of two $\frac{1}{2}^+$ resonances in this energy interval, one at $\varepsilon_d \approx 0.36$ MeV with $\Gamma \approx 140$ keV and $\Gamma' \approx 50$ keV, and the second at $\varepsilon_d \approx 0.7$ MeV with $\Gamma \approx 160$ keV and $\Gamma' \approx 100$ keV, although ambiguities make the proposed properties of the higher-energy resonance somewhat uncertain.

While the existence of resonance properties is a necessary condition for the observed intermediate-width peak to be interpreted as a doorway state, a more definitive test of the doorway-state model can be obtained by investigating the fine structure in the region of the resonance. To do this, the K matrix that describes the scattering in a basis in which all model states are coupled directly to the entrance channel is equated to the K matrix in a basis in which a single (doorway) state is so coupled. From this relation the doorway-state parameters can be obtained and their distributions can be compared with predictions of the doorway-state model.

The total neutron cross section of ^{56}Fe has been measured[1] with ~1-keV spread in neutron energy for energies up to 0.65 MeV. The doorway-state parmeters obtained from these fine-structure measurements are found to obey the distribution laws predicted by the model. The results show that the properties of the fine structure are consistent with the interpretation[2] that the intermediate resonance at $\varepsilon_d \approx 0.36$ MeV is an "almost pure" doorway state in the compound nucleus. The properties of this state as constructed from its fine structure agree with those obtained from the phase-shift analysis of the measured angular and polarization distributions.

---

[1] C. D. Bowman, E. G. Bilpuch, and H. W. Newson, Ann. Phys. (N.Y.) 17, 779 (1962).

[2] J. E. Monahan and A. J. Elwyn, Phys. Rev. Letters 20, 1119 (1968).

d. Systematic Study of the Small-Angle Scattering of Neutrons by Heavy Nuclei

F. T. Kuchnir, A. J. Elwyn, A. Langsdorf, Jr., F. P. Mooring, and J. E. Monahan

A systematic study of the differential cross section and polarization in the elastic scattering of fast neutrons was undertaken

during the past year. Measurements which are now completed were performed with nearly monoenergetic neutrons in the energy range from 0.6 to 1.6 MeV for U, Th, Pb, Au, W, and Cd. Data at a number of angles between 1.75° and 15° were taken with four neutron detectors simultaneously. These are a part of a neutron detection system designed and built at Argonne[1]; it consists of seven stilbene scintillators used with pulse-shape discrimination to reduce the high gamma-ray background. The data were corrected for multiple and inelastic scattering as well as for the effects of the spatial extension of the scatterer and detector. As the scattering angle decreased from 6° to 1.75°, the differential cross section of U was observed to increase by approximately 0.7 b/sr— independent of the neutron energy. The corresponding increase in other nuclei was found to be proportional to Z^2. At all energies and for all nuclei, the measured polarizations are negative and reach maximum values of 0.4— 0.6 at 1.75°.

Both the differential cross sections and the polarizations are compared with calculations[2] based on an optical-model potential for the nuclear interaction with parameters determined by the analysis of large-angle scattering. The model also includes terms describing the electromagnetic interaction between the Coulomb field of the nucleus and the magnetic moment of the neutron (Schwinger scattering) as well as its induced electric dipole moment (polarizability). Good agreement in the angular dependence is obtained between all experimental results and the calculated cross sections and polarizations (as shown in Figs. 10 and 11). There is therefore no evidence that the cross section behaves in an anomalous manner as had been reported on the basis of earlier experiments.

---

[1] F. T. Kuchnir and F. J. Lynch, IEEE Trans. Nucl. Science NS-15 (3), 107 (June 1968).

[2] J. E. Monahan and A. J. Elwyn, Phys. Rev. 136, B1678 (1964); A. J. Elwyn, J. E. Monahan, R. O. Lane, A. Langsdorf, Jr., and F. P. Mooring, Phys. Rev. 142, 758 (1966).

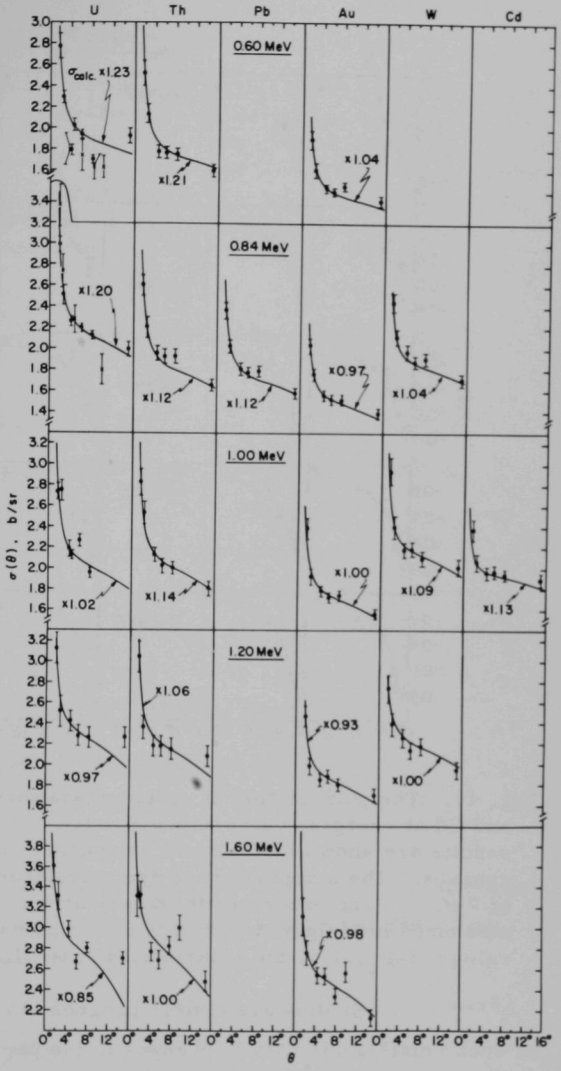

Fig. 10. Differential cross sections for neutrons scattered from U, Th, Pb, Au, W, and Cd at energies between 0.6 and 1.6 MeV. The present experimental values are shown as solid points; previous measurements are shown as crosses. The smooth curves are calculations based on the formalism of Ref. 2. The numbers near unity shown on the smooth curves are scale factors by which the calculations had to be multiplied to obtain agreement with the measurements. In its effect, such a normalization is equivalent to small changes in the nuclear optical-model parameters.

Further analysis of these data have led to the following conclusions: (i) For scattering angles $\theta \lesssim 10^{\circ}$, measurements of $\langle\sigma(\theta)P(\theta)\rangle$, $\langle\sigma(\theta)\rangle$, and $\langle\sigma_t\rangle$ for these heavy elements provides an absolute polarization analyzer. (ii) The imaginary part and an upper limit for the real part of the nuclear forward-scattering amplitude can be extracted from the measurements.

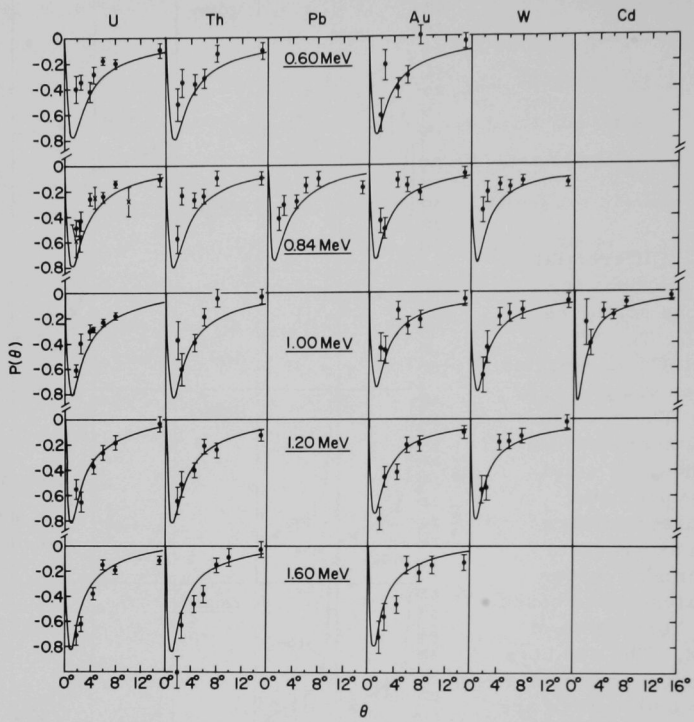

Fig. 11. The polarization of neutrons scattered by U, Th, Pb, Au, W, and Cd at energies between 0.6 and 1.6 MeV. The present experimental results are shown by the solid points; previous measurements by the crosses. The smooth curves are calculations based on the formalism of Ref. 2. The experimental polarizations have been obtained from measured left/right asymmetry ratios by use of previously measured values of $P_1(51^\circ)$, the polarization in the $Li^7(p,n)Be^7$ source reaction.

Studies are also in progress to determine the sensitivity of such small-angle data to changes in the parameters of an optical-model potential. In particular, the possible indication of any "long-range" nuclear force is being studied. Finally, the possibility of a measurement of the compound-elastic cross section is being investigated.

e. Lifetimes of Nuclear Excited States

This program of measuring the lifetimes of γ-ray-emitting states is based on the attenuated-Doppler-shift method, with the γ rays detected by lithium-drifted Ge detectors. A number of issues have been investigated: M1 transitions have been compared with their analogous Gamow-Teller beta decay, transitions in nuclei with a closed shell plus one nucleon have been measured, and other investigations linked to various predictions of the shell model are under way.

(i) Lifetime of the 1.042-MeV State in ^{18}F

A. E. Blaugrund, D. H. Youngblood, G. C. Morrison, and R. E. Segel

The lifetime of the 1.042-MeV T=1 state in ^{18}F was measured by use of the attenuated-Doppler-shift method. Analysis of the measurements by use of the universal stopping cross section given by Lindhard, Scharff, and Schiott gives a mean life $\tau = (0.4^{+0.3}_{-0.2}) \times 10^{-14}$ sec. The experimental lifetime agrees with the value calculated from the corresponding Gamow-Teller β transition according to a relation given by Kurath. The accuracy of the universal stopping cross section was discussed. The results of this work have been published.[1]

(ii) Speed of the ΔJ=1, ΔT=1 M1 Transition in ^{26}Al

D. H. Youngblood, R. C. Bearse, N. Williams, A. E. Blaugrund, and R. E. Segel

The attenuated-Doppler-shift technique (Fig. 12) has been used to determine the mean life of the 1.059-MeV third excited state in ^{26}Al. The value was found to be $(3.1^{+1.1}_{-0.8}) \times 10^{-14}$ sec. The state decays primarily to the $J^{\pi} = 0^{+}$, T = 1, 0.229-MeV first excited state. The spin component in this pure M1 transition can be deduced from the analogous Gamow-Teller β decay from the ^{26}Si ground state to the 1.059-MeV state in ^{26}Al. The observed lifetime is only about half what would be predicted from the spin component alone. This indicates a strong orbital contribution which, in turn, implies a large $(d_{5/2})^{-2}$

[1] A. E. Blaugrund, D. H. Youngblood, G. C. Morrison, and R. E. Segel, Phys. Rev. 158, 893 (1967).

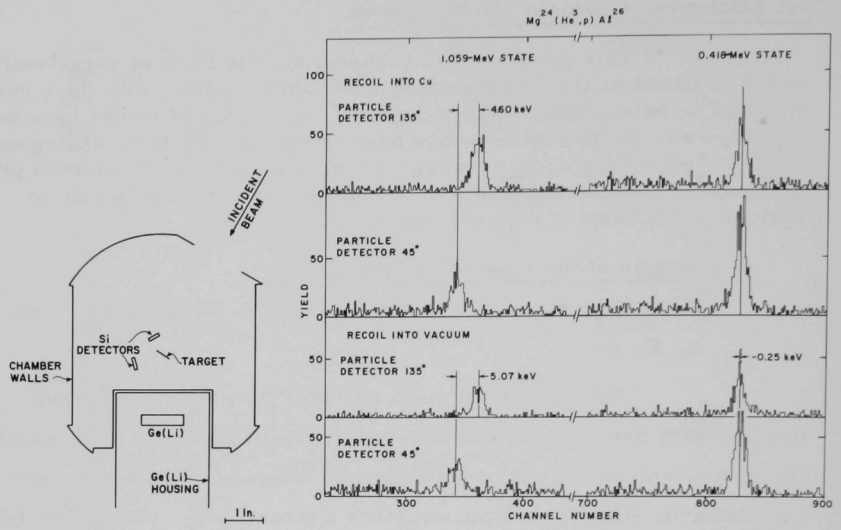

Fig. 12. Lifetime measurement by the attenuated-Doppler-shift technique. Left: Schematic diagram showing the Doppler shifts for the 830- and 418-keV gamma rays from the $^{24}Mg(^3He,p)^{26}Al$ reaction when the recoils were stopped in copper (upper graphs) and when they were allowed out into the vacuum (lower graphs).

component in the wave function. The M1 transitions whose spin components are known from analogous β decays are summarized in Table I. A mean life of $(4.8 \pm 2.5) \times 10^{-14}$ sec was found for the second excited state of ^{26}Mg. This work has been reported in the Physical Review.[1]

(iii) Lifetimes of the First and Third Excited States of ^{41}Ca and ^{41}Sc

P. P. Singh,* R. E. Segel, R. H. Siemssen,** S. Baker, A. E. Blaugrund, R. C. Bearse, and D. H. Youngblood

The lifetimes of the $\frac{3}{2}^-$ first excited state of ^{41}Ca at $E_x = 1.95$ MeV and the $\frac{3}{2}^-$ third excited state at $E_x = 2.47$ MeV have been

[1] D. H. Youngblood, R. C. Bearse, N. Williams, A. E. Blaugrund, and R. E. Segel, Phys. Rev. 164, 1370 (1967).

* Indiana University, Bloomington, Indiana.

** Yale University, New Haven, Connecticut.

TABLE I. Comparison between M1 decay rates and the speed expected if only the spin component were present. The spin component is taken for the analogous Gamow-Teller β decay by use of the formula of Kurath.[a] The estimates of Moszkowski[b] are used in determining $|M|^2$, the ratio of observed transition speed to single-particle speed. Here J_f and $J_{f\beta}$ are the spins of the final states in the γ and β transitions, respectively.

Nucleus	$E_i(J_i, T_i)$	E_f	(J_f, T_f)	$\log(2J_{f\beta}+1)ft$	$T^{-1}(\sec^{-1})$ From spin	Measured	$\lvert M\rvert^2/(2J_f+1)$	Ref.
Li^6	3.56(0, 1)	0	(1, 0)	3.40	0.85×10^{16}	$(1.25 \pm 0.20) \times 10^{16}$	3.3	c
F^{18}	1.04(0, 1)	0	(1, 0)	3.62	1.83×10^{14}	$(2.5^{+2.5}_{-1.1}) \times 10^{14}$	2.7	d
C^{12}	15.11(1, 1)	0	(0, 0)	3.62	5.4×10^{16}	$(6.1 \pm 0.8) \times 10^{16}$	0.63	e
Al^{26}	1.06(1, 0)	0.23	(0, 1)	3.84	1.59×10^{13}	$(3.3^{+1.7}_{-0.8}) \times 10^{13}$	2.1	f
P^{30}	0.677(0, 1)	0	(1, 0)	4.84	2.5×10^{12}	$(6.8 \pm 1.1) \times 10^{12}$	0.29	g

[a] D. Kurath, quoted in Ref. d and private communication.

[b] S. A. Moszkowski, in Alpha-, Beta-, and Gamma-Ray Spectroscopy, edited by Kai Siegbahn (North-Holland Publishing Company, Amsterdam, 1965), Vol. II, p. 865.

[c] L. Cohen and R. A. Tobin, Nucl. Phys. 14, 243 (1959).

[d] A. E. Blaugrund, D. H. Youngblood, G. C. Morrison, and R. E. Segel, Phys. Rev. 158, 893 (1967)

[e] S. J. Skorka, R. Hübner, T. W. Retz-Schmidt, and H. Wahl, Nucl. Phys. 47, 417 (1963).

[f] Present work.

[g] E. F. Kennedy, D. H. Youngblood, and A. E. Blaugrund, Phys. Rev. 158, 897 (1967).

measured by the attenuated-Doppler-shift method.[1] The two states were populated through the $^{41}K(p, n)^{41}Ca$ reaction at bombarding energies only a little above threshold. The γ rays were detected with a lithium-drifted germanium detector. Measurements were made at 0° and 90° to the beam and with ^{41}Ca ions recoiling into vacuum, carbon, KCl, and gold. Some attenuation of the Doppler shift results from the recoiling ion changing its direction on collision with a nucleus. At the low recoil velocities encountered, this effect is comparable to the attenuation due to the energy loss in electronic collisions and it was explicitly taken into account. The lifetime of the first excited state was found to be $(4.7^{+2.5}_{-1.0}) \times 10^{-13}$ sec; that of the third excited state is $\geq 7 \times 10^{13}$ sec. The speed of the E2 transition to ground state from the first excited state is thus about three times the Moszkowski single-particle estimate. In

[1] P. P. Singh, R. E. Segel, R. H. Siemssen, S. Baker, and A. E. Blaugrund, Phys. Rev. 158, 1063 (1967).

TABLE II. Radiation widths for the ground-state transitions from the low-lying $\frac{3}{2}^-$ states in ^{41}Sc and ^{41}Ca.

Nucleus	E_x (MeV)	Γ_γ (MeV)	$\|M\|^2$ (single-particle units)[a] Exp.	Theory[b]
^{41}Sc	1.71	1.3 ± 0.4[c]	4.8 ± 1.5	5.2
	2.41	< 0.01[d]	< 0.006	0.06
^{41}Ca	1.95	1.5 ± 0.5[e]	2.9 ± 0.9	3.8
	2.47	< 0.01[e]	< 0.006	0.06

[a] S. A. Moszkowski, in Alpha-, Beta-, and Gamma-Ray Spectroscopy, edited by K. Siegbahn (North-Holland Publishing Company, Amsterdam, 1965), Vol. II, p. 865.

[b] W. A. Gerace and A. M. Green, Nucl. Phys. A93, 110 (1967).

[c] D. H. Youngblood, J. P. Aldridge, and C. M. Class, Phys. Letters 18, 291 (1965).

[d] Present work.

[e] P. P. Singh, R. E. Segel, R. H. Siemssen, S. Baker, and A. E. Blaugrund, Phys. Rev. 158, 1063 (1967).

contrast, the speed of the E2 ground-state transition from the third excited state (which decays mainly to the first excited state) is less than 6×10^{-3} of the single-particle estimate. These results were compared with theoretical predictions.

In addition, the ^{40}Ca(p, γ_0)^{41}Sc yield curve was examined in a search for the transition from the $\frac{3}{2}^-$ third excited state to the $\frac{7}{2}^-$ ground state in ^{41}Sc.[1] No resonance was found; an upper limit was set at $\Gamma_{\gamma 0} = 10$ μeV, which corresponds to 6×10^{-3} single-particle units. The results for ^{41}Sc and ^{41}Ca are summarized in Table II.

[1] R. C. Bearse, D. H. Youngblood, and R. E. Segel, Nucl. Phys. A111, 678 (1968).

f. Measurements of Scintillator Properties

Scintillators continue to be important detectors for neutrons, gamma rays, and beta particles— especially where good time resolution is required. The present measurements of the intensity of the scintillation light as a function of the time since the excitation occurred were undertaken (1) to evaluate scintillators for these applications and (2) to improve the understanding of the scintillation processes. Calculations of the expected time resolution have indicated the relative importance of the scintillator

and photomultiplier parameters as they affect the time resolution and have guided the optimization of the technique used to obtain the best time resolution from a specific scintillator. One concrete result is the development of a fixed-fraction discriminator which provides excellent time resolution independent of pulse height.

(i) Time Dependence of Scintillations and the Effect on Pulse-Shape Discrimination

F. T. Kuchnir and F. J. Lynch

In a comparative study of commercially available organic scintillators for pulse-shape discrimination (PSD) we have measured the time dependence of the light following excitations by neutrons and gamma rays for stilbene and for the liquids NE213, NE213M, and NE218. The experimental results obtained in the region 0—500 nsec were fitted to the sum of three exponentials and values for the three decay constants were extracted. In addition, the number of photoelectrons produced at the cathode of an RCA-8575 photomultiplier per keV energy loss in each scintillator was determined. As a result of this study it was concluded that stilbene is the best choice for PSD when small detectors can be used. Among the liquids, NE218 seems to be a somewhat better choice than the other two.

A PSD system using stilbene scintillators was built at Argonne. It is based on the simple technique of measuring the time difference between the start and the instant at which the integrated photomultiplier pulse reaches a specified fraction of its final amplitude. In practice it is operated for pulses within a certain range in pulse height. In order to be able to compare calculations based on the measured scintillation decays with the performance of the PSD system, it was necessary to know the light-output-vs energy-loss relation for both Compton electrons and recoil protons. The Argonne 4-MeV Van de Graaff and standard γ-ray sources were used for these measurements.

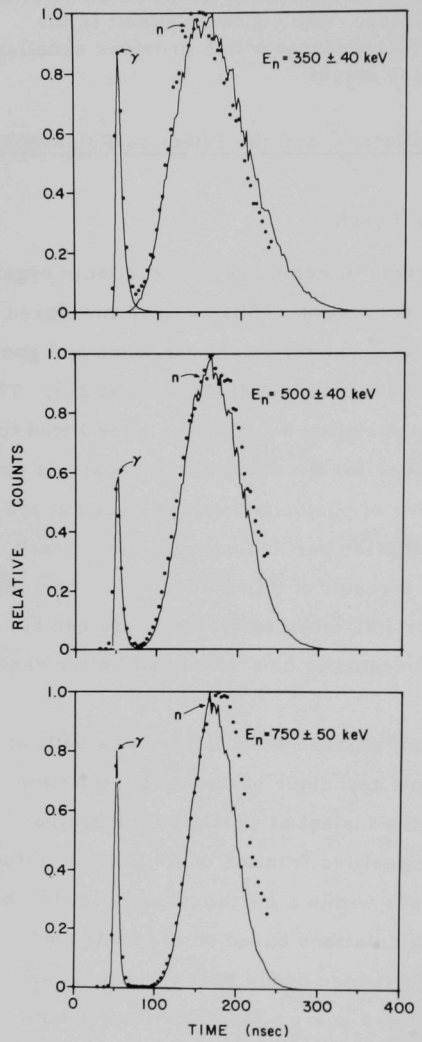

Fig. 13. Rise-time distributions for γ rays and neutrons. The points are the experimental values; the curves are the calculated distributions.

With the single assumption that the photoelectron emission follows Poisson statistics, and by using the measured decay curves and the experimentally determined 2.3 photoelectrons/keV energy loss by electrons in stilbene, one can calculate the rise-time distribution function. This is directly comparable with the experimental results obtained with the PSD system. Figure 13 illustrates the type of agreement between the calculated (solid line) and actual performance (points) of the PSD system for different pulse-heights corresponding to the neutron energies indicated. The calculations assumed that the triggering fraction was 0.895. Good over-all agreement was obtained.

(ii) New Liquid Scintillators with Higher Speed and Efficiency

F. J. Lynch

Further measurements of the variation of light intensity with time following excitation by gamma rays have been made for

toluene solutions of quaterphenyl, quinquiphenyl, and sexiphenyl compounds whose solubilities were enhanced by substitution of alkyl groups. The decay curves, measured by use of a light-intensity-sampling technique, were analyzed to yield the mean lives τ_1 for energy transfer from solvent to solute, τ_2 for decay of the fast component (from the singlet state), and τ_3 for decay of the slower component (probably from excimers). Preliminary estimates of τ_2 for quaterphenyl, quinquiphenyl, and sexiphenyl are 1.27, 1.22, and 1.02 nsec, respectively. As expected, τ_1 appears to vary inversely with solute concentration, and at the highest concentration of quaterphenyl in toluene ($\sim$ 65 g/liter, mole fraction = 1.12×10^{-2}) was < 0.1 nsec. At this concentration, the amount of light in the slower component was only about 1/6 of the total light. This indicates that formation of excimers is inhibited. In addition, the photoelectrons produced in an RCA-8575 photomultiplier per keV of energy lost in the scintillator was measured to be 2.1 for quaterphenyl, 2.2 for quinquiphenyl, and 1.9 for sexiphenyl solutions. The efficiency and speed are higher than in the commonly-used plastics, and this improvement is reflected in a corresponding enhancement of the time resolution achievable with these scintillators. For a 300-keV energy loss in the quaterphenyl solution, the FWHM was 0.20 nsec and the effective half-life was 0.035 nsec.

(iii) Calculation of Time Resolution

F. J. Lynch

The expected time resolution has been calculated from the photoelectron current measured as a function of time for the two cases in which the pulse was timed (1) by a fixed-level discriminator and (2) by a fixed-fraction discriminator. Similar calculations have also been made with a photoelectron current simulated by analytic functions that approximate the responses of the scintillator and photomultiplier.

These show the relative effectiveness of scintillator and photomultiplier parameters in determining the time resolution.

(iv) Fixed-Fraction Discriminator

F. J. Lynch

The calculations described in Sec. (iii) show that the optimum time resolution is obtained when the discriminator triggers at a particular fraction of the integrated final pulse height. A fixed-fraction discriminator to fulfill the theoretical requirements has been under development for the last two years. The final circuit shows excellent time resolution over a range of 10:1 in pulse hight, with virtually no walk in the time spectrum throughout this range.

C. RESEARCH AT THE TANDEM VAN DE GRAAFF ACCELERATOR

The newly-converted Tandem Van de Graaff accelerator, now an FN-model machine, provides the principal research tool for about 15 Argonne scientists in the Physics Division and several in the Chemistry Division. Also, running time is made available to qualified physicists from universities. Currently, research groups from six universities are using the system.

The Tandem is used to full capacity on an operating schedule of 24 hours per day. The new machine has proved to be exceptionally reliable in operation. A terminal voltage of 8.5 million volts is attained with ease and 9.0 MV has been achieved on occasion. Also, the beam current from the new machine is much higher than it had been at the EN Tandem.

The research carried out at the Tandem under the low-energy physics program is very broad in scope, reflecting the diverse interests of the physicists involved. The major permanent facilities for these investigations are indicated in Fig. 14. Most of the program is concerned with some aspect of charged-particle nuclear reactions. Recently, studies of direct reactions, the giant dipole resonance, lifetimes of excited states, and isobaric-spin analog states have received special emphasis. A study of reactions induced by Li ions has been initiated.

a. Operation of the Tandem Van de Graaff Accelerator

Jack R. Wallace

The EN tandem operated 1368 hours in the period from 1 April to 8 June 1967. The total number of hours on the EN tandem from its first operation in January 1962 until it was converted to the FN model was 29 001 hours. Since the changeover, the new FN tandem (Fig. 15) has operated 3558 hours in the period from 8 August 1967 to 31 March 1968. Thus, the total operating time in the period from 1 April 1967 to 31 March 1968 was 4926 hours.

The changeover from the EN Tandem to the FN Tandem took place in the period 8 June to 30 August 1967. A handling and storage system for SF_6 insulating gas for the FN Tandem was also installed at this time and was put in use on 22 October 1967. We have been able to operate at terminal voltages up to 9 MV.

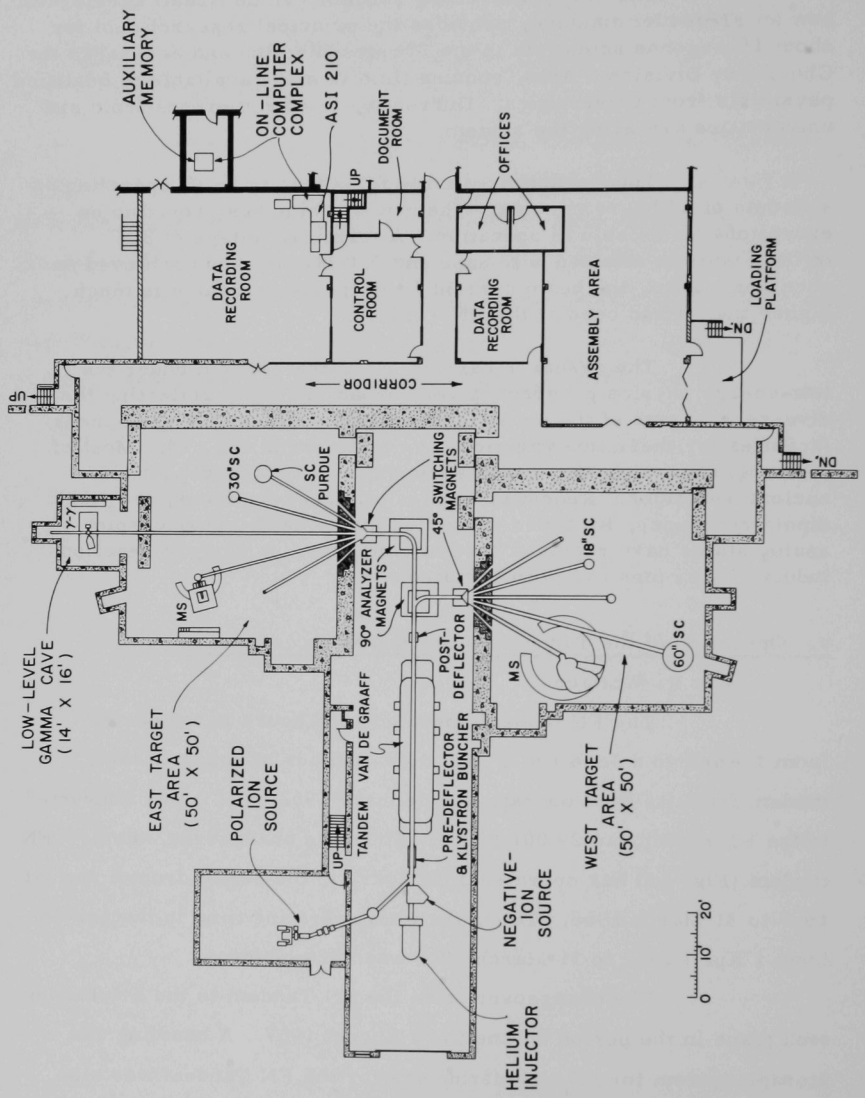
AUXILIARY MEMORY
ON-LINE COMPUTER COMPLEX
ASI 210
DOCUMENT ROOM
OFFICES
UP
DATA RECORDING ROOM
CONTROL ROOM
DATA RECORDING ROOM
ASSEMBLY AREA
LOADING PLATFORM
DN
CORRIDOR
UP
DN
30°SC
SC PURDUE
45° SWITCHING MAGNETS
18°SC
MS
90° ANALYZER MAGNETS
POST-DEFLECTOR
MS
60°SC
LOW-LEVEL GAMMA CAVE (14' X 16')
EAST TARGET AREA (50' X 50')
POLARIZED ION SOURCE
UP
TANDEM VAN DE GRAAFF
PRE-DEFLECTOR & KLYSTRON BUNCHER
NEGATIVE-ION SOURCE
WEST TARGET AREA (50' X 50')
HELIUM INJECTOR
0 10' 20'

Changes and improvements since installation of the FN include a lithium-gas-exchange duo-plasmatron ion source, and turbo-molecular pumping systems to replace the oil diffusion pumps in the pumping stations for the low-energy and high-energy accelerating tubes and for both analyzing magnets. We have also installed turbo-molecular pumping systems in the experimental areas. An automatic beam-steering system in the experimental areas is now operational. The polarized-ion source has been installed and is currently being tested. The recent enlargement of the data-handling area (Fig. 16) has greatly enhanced the convenience and efficiency with which the on-line computer system can be used by all experimenters employing the tandem facilities.

A beam-profile monitoring system is under construction and will soon be installed.

Fig. 14. Floor plan of the tandem wing of the Physics Building. In the two target areas, SC designates a scattering chamber, MS a magnetic spectrograph, and γ-γ the gamma-gamma angular-correlation apparatus.

b. Radiative-Capture Studies of the Giant Dipole Resonance

(i) The Giant Dipole Resonance Excited by α Capture

L. Meyer-Schützmeister, Z. Vager, R. E. Segel, and P. P. Singh*

We have studied the reactions $^{24}Mg(\alpha,\gamma)^{28}Si$ from E_α = 5.3 MeV to 14.5 MeV, $^{26}Mg(\alpha,\gamma)^{30}Si$ from 4.0 MeV to 13.5 MeV, and $^{28}Si(\alpha,\gamma)^{32}S$ from 7.0 MeV to 12.0 MeV. These α energies lead into the region of the giant dipole resonance in the compound nucleus. The yield of gamma rays γ_0 leading to the ground state of the final nucleus (Fig. 17) was studied for each of the three targets; and for $^{24}Mg(\alpha,\gamma)$ the radiation γ_1 going to the first excited state was also studied with reasonable

*Indiana University, Bloomington, Indiana.

Fig. 15. Output end of the new 18-MeV FN tandem, with the 90° analyzing magnets and the switching magnets in the foreground.

Fig. 16. The ASI-210 computer and some experimental electronics in the newly-expanded data-handling area for the tandem.

accuracy. The angular distributions of γ_0, which were measured in 100-keV steps over a wide range of energies for the ^{24}Mg and ^{26}Mg targets and at two energies for the ^{28}Si target, showed a dominant electric-dipole transition. This indicates that the (α, γ_0) reactions lead predominantly through the giant dipole resonance in ^{28}Si and ^{30}Si and most likely also in ^{32}S. The gamma-ray yield, which was measured in steps of 30 or 100 keV over the energy ranges studied, exhibited strong fluctuations in each case. For α capture both in ^{24}Mg and in ^{26}Mg, statistical analysis of the fluctuations showed that the reactions proceed nearly 100% through compound-nucleus formation and that the average width of the compound-nucleus resonances is about 60 keV. The integrated cross sections of these three alpha-capture reactions led to the conclusion that formation of the giant resonance by alpha capture is strongly inhibited— even in cases in which the alpha capture is isospin allowed. This is expected since the giant dipole resonance is supposed to consist predominantly of particle-hole states. Earlier experiments on proton capture by ^{27}Al had shown that only a small part of the giant dipole resonance in ^{28}Si leaks into the more

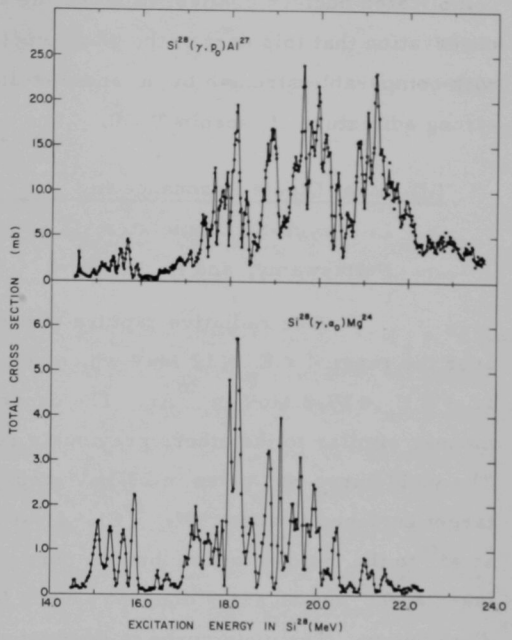

Fig. 17. Yield curves for the $^{28}Si(\gamma, p_0)$ and $^{28}Si(\gamma, \alpha_0)$ reactions in the giant-resonance region. The (γ, p_0) curve is computed from the $^{27}Al(p, \gamma_0)$ data, the (γ, α_0) curve from the ^{24}Mg (α, γ_0) data.

complicated nucleon configurations of the compound nucleus. The observation that this part of the giant dipole resonance in ^{28}Si decays with comparable strength by α and p emission indicates that it has a strong admixture of isospin T = 0.

(ii) Giant Dipole Resonance in ^{36}Ar

L. Meyer-Schützmeister, D.S. Gemmell, R. C. Bearse, N. G. Puttaswamy, and R. E. Segel

The radiative capture of protons by ^{35}Cl has been studied over the range $4 \leq E_p \leq 12$ MeV which covers the excitation region $12.4 \leq E_x \leq 19.2$ MeV in ^{36}Ar. The experiments were performed in a manner similar to the others previously reported by the Argonne group. The yield curve was taken in 25-keV steps with a 1.5 mg/cm^2 $BaCl_2$ target enriched to about 99% ^{35}Cl. Most of the yield curve was taken at 45° to the incident beam, but the portion from 7.0 to 8.5 MeV was taken at 90° and an adjustment was made for the gamma-ray angular distribution. The yield curve is dominated by the onset of the giant resonance but, because of the comparatively low Q and also because the giant resonance appears to come at a higher energy in ^{36}Ar than in neighboring nuclides, the beam energy was not high enough to reach the peak of the giant resonance. There is a great deal of fine structure but, at least in the giant-resonance region, the direct-interaction component contributes most of the cross section.

The γ_1 yield curve (for reactions to the first excited state) is qualitatively similar to that obtained for γ_0 except that the γ_1 yield is still rising at the high-energy end. This indicates that the peak of the γ_1 giant resonance has not yet been reached. The integrated (γ, p_0) yield, obtained by detailed balance, is 0.060 MeV-b which is about 11% of the dipole sum [taken as $(2\pi^2 e^2 \hbar/Mc)(NZ/A)$].

Angular distributions, taken every 100 keV over the entire range, show marked variations below the giant-resonance region

but then settle down to the usual near-invariance at higher energy. The greater yield in the forward direction, indicative of E1-E2 interference, is quite marked. Some yields from $^{37}Cl(p, \gamma)$ have also been measured.

c. Nuclear Spectroscopy ($A < 40$)

(i) The (d, p) Reaction in the 1p Shell

G. C. Morrison, J. P. Schiffer, R. H. Siemssen,* and B. Zeidman

Angular distributions of the (d, p) reaction at $E_d = 12$ MeV in the angular range 10°—155° were obtained for targets of all stable isotopes between ^6Li and ^{14}N. The experimental absolute cross sections were analyzed by use of DWBA calculations with a single, average set of distorting parameters for light nuclei. The spectroscopic factors were found to be in reasonable agreement with those obtained in shell-model calculations. The sensitivity of the results to distorting parameters and to nonlocal, finite-range effects was investigated. Persistent J-dependent effects were observed and attempts were made to extract fractional-parentage coefficients for mixed $p_{1/2}$ and $p_{3/2}$ transitions. The results have been published.[1]

(ii) Inelastic Scattering of Protons by ^{10}B

B. A. Watson, R. E. Segel, and P. P. Singh†

The inelastic scattering of protons by ^{10}B has been studied at proton bombarding energies from 5 to 16 MeV. Data were taken every

---

*Yale University, New Haven, Connecticut.

[1] J. P. Schiffer, G. C. Morrison, R. H. Siemssen, and B. Zeidman, Phys. Rev. 164, 274 (1967).

†Indiana University, Bloomington, Indiana.

100 keV at six angles while complete angular distributions in 5° steps from 15° to 165° were measured every 300 keV. The groups studied were those feeding the 0.72-, 1.74-, 2.15-, 3.59-, 4.77-, and 6.04-MeV states. The integrated cross sections for feeding the 1.74-, 2.15-, and 3.59-MeV states are in reasonable agreement with those reported by Segel et al., but our value for feeding the 0.72-MeV state is only about half theirs. By far the largest cross section observed is that for feeding the 6.04-MeV state. Above 11 MeV bombarding energy, its cross section was more than five times that of any other state. This supports the notion that the 6.04-MeV state is the first excited state of a rotational band built upon the ground state. Calculations involving the DWBA indicate that excitation of the first five excited states proceeds by $\ell = 2$ transfer. Excitation of the 6.04-MeV state appears to have an appreciable $\ell = 0$ component— in contrast to an $\ell = 2$ transition expected for a strong rotational state.

(iii) The ^{10}Be(d, p)^{11}Be, ^{10}Be(d, t)^{9}Be, and ^{10}Be(p, p')^{10}Be Reactions

D. L. Auton

Experimental angular distributions for these reactions are being studied with solid-state detectors and the magnetic spectrograph at the Argonne tandem accelerator. The ^{10}Be target being used was produced at the Argonne isotope separator, and has a thickness of approximately 1 $\mu g/cm^2$ and an enrichment of 90%. Preliminary results for the ^{10}Be(d, p) reaction to the ground state and first excited state of ^{11}Be indicate spins and parities of $\frac{1}{2}^+$ and $\frac{1}{2}^-$ or $\frac{3}{2}^-$, respectively, by comparison of the observed cross sections with those calculated by means of the JULIE program. The ^{10}Be(d, t)^{9}Be reaction will be studied in an effort to determine the existence of a state at 1.75 MeV in ^{9}Be. The ^{10}Be(p, p')^{10}Be reaction to the 2^+ first excited state at 3.368 MeV is being studied with a view toward determining B(E2), which is proportional to the probability of the upward transition from the 0^+ ground state to the 2^+ first excited state.

(iv) The $^{11}B(^3He, \alpha)^{10}B$ Reaction at 33.0 MeV

D. Dehnhard,* N. Williams, and J. L. Yntema

Several neutron pickup reactions, including (d, t) and (p, d), have been performed on ^{11}B to investigate both the reaction mechanism and the variations in spectroscopic factors obtained from DWBA analyses. The $(^3He, \alpha)$ reaction was studied at 33 MeV to supplement the existing data and to allow a comparison of spectroscopic factors with the theoretical predictions of Cohen and Kurath. The relative spectroscopic factors obtained are in good agreement with theory for both $T_<$ and $T_>$ states, and no significant j dependence was observed for levels populated principally by $j^\pi = \frac{3}{2}^-$ and $\frac{1}{2}^-$. The angular distributions and the distorted-wave Born approximation fits to the data are shown in Fig. 18.

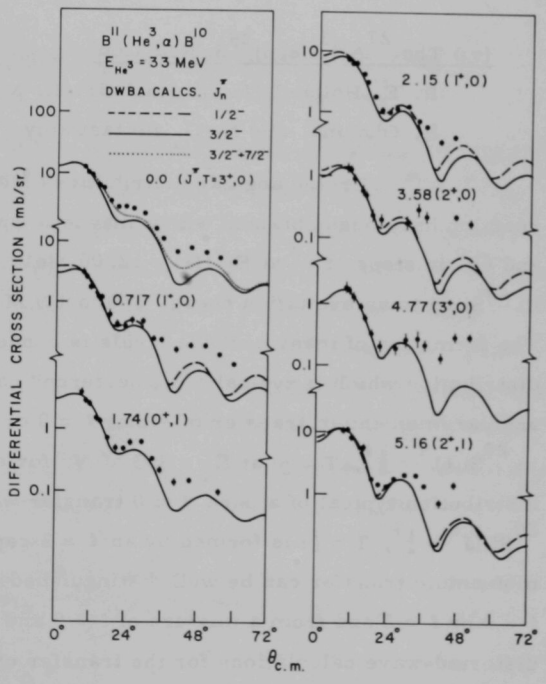

Fig. 18. Angular distributions of the $^{11}B(^3He, \alpha)^{10}B$ reaction. The curves are DWBA fits to the data.

(v) The Reaction $^{25}Mg(^3He, d)^{26}Al$ at 12 MeV

A. Weidinger,† R. H. Siemssen,† G. C. Morrison, and B. Zeidman

The $^{25}Mg(^3He, d)^{26}Al$ reaction was studied

*University of Minnesota, Minneapolis, Minnesota.

†Yale University, New Haven, Connecticut.

at E(^{3}He) = 12 MeV by use of the Argonne tandem Van de Graaff and a broad-range magnetic spectrograph. All known states up to 4.2 MeV were observed in this experiment; but the doublets at 2.07 MeV and 4.20 MeV have not been resolved. For the 15 strongest transitions, angular distributions between 5° and 25° were measured. They all have characteristic $\ell = 0$, $\ell = 2$, or $\ell = 0 + 2$ stripping patterns. The $\ell = 0$ admixtures in the angular distributions limit spins and parities to 2^+ or 3^+ for the states at 2.55, 2.92, 3.59, 3.68, and 3.75 MeV, for which no spins and parities were previously known. Spectroscopic factors have been extracted with the Oak Ridge DWBA code JULIE. The published report[1] discusses the results in the framework of the unified model.

(vi) The ^{27}Al(^{3}He, p)^{29}Si Reaction

R. E. Holland, F. T. Kuchnir, L. Meyer-Schützmeister, H. Ohnuma, and N. G. Puttaswamy

Proton angular distributions from the ^{27}Al(^{3}He, p)^{29}Si reaction have been obtained with a magnetic spectrograph between 5° and 69° in steps of 8° at E(^{3}He) = 12.00 MeV. All known energy levels in ^{29}Si up to an excitation energy of about 9 MeV have been observed. The formation of many of these levels is connected with an angular distribution which is typical of a "deuteron" capture process with an angular-momentum transfer of either $\ell = 0$ or $\ell = 2$. The analog state in ^{29}Si ($J^\pi = \frac{5}{2}^+$, $T = \frac{3}{2}$) at $E_x = 8.3$ MeV, for example, shows an angular distribution typical of a pure $\ell = 0$ transfer while the ground state of ^{29}Si ($J^\pi = \frac{1}{2}^+$, $T = \frac{1}{2}$) is formed by an $\ell = 2$ capture process. Odd angular-momentum transfer can be well distinguished from those with pure $\ell = 0$ or $\ell = 2$ and from a mixture of $\ell = 0$ and $\ell = 2$. Theoretical distorted-wave calculations for the transfer of a "neutron-proton" pair (JULIE code) show fairly good agreement with the experimental results.

[1] A. Weidinger, R. H. Siemssen, G. C. Morrison, and B. Zeidman, Nucl. Phys. A108, 547 (1968).

(vii) The $^{30}Si(^{3}He, \alpha)^{29}Si$ Reaction

D. Dehnhard* and J. L. Yntema

The results from the neutron-pickup reaction indicate that the $d_{5/2}$ neutron shell is nearly filled and that the remaining neutrons are split about equally between the $2s_{1/2}$ and $1d_{3/2}$ shells. A rather weak transition to the known $\frac{7}{2}^-$ level indicates an admixture of a few percent of f-wave neutrons in ^{30}Si. The weak single-particle neutron-hole component in the 3.027-MeV level and the strong component in the 2.027-MeV level disagree with the conclusions one would draw from the gamma decay of these levels. The isobaric analog of the ^{29}Al ground state was found at 8.32 MeV. The strength of the transition appears to exhaust the available $d_{3/2}$ strength.

(viii) Study of the $(^{3}He, d)$ Reaction on Nuclei with A Near 30

R. A. Morrison, J. P. Schiffer, and B. Zeidman

We plan to measure the angular distributions and absolute cross sections for the $(^{3}He, ^{3}He)$ and $(^{3}He, d)$ reactions on ^{30}Si, ^{31}P, ^{32}S, and ^{34}S at an incident energy of 15.0 MeV. From the angular distribution obtained in elastic scattering, an optical model for the input channel will be chosen; and an output optical model will be chosen from data already available and other data taken if necessary. The parameters of these models will be used in a DWBA analysis to extract the spectroscopic factors. The work on ^{31}P is almost completed and about a third of the work on ^{30}Si is done. Spectroscopic factors for the $^{31}P(^{3}He, d)$ reaction agree well with the limited shell-model calculation of Glaudemans et al.

*University of Minnesota, Minneapolis, Minnesota.

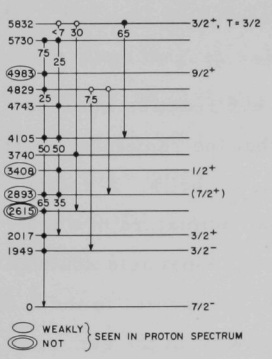

Fig. 19. Gamma-ray decay scheme of ^{41}Ca levels observed in the ^{39}K(^{3}He, pγ)^{41}Ca reaction. The proton detector was at 0°.

d. Nuclear Spectroscopy (A > 40)

(i) The ^{39}K(^{3}He, pγ)^{41}Ca Reaction

L. Meyer-Schützmeister, D. S. Gemmell, H. Ohnuma, and N. G. Puttaswamy

The gamma-decay properties of some ^{41}Ca levels have been studied with the ^{39}K(^{3}He, pγ)^{41}Ca reaction at E(^{3}He) = 12 MeV. The target was made of natural KI evaporated on gold foil which stopped the ^{3}He beam. The gammas were detected by a 25-cc Ge(Li) counter in coincidence with the protons at 0°. Such an arrangement restricts observation to those states in ^{41}Ca that have even parity and dominant 2p-1h configuration. We find (Fig. 19) that these states decay preferentially to similar states, although in some cases strong transitions to the ground state ($J^{\pi} = \frac{7}{2}^{-}$, $T = \frac{1}{2}$) have been observed. The analog state at 5.83 MeV ($\frac{3}{2}^{+}$, $\frac{3}{2}$) decays mainly to the 4.11-MeV state and not to the 2.02-MeV state ($\frac{3}{2}^{+}$, $\frac{1}{2}$) believed to be the "anti-analog" of the 5.83-MeV state. This is in contrast to the strong and predominant γ transition between the analog state ($J^{\pi} = \frac{7}{2}^{-}$, $T = \frac{3}{2}$) and the "anti-analog" state ($J^{\pi} = \frac{7}{2}^{-}$, $T = \frac{1}{2}$) observed in a number of sd-shell nuclei.

(ii) Study of ^{48}Ca(^{3}He, t)^{48}Sc and ^{48}Ca(^{3}He, p)^{50}Sc Reactions

J. R. Erskine, J. A. Nolen, and H. Ohnuma

We have taken new data on these reactions with the higher beam currents available from the improved negative-ion source. Some of the data were read from the nuclear emulsions with an automatic track-counting machine. Preliminary analysis of these superior-quality data confirms our preliminary conclusions reported last year. The

relative ease with which we can now obtain good (^{3}He, t) data has encouraged us to start a program of using this same reaction on other medium-weight nuclei. The angular distributions obtained for the (^{3}He, p) reactions were compared with the DWBA theory, and possible spin and parity assignments were given for the low-lying states of ^{50}Sc. The results were in good agreement with shell-model calculations, as can be seen in Fig. 20.

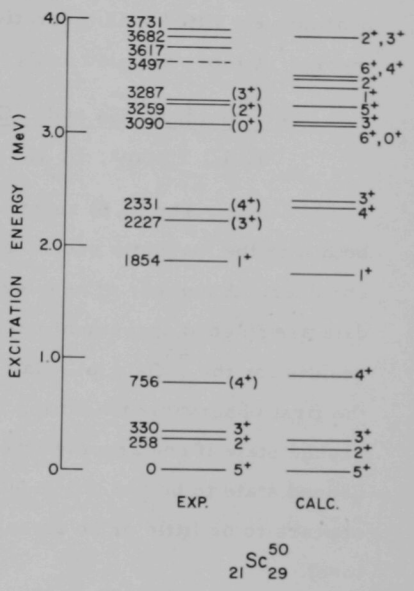

Fig. 20. Comparison between the results of the present experiment and the shell-model calculations by T. A. Hughes and M. Soga (preprint).

(iii) The ^{54}Fe(d, p)^{55}Fe Reaction

J. L. Yntema, H. Ohnuma, and H. T. Fortune

This reaction was first investigated at the cyclotron to see whether the j-dependence—the differences between the angular distributions of the protons from the ground state ($\frac{3}{2}^-$) and the first excited state ($\frac{1}{2}^-$) of ^{55}Fe, first observed at lower energies by Lee and Schiffer—persisted at higher energies. The cyclotron results indicated that the differences observed between the $p_{3/2}$ and $p_{1/2}$ neutron transfer at 23 MeV were predicted by the distorted-wave theory, provided that one damps the contributions from the interior of the nucleus. The damping provided by the Perey-Buck nonlocal potential is insufficient.

Subsequently, both elastic scattering of deuterons and the (d, p) reaction were measured at the tandem at a number of energies between 12 and 18 MeV. The data obtained at the tandem have been

qualitatively fitted with theoretical curves from the distorted-wave theory. A more detailed analysis is in progress.

(iv) ^{69}Ga(d, p)^{70}Ga and ^{71}Ga(d, p)^{72}Ga

J. L. Yntema, H. H. Bolotin, and J. Vervier

The (d, p) reactions on ^{69}Ga and ^{71}Ga have been studied both with the magnetic spectrograph and with the 60-in. scattering chamber. A number of new levels have been found, and the analyzed data are in good agreement with the low-energy neutron-capture results for the ^{69}Ga(d, p)^{70}Ga case. In the ^{71}Ga(d, p)^{72}Ga reaction, the first observable transition is to a level about 165 keV above the ground state if one assumes the energy of the (n, γ) transition to the ground state to be 6.520 ± 0.001 MeV. It is disturbing that there appears to be little or no strength for transitions below the 165-keV level.

(v) Energy Levels of ^{103}Ru and ^{105}Ru from the $^{102, 104}$Ru (d, p) Reactions

J. A. Nolen, Jr., H. T. Fortune, P. Kienle, and G. C. Morrison

The $^{102, 104}$Ru(d, p) reactions in isotopically enriched targets were studied at a bombarding energy of 14 MeV with a broad-range magnetic spectrograph. The Q values of the ground-state transitions were determined to be 4.005 ± 0.015 MeV for ^{102}Ru and 3.663 ± 0.015 MeV for ^{104}Ru. Angular distributions (Fig. 21) were obtained for the levels below 1 MeV excitation energy (12 levels in ^{103}Ru and 17 levels in ^{105}Ru). The ground-state transitions were both $\ell = 2$. There is a low-lying $\frac{1}{2}^+$ state at 0.170 MeV in ^{103}Ru and at 0.140 MeV in ^{105}Ru. Spectroscopic factors and ℓ values for these and the other levels have been determined. The sum of the spectroscopic factors for the $\ell = 4$ transitions indicates that the $g_{7/2}$

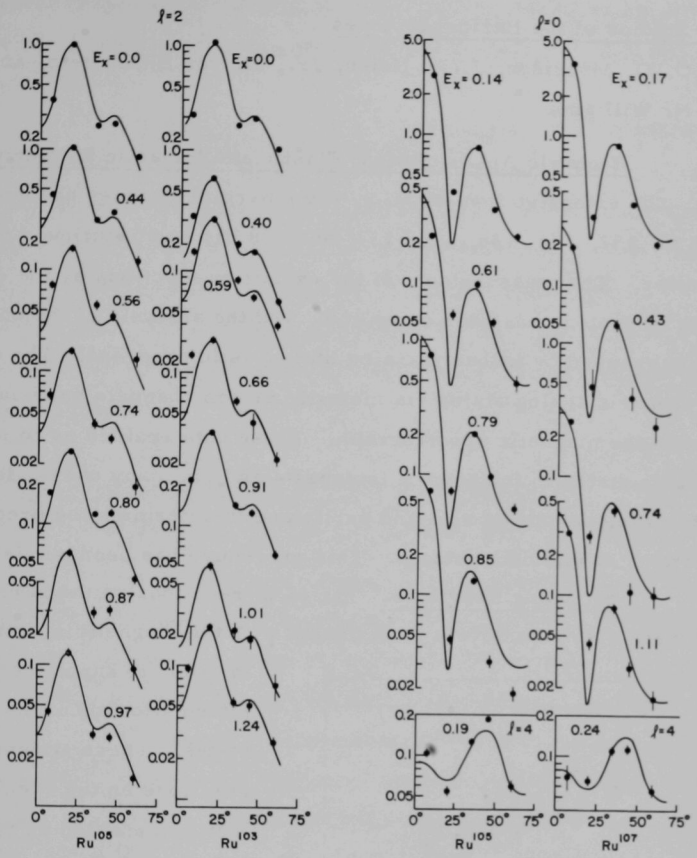

Fig. 21. Angular distributions from the (d, p) reaction on ^{102}Ru and ^{104}Ru. The curves are local, zero-range DWBA calculations.

state seems to be almost empty in both isotopes. This agrees with and extends the trend Cohen et al.[1] observed for nuclei near A = 110.

---

[1] B. L. Cohen (private communication).

(vi) Studies of the Barium Isotopes

G. C. Morrison, J. A. Nolen, Jr., D. von Ehrenstein, and N. Williams

Isobaric Analog States; Elastic and Inelastic Scattering of Protons. The extensive investigation of the barium isotopes of mass number 130, 132, 134, 135, 136, 137, and 138 has been continued during the past year. The measurement of the excitation functions by the elastic scattering of protons has been completed, and the analysis of the observed resonances (caused by isobaric analog states) is in progress. The decay of these isobaric analog states via inelastic proton channels has been studied with the magnetic spectrograph. These data enabled us to identify particle-hole states in the even-A isotopes — and, in many cases, to make reasonable assignments of spin and parity and to determine the predominant configurations of individual states. This procedure has been published.[1]

Stripping Reactions. The (d, p) reactions on the barium isotopes were also extensively investigated with the magnetic spectrograph in order to supplement the information about the analog states. These stripping reactions on the even-A isotopes enabled us to determine the energies, spins, parities, and spectroscopic factors of many previously unknown levels, among which are the parents of the isobaric analog resonances observed in the proton scattering.

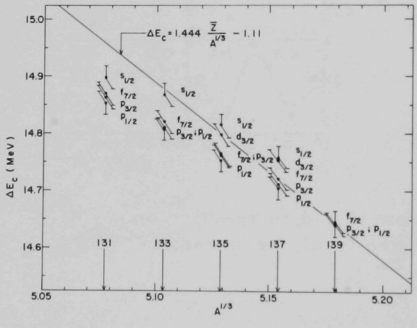

Fig. 22. Coulomb-energy differences ΔE_c for various La-Ba isobaric pairs. These differences (MeV) were computed from the expression

$$\Delta E_c = E_p(\text{c.m.}) + Q_{d,p} + 2.226 \text{ MeV},$$

where E_p(c.m.) and $Q_{d,p}$ are the values obtained in the present experiments.

[1] G. C. Morrison, J. A. Nolen, Jr., D. von Ehrenstein, and N. Williams, Phys. Rev. Letters 19, 592 (1967).

Coulomb displacement energies (Fig. 22) for odd-mass La-Ba pairs have been computed for the strong levels seen in the (d, p) and (p, p) reactions.

Inelastic Scattering of Deuterons. To complement these (p, p), (p, p') and (d, p) data, which are discussed in terms of the shell model, we have gathered data on the (d, d') reactions on the even-A barium isotopes. These reactions predominantly populate collective 2^+ and 3^- states, which are easily identified by their angular distributions. The collective properties of these isotopes are demonstrated to depend markedly on the neutron number because of the shell closure at ^{138}Ba.

(vii) (^{3}He, d) Reactions on Rare Earth Nuclei

J. R. Erskine, A. M. Friedman,* and B. Zeidman

A preliminary investigation of the feasibility of extracting spectroscopic information on proton levels of rare earth nuclei was carried out at the FN tandem. The 24-MeV ^{3}He beam was used to initiate (^{3}He, d) reactions. Higher energies would have been more desirable, but the Bρ limitations of the Browne-Buechner spectrograph limited the maximum energy. Additional data will be obtained when the split-pole magnetic spectrograph becomes operational.

(viii) Study of Actinide Nuclei with Charged-Particle Reactions

T. H. Braid, J. R. Erskine, and A. M. Friedman*

We have extended this investigation to include new targets and studies of our old odd-A targets at the higher bombarding energies of the new FN tandem accelerator. Most of the effort on this

---

*Chemistry Division.

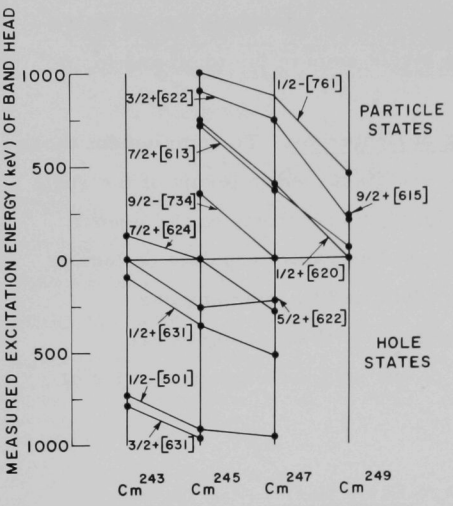

Fig. 23. A summary of the energies of 1-quasiparticle states found in the present investigation of the curium isotopes. The crossing of the $\frac{5}{2}+[622]$ and $\frac{7}{2}+[624]$ states at ^{247}Cm is rather unusual; it may result from some local peculiarity of the deformed potential felt by the nucleons.

project has gone into data analysis. Our results for the four curium isotopes ^{243}Cm, ^{245}Cm, ^{247}Cm, and ^{249}Cm are summarized in Fig. 23, which shows the measured energies of 1-quasiparticle states. These data were derived from spectra of the kind shown in Fig. 24, which presents the spectra of (d, p) and (d,t) reactions leading to ^{245}Cm.

e. Nuclear Reaction Mechanisms

(i) Optical-Model Analysis of Proton Elastic Scattering from Boron and Beryllium

R. E. Segel, B. A. Watson, and P. P. Singh†

We have found an optical-model potential that fits the 10—20-MeV range of the recently obtained elastic-scattering data on ^{10}B as well as the published data on elastic scattering on ^{9}Be and ^{11}Be. The real-potential and radius parameters are those used for heavy nuclei. The other parameters depended on energy and (N - Z)/A. The model

†Indiana University, Bloomington, Indiana.

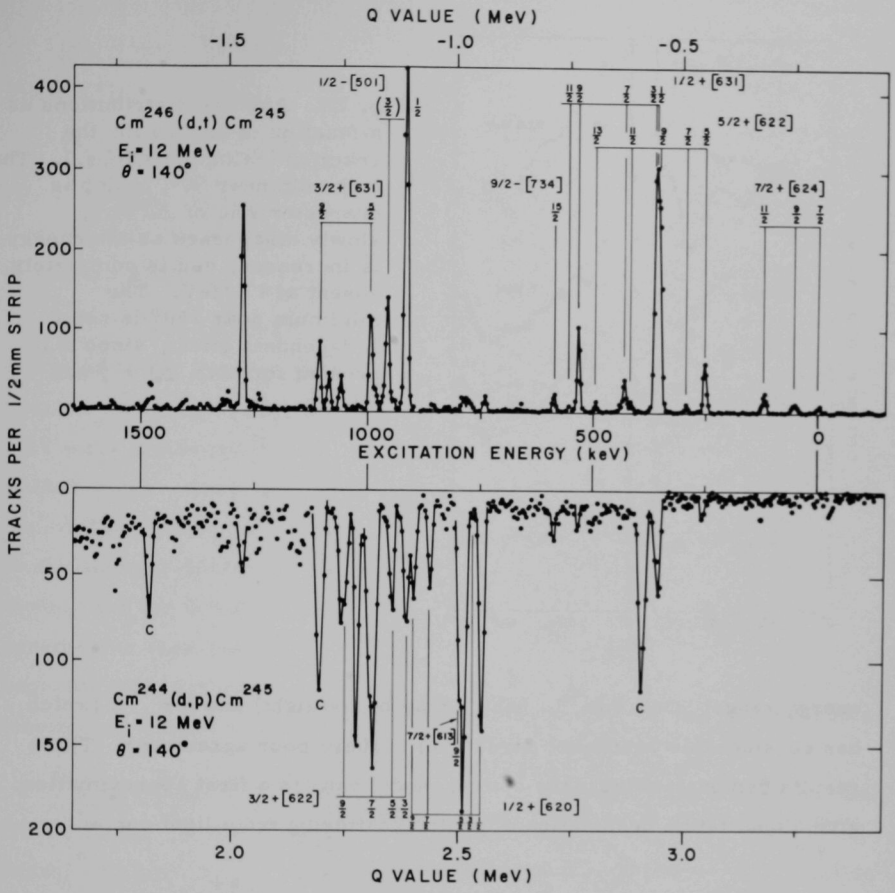

Fig. 24. Proton and triton spectra from (d, p) and (d, t) reactions leading to final states in ^{245}Cm. The energy scales of the two reactions are adjusted so that the same energy levels are adjacent to each other. The various rotational bands are indicated. Particle states are most strongly excited in the (d, p) reaction and hole states in the (d, t).

predictions with this set of parameters gave good fits for ^{9}Be, ^{10}Be, and ^{11}Be for proton bombarding energies between 10 and 20 MeV. Below this energy the general trends of the data with respect to mass and energy were reproduced, although the quality of the fits was poor. This same set of parameters fits published elastic-scattering data on ^{14}N and ^{13}C in this

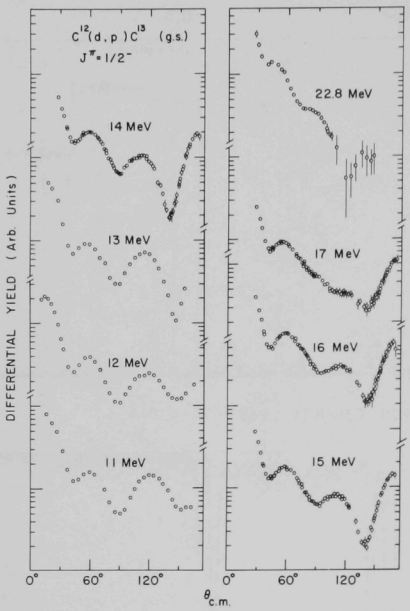

Fig. 25. Angular distributions as a function of energy for the reaction $^{12}C(d,p)^{13}C(g.s.)$. The large dip near 90°, which is characteristic of $\Delta J = \frac{1}{2}$, slowly disappears as the energy is increased, and is completely absent at 17 MeV. The minimum near 150° is not a J-dependent effect, since it is present for both $\Delta J = \frac{1}{2}$ and $\Delta J = \frac{3}{2}$.

energy range. Only for ^{6}Li (which may be too light) and for ^{12}C (which has considerable resonance structure) is there poor agreement. These results demonstrate that the optical model can, to a first approximation, give a qualitative description of proton scattering from light nuclei.

(ii) Energy Variation of the J Dependence in the $^{12}C(d,p)$ Reaction

H. T. Fortune, R. C. Bearse, J. L. Yntema, and H. Ohnuma

The J dependence in $\ell = 1$ stripping angular distributions[1] from ^{12}C has been investigated in the energy range $E_d = 9.6—17$ MeV and at 23 MeV. Preliminary results (Figs. 25 and 26) indicate a correlation between the magnitude of the J dependence and the magnitude of the "direct" contribution to the reaction mechanism.

---

[1] J. P. Schiffer, G. C. Morrison, R. H. Siemssen, and B. Zeidman, Phys. Rev. 164, 1274 (1967) and references therein.

(iii) Elastic Scattering of Alpha Particles

$^{44}Ca(\alpha, \alpha)^{44}Ca$

(P. P. Singh,* J. J. Kroepfl,* D. W. Devins,* and A. J. Elwyn).

The angular distributions in the range E_α = 11.8—13.8 MeV were measured in 40-keV steps. They are well accounted for by the smooth-cutoff model, and the cutoff parameters show the expected behavior as a function of energy.

$^{28}Si(\alpha, \alpha)^{28}Si$

(P. P. Singh,* J. W. Smith,* R. Li,* J. J. Kroepfl,* and A. J. Elwyn).

A phase-shift analysis of the differential cross sections in the range E_α = 10—12 MeV, measured in 40-keV steps, has revealed resonance structures 140 keV

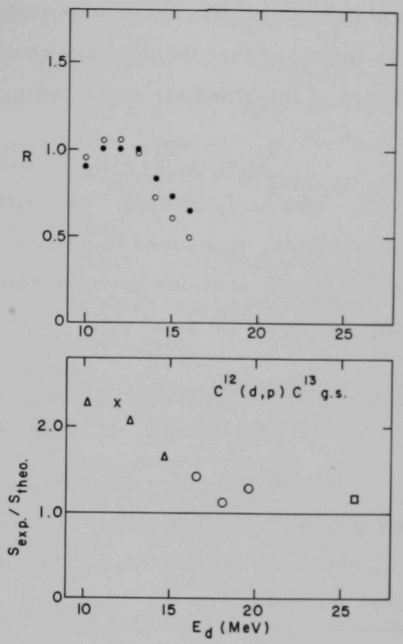

Fig. 26. Energy dependences of the spectroscopic factor (bottom) and the magnitude of the J-dependent dip (top) for the reaction $^{12}C(d, p)^{13}C$ (g. s.). The ratio of the experimental to the theoretical spectroscopic factor is from Ref. 1. In the upper figure, the filled circles represent values of R calculated from the relation

$$R = \frac{\frac{1}{2}(\sigma_{Lmax} + \sigma_{Rmax}) - \sigma_{min}}{\frac{1}{2}[\frac{1}{2}(\sigma_{Lmax} + \sigma_{Rmax})] - \sigma_{min}}$$

while the open circles represent values from

$$R = \left(\frac{(\sigma_{Lmax} - \sigma_{min})(\sigma_{Rmax} - \sigma_{min})}{[\frac{1}{2}(\sigma_{Lmax} + \sigma_{min})][\frac{1}{2}(\sigma_{Rmax} + \sigma_{min})]} \right)^{\frac{1}{2}}.$$

*Indiana University, Bloomington, Indiana.

wide and primarily with spins and parities of 1^-, 3^-, and 5^-. Statistical analysis indicates that the data are consistent with the existence of resonances of intermediate width and give a coherence width of 50 keV.

^{30}Si(α, α)^{30}Si (P. P. Singh,* R. N. Verma,* D. J. Plummer,* and A. J. Elwyn). The data in the energy range E_α = 10—13 MeV, measured in 40-keV steps, are being analyzed. The differential cross sections have the same general features as those from the ^{28}Si(α, α)^{28}Si reaction.

(iv) Inelastic Proton Scattering in the 1f-2p Shell

J. C. Legg† and J. L. Yntema

Preliminary measurements of the inelastic scattering of 14-MeV protons by odd-A nuclei in the 1f-2p shell have been made. Of particular interest are the angular distributions of protons inelastically scattered from the $\frac{1}{2}^-$ and $\frac{3}{2}^-$ levels.

*Indiana University, Bloomington, Indiana.

†Kansas State University, Manhattan, Kansas.

f. Studies of Isobaric Analog States

(i) Gamma Decay of the Two Lowest T = $\frac{3}{2}$ States in ^{25}Al

G. C. Morrison, D. Youngblood, R. C. Bearse, and R. E. Segel

We have previously shown[1] how proton capture can be a good method for locating low-lying T = $\frac{3}{2}$ states in T_z = $-\frac{1}{2}$ nuclei. Such states may stand out in proton-capture yield curves since the gamma decay to the lower T = $\frac{1}{2}$ states is not forbidden, and in fact, can be especially strong because of the simple configurations that are characteristic of low-lying analog states. Proton capture to these states

[1]D. Youngblood, G. C. Morrison, and R. E. Segel, Phys. Letters 22, 625 (1966).

by a T = 0 target is, of course, T forbidden. Consequently, the states will be much narrower than their $T_<$ neighbors but, unless isotopic-spin conservation inhibits the protons by a factor greater than about 10^4, the area under a capture resonance will still be proportional to the radiation width. Thus, one seeks strong, narrow capture resonances; and such were indeed found for the lowest T = $\frac{3}{2}$ state in ^{29}P.

Since the positron activity of ^{25}Al was counted (between bursts of a mechanically chopped beam), the yield curve for the ^{24}Mg(p, γ) reaction represents the sum of the transitions to the five bound states in ^{25}Al. The two strong, narrow (< 3.5 keV wide) resonances represent ^{25}Al states at 7.916 ± 0.012 and 7.985 ± 0.012 MeV. A 700-keV interval was searched and no other strong resonances were found. These are the two lowest T = $\frac{3}{2}$ states in ^{25}Al. Their integrated yields $(J+\frac{1}{2})\times \Gamma_p \Gamma_\gamma / \Gamma$, approximate 1.0 and 1.5 eV, respectively. In ^{25}Na, their analogs are separated by 90 keV.

Gamma-ray spectra were taken on the two resonances with a lithium-drifted germanium detector. Spectra were also taken off-resonance, where no strong lines were seen. Figure 27 shows the branching ratios for the observed transitions. The decay of the lower state is consistent with the $\frac{5}{2}^+$ expected from the ^{25}Na analog. The decay of the upper state indicates that $\frac{3}{2}^+$ is the most likely assignment. The γ-ray transition probabilities are well explained by a rotational picture in which the K = $\frac{3}{2}$ band predominates for the low T = $\frac{3}{2}$ states.

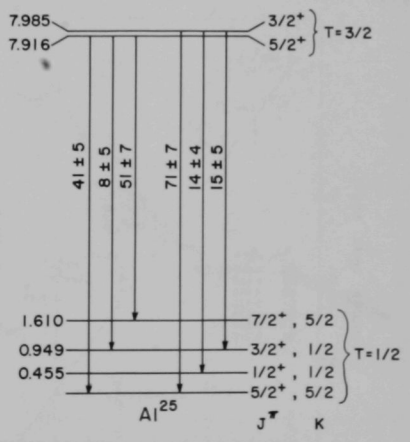

Fig. 27. Energy level diagram showing the γ-ray decay of the two lowest T = $\frac{3}{2}$ states in ^{25}Al.

(ii) Coulomb Displacement Energies of the Nickel Isotopes

J. A. Nolen, Jr., J. P. Schiffer, N. Williams, and G. C. Morrison

The ground-state Coulomb displacement energies of the Ni-Cu isobaric pairs of mass 58, 59, 60, 61, 62, 64, and 66 have been measured to ±15 keV by the (^{3}He, p), (^{3}He, d), and (^{3}He, t) reactions at the Argonne tandem Van de Graaff and magnetic spectrograph. The Coulomb shifts for ^{59}Ni and ^{61}Ni were obtained with the (^{3}He, d) reaction—those for ^{58}Ni and ^{66}Ni with (^{3}He, t) and (^{3}He, p), respectively. Both (^{3}He, p) and (^{3}He, t) reactions were used to determine the shifts in ^{60}Ni and ^{64}Ni, and all three reactions were used in the determination for ^{62}Ni. The data (Fig. 28) have been analyzed to extract neutron well radii as was done for the calcium isotopes, but with configuration mixing and antisymmetrization effects taken into account.

(iii) Isobaric Analog States in ^{97}Nb

N. Williams, G. C. Morrison, and C. F. Moore*

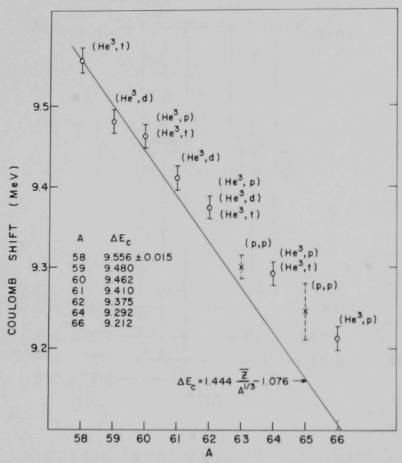

Fig. 28. Experimental ground-state Coulomb shifts in the Ni-Cu isotopes.

Elastic and inelastic proton scattering on ^{96}Zr have been studied with both the University of Texas and Argonne tandem Van de Graaff accelerators. The elastic-scattering excitation functions (Fig. 29) at several angles, along with level systematics, have enabled us to determine the spins and parities of some previously unobserved isobaric-analog resonances.

*University of Texas, Austin, Texas.

The strong inelastic scattering to the low-lying 2^+ and 3^- states has yielded information about the nature of both these and the intermediate analog states. The reactions $^{96}Zr(d, p)$ and $^{96}Zr(\alpha, \alpha')$ are being employed to investigate the parent analogs and the residual states.

Less extensive experiments on the other Zr isotopes have been performed and several trends are being investigated, including the consequences of the weak-coupling excited-core model.

(iv) The Neutron Radius of ^{208}Pb

J. A. Nolen, Jr., J. P. Schiffer, and N. Williams

The wave function of the analog state of a nucleus such as ^{208}Pb is given by operating with the T_- operator on the ground state of ^{208}Pb. In this process one of the excess neutrons in the target is replaced by a proton with the same quantum numbers (except T_z). The corresponding Coulomb displacement energy ΔE_c is then given by the Coulomb interaction between one proton and the charge distribution of the parent nucleus. We assume that the radial distribution of the proton in the analog state is the same as that of the neutron excess in the parent. With ΔE_c and the parameters of the charge distribution measured experimentally, the radius of the neutron excess can be determined. We have calculated the direct and exchange contributions to ΔE_c for ^{208}Pb. (The exchange contribution is about -3%.) The preliminary result is that the rms radius of the neutron excess of ^{208}Pb is on the order of 0.1 ± 0.1 F larger than that of the proton distribution.

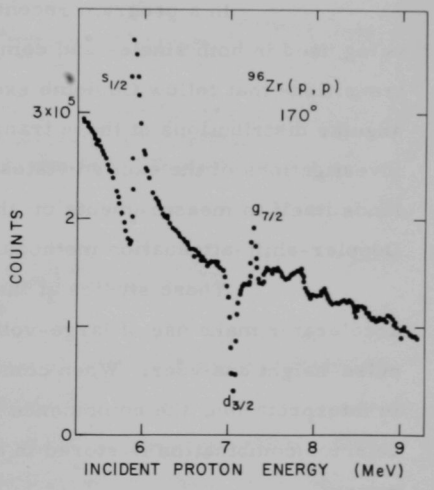

Fig. 29. $^{96}Zr(p, p)$ elastic scattering at 170°. Three prominent isobaric analog resonances are shown.

g. Coulomb Excitation: Investigation of the Excited States of ^{103}Rh and ^{105}Pd

H. H. Bolotin, D. A. McClure, and B. Zeidman

The Coulomb excitation process has proved to be a powerful technique with which to establish detailed parameters of excited nuclear levels and of radiative transitions proceeding between states. Until quite recently, NaI(Tl) detectors have provided the bulk of the experimental spectroscopic information in this field. However, except in special and relatively simple cases, the energy resolution and sensitivity of these scintillators were not high enough for the study of most states populated by Coulomb excitation. The much higher resolution obtainiable with Ge(Li) detectors makes many more levels accessible to study by Coulomb excitation. Studies of the depopulation of levels reached by Coulomb excitation can be used to determine B(E2), and in addition can yield detailed information on the lower excited states and the transitions between them.

In a program recently initiated, Ge(Li) detectors are being used in both singles and coincidence spectroscopic studies of the transitions that follow Coulomb excitation, and in measurements of the angular distributions of these transitions. In addition to these investigations of the excited states of stable nuclei, Coulomb excitation lends itself to measurements of the lifetimes of excited states by Doppler-shift-attenuation methods.

These studies at the Argonne tandem Van de Graaff accelerator make use of large-volume Ge(Li) detectors and a 4096-channel pulse-height analyzer. When coincidence studies are required as an aid in interpretation, the coincidence information from a Ge(Li)-NaI(Tl) detector combination is stored in a 1024 × 4096-channel two-parameter matrix.

Coulomb-excitation studies of the characteristics of the excited states of ^{105}Pd have been initiated to test various applicable nuclear models and the suggestions that some of the excited states of nuclei with A ≈ 100 are rotational in character. Preliminary analyses of these experiments have demonstrated the population of states not reported in previous studies. A total of ten excited states have been observed to be Coulomb excited, and their yields have been found to be consistent with E2 excitation. Figure 30 displays a typical thick-target yield of the de-excitation γ rays observed in a bombardment with 7.2-MeV alpha particles. To establish additional information concerning the spins of these states and the characteristics of the transitions issuing from them, the angular distributions of the transitions depopulating these states will be studied.

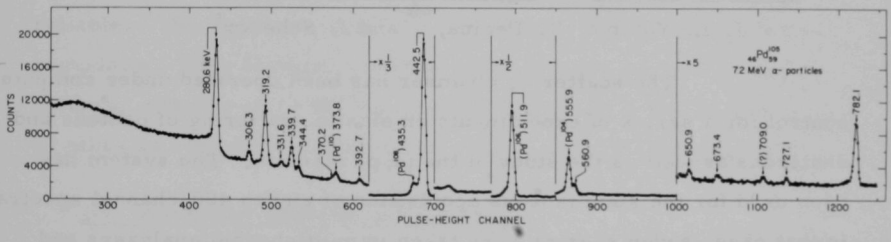

Fig. 30. Typical spectrum of de-excitation γ rays following Coulomb excitation in a thick ^{105}Pd target bombarded with α particles. All energies are in keV. Contributions from other Pd isotopes are so labeled.

h. Lifetime Measurements by Direct Electronic Methods

R. E. Holland and F. J. Lynch

Measurements of lifetimes of low-lying nuclear levels in ^{47}V and ^{48}V have been begun. Because several levels of nearly the same energy are excited in these cases, one needs the excellent energy resolution available with lithium-drifted germanium detectors. However, the time resolution of such detectors at present severely limits the accuracy of the lifetime measurement. By combining these data with those from NaI detectors, we expect to obtain values of the lifetimes.

i. Development of Instrumentation at the Tandem

(i) High-Resolution Charged-Particle Spectroscopy with Silicon Surface-Barrier Detectors

E. Klema* and J. A. Nolen, Jr.

High-resistivity silicon surface-barrier detectors 3—5 mm deep have been fabricated at Northwestern and tested at the Argonne tandem Van de Graaff. Used in conjunction with a commercial transmission-type detector in a detector telescope, these detectors have yielded energy spectra with over-all resolution width as small as 25 keV for 20-MeV protons. These detectors are currently being used in (α, p) experiments with the 25-MeV negative ^{4}He beam.

(ii) Automation of the 60-in. Scattering Chamber

J. L. Yntema, R. Pecina,** and J. Scherer†

The scattering chamber has been operated under computer control for a series of experiments on elastic scattering of protons and deuterons as well as the study of the (d, p) reaction. The system has been used for the simultaneous acquisition of eleven 400-channel spectra. In that case, seven spectra were taken in multichannel analyzers and four were accumulated in the external memory associated with the ASI-210 computer. The analyzers are stopped by the computer and memories are dumped into the computer memory at the end of the run. The data are then transferred onto magnetic tape and printed on the line printer. The computer then clears the memory of the analyzers. The use of the external memory will be expanded when a more flexible system of ADC's is acquired.

---

*Northwestern University, Evanston, Illinois.

**Electronics Division

†Applied Mathematics Division.

(iii) New Split-Pole Magnetic Spectrograph

J. R. Erskine and M. Macháłek

An Enge split-pole spectrograph is being installed at the tandem Van de Graaff accelerator. The assembled magnet and carriage system are being purchased from the Scanditronix Co. The camera system (including plate holders), the target chamber, and vacuum systems are being designed and built by Argonne personnel. The plate-holder system is intended to give greater reproducibility and flexibility of operation than previous camera systems for this type of spectrographs. This increase in mechanical precision is needed to fully use the increased resolving power of the new spectrograph. The target chamber will incorporate an improved sliding seal which is expected to make operation of the target chamber simpler and more reliable. The vacuum system for the camera is designed for rapid pumpdown. This feature, together with two interchangeable plate holders, should reduce the time needed to change plates to about 10 min—as compared with about 45 min for the old spectrograph.

(iv) Automatic Plate-Scanning Machine

J. R. Erskine, R. H. Vonderohe,* M. Macháłek, and N. Sobol*

The scanning machine has reached a sufficiently advanced stage that a relatively unskilled operator can take a good-quality plate from the magnetic spectrograph and produce a satisfactory scan of the data. Improvements in the hardware and software, together with operating experience, have made this possible. With poor-quality data, a more skilled operator is needed. The machine is currently being used on a limited basis to process research data. We are acquiring a new camera tube that has two or three times the resolving power of our present system. With this refinement, we expect that

*Applied Mathematics Division

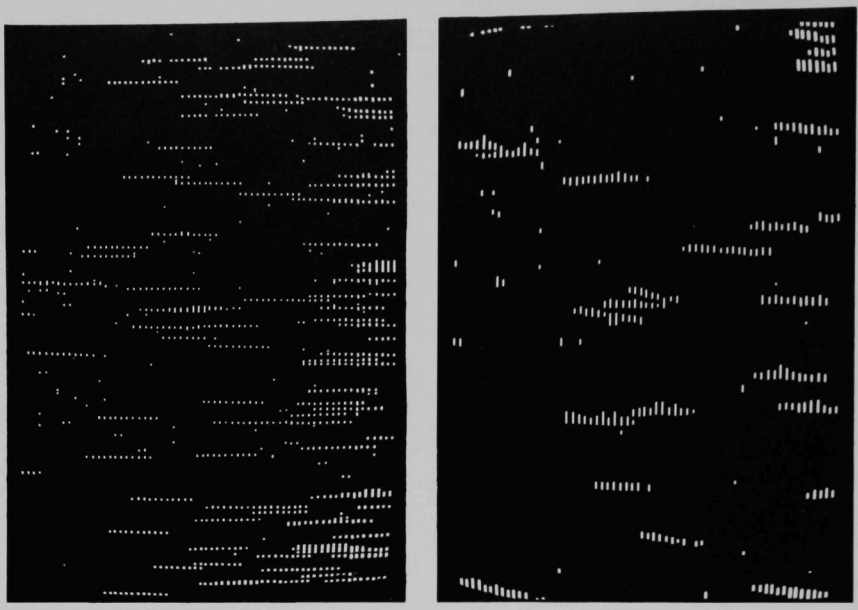

Fig. 31. Views of tracks as they appear on the display scope of the plate-scanning machine. In the figure on the right, the horizontal magnification has been increased about 10-fold; it corresponds to a region measuring 0.64 × 5 mm in the emulsion. In the center of this view, a group of three tracks can be seen well resolved. The width of the tracks corresponds to about 7 microns in the emulsion and results primarily from aberrations in the scanning tube. The tracks are about 100 microns long. In the scanning process, the electronic sweep proceeds from left to right along lines separated by a vertical step of 10 microns. This gives the tracks the appearance of dotted lines.

less skill will be demanded of the operator.

One of the recent refinements of the system is the addition of a display scope that shows exactly what the camera tube is seeing. Typical views of tracks on this display scope are shown in Fig. 31. This information helps the operator to correctly set various parameters describing the tracks and also assists in monitoring the performance of the system while it is scanning.

(v) Processing of Nuclear Emulsions to Enhance Track Brightness for Machine Scanning

J. R. Erskine and M. D. Machálek

In order to maximize the usefulness of the automatic scanning machine [Sec. (iv)], we are continually investigating ways to consistently obtain high contrast between tracks and background in the emulsion. We have found a method (based on an Amidol development at 0°C) which produces an enhancement of about 30% over the standard D-19 procedure. We have evidence that further enhancements are achieved with this method when the emulsion fogging is due to radiation.

(vi) Construction of the Source of Polarized Ions for the Tandem Van de Graaff

D. von Ehrenstein, C. W. Schmidt, and D. C. Hess

The testing of the individual components of the polarized-ion source and the beginning of its transfer to its final location were reported last year. It is now reassembled as originally planned in a room built for it adjacent to, but separated from, the tandem vault. The general layout of the source and the beam line is shown in Fig. 32. It has been connected to the FN tandem and a first beam has been accelerated.

In the light of our earlier experience, we built and successfully tested a charge-exchange unit operating with alkali vapor. An earlier version of this vapor adder (which converts the positive ions from our ionizer into negative ions to be injected into the tandem) had been built into the (positive) ionizer unit to take advantage of the strong guide field already present there. However, this design introduced too much potassium vapor into the ionizer and hence was abandoned in favor of the present arrangement, in which the vapor region is separated from the ionizer by some distance. It features a solenoid to supply the

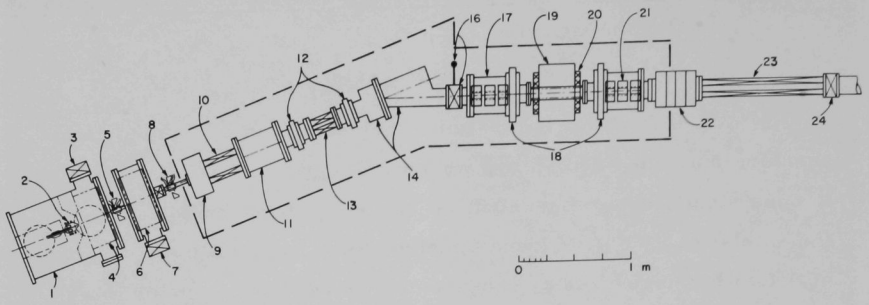

Fig. 32. Schematic diagram of the polarized-ion source (POLISO).

1. Vacuum chamber for dissociator and first 6-pole magnet.
2. Dissociator.
3. Valve to 6-in. mercury pump.
4. First 6-pole magnet.
5. First transition assembly. The vacuum chamber here is a Teflon tube.
6. Second 6-pole magnet.
7. Valve to 6-in. mercury pump.
8. Second transition assembly. As in the first, the vacuum chamber is a Teflon tube.
9. Cathode chamber, now used for access to ionizer.
10. Solenoid surrounding the ionizer region.
11. Extraction chamber. Contains part of system to draw out ions.
12. Insulating flanges (G-10 fiberglass-filled epoxy) to permit operation of the adder at a potential different from reference ground. (See item 15).
13. Solenoid and adder unit. The furnace and valve system for controlling the density of potassium vapor is below and is not shown.
14. Chamber containing the 20° deflection magnet to separate out the desired ions from background ions such as N_2^- and to remove the un-ionized part ($\gtrsim$99.9%) of the polarized beam.
15. Corona shield (a box mode of $\frac{1}{2}$-in. Lucite) to permit operation of the enclosed portion at -60 kV so that a stiffer beam can be used. This -60 kV potential is "reference ground" for various elements in the box.
16. Ion collector used in adjusting the 20° magnet and other beam-handling devices. It is designed to collect the 1-cm-diameter central portion of the beam and, separately, the 1-cm-wide annulus surrounding this. The collector plate for the annular region is divided

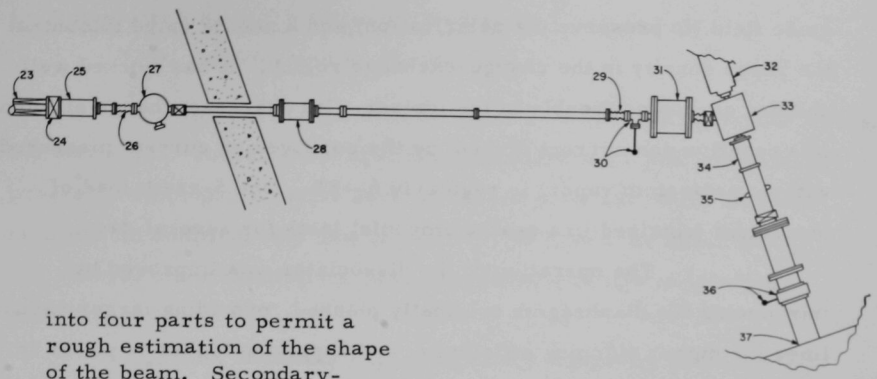

into four parts to permit a rough estimation of the shape of the beam. Secondary-electron emission is suppressed by a mesh of 0.5-mil tungsten wires spaced 1.25 mm apart and held at -67.5 V. The collector can be moved into and out of the beam by means of a mechanism operated from outside the system.

17. Chamber containing an electrostatic quadrupole triplet.
18. Insulating flanges (G-10) to allow operation of the Wien filter at a potential different from reference ground.
19. Wien filter. This allows precession of the polarization direction without deflection of the beam.
20. Coils for the Wien filter.
21. Second triplet of electrostatic quadrupoles—identical to that in 17.
22. Acceleration tube.
23. Solenoid to change the direction of polarization from horizontal to vertical.
24. Six-inch gate valve (shown in each half of the figure).
25. Chamber containing an electrostatic quadrupole doublet.
26. Metal bellows.
27. Chamber which may house a beam-switching mirror (whose repelling electrode will be a high-transmission grid) to deflect the beam into a DT reactor to measure the polarization of deuterium.
28. Electrostatic quadrupole doublet.
29. Bellows.
30. Ion collector identical to 16.
31. Electrostatic quadrupole triplet.
32. Output of the usual tandem ion source.
33. Chamber for electrostatic mirror that deflects the beam into the tandem. This mirror can be moved out of the beam line for normal operation of the tandem.
34. Electrostatic doublet.
35. Einzel lens, part of the normal tandem facilities.
36. Beam detector, same as 16.
37. Entrance to the accelerating tube of the tandem. The usual beam-steering plates are in this region.

guide field (to preserve the polarization) and a needle valve to control the vapor density in the charge-exchange region. It has worked well and has caused no trouble in the ionizer. Its charge-exchange efficiency (the negative-ion current divided by the positive-ion current measured with no potassium vapor) is regularly 6—8%. One 5-gram load of potassium (obtained in a sealed ampoule) lasts for several days.

The operation of the dissociator was improved by introducing the diaphragms originally planned, providing larger vacuum lines for higher pumping efficiency, and supplying higher rf power in the discharge region.

Where the beam emerges from the 20° mass-analyzing magnet at the output end of our ion source proper, we have observed H^- ion currents up to 25 nA.

Along the 50-ft beam path from the 20° magnet to the injection end of the tandem, the beam traverses spin-turning devices (the Wien filter and solenoid), focusing elements (quadrupoles and einzel lenses), and an electrostatic mirror that deflects the beam through 70°. This beam line, including all its elements, was assembled and successfully tested during the past year. In addition part of the source (ionizer, potassium-adder, 20° magnet, Wien filter, and quadrupoles) has been insulated for high potential in order to obtain a more energetic beam for transmission through the rest of the beam line and for injection into the tandem. (Without this high-voltage insulation, a beam of only 24 keV could be obtained and the resulting current was only 0.18 nA at the Faraday cup after acceleration in the tandem.) With this installation partially completed, a negative hydrogen-ion beam of 60 keV could be achieved. Its over-all transmission through the beam line to the low-energy end of the tandem was around 60%; and after acceleration through the tandem, a current of 3 nA has been observed at the Faraday cup at the output of the tandem. (During this test the output of the ion source was around 10 nA.)

j. University Use of the Argonne Tandem

J. P. Schiffer and F. P. Mooring

Interest in the outside-users program has increased during the last year. Though several universities no longer participate in the program, other participants have increased their use of the Tandem facility. In addition, one new university has joined the users group and several other institutions have expressed a desire to join the program.

The following experiments are currently active at the Tandem.

(a) Multiple Coulomb Excitation and Reorientation Effect

R. P. Scharenberg, J.W. Tippie, G. Schilling, D. Grissmer, R. Beyer, and W. Lutz

Purdue University, West Lafayette, Indiana

(b) Studies of Energy Levels in Light Nuclei

C. P. Browne, W. D. Callender, G. Marolt, J. Duray, E. Berkowitz, A. Rollefson, and J. Sobol

Notre Dame University, South Bend, Indiana

(c) Scattering of Alpha Particles

P. P. Singh, B. A. Watson, J. Smith, A. Sauter, J. Kroepfl, R. Li, R. Verma, T. Marvin, and T. Hall

Indiana University, Bloomington, Indiana

(d) J Dependence of Inelastic Scattering

J. Legg

Kansas State University, Manhattan, Kansas

(e) Investigation of States in ^{42}K by the $^{41}K(d, p)^{42}K$ Reaction

R. T. Carpenter and R. A. Mendelson, Jr.

University of Iowa, Iowa City, Iowa

(f) Investigation of the $^{31}P(^{3}He, p)^{33}S$ Reaction

Richard W. West, Richard S. Cox, and William A. Dobra

University of Kansas, Lawrence, Kansas

D. RESEARCH AT THE 60-in. CYCLOTRON

The 60-in. cyclotron is one of the low-energy accelerators operated by the Chemistry Division. The beam energies are 46.5 MeV for α particles, 36 MeV for ^{3}He, 23 MeV for deuterons, and 11.5 MeV for protons. These values are the maximum possible with the components currently in use.

The beam-handling equipment currently consists of a beam squeezer, three sets of quadrupole lenses, and two sets of left-right and up-down deflection magnets. A switching magnet permits the use of five different experimental stations. The energy of the incident particles can be lowered by use of a remotely-controlled foil changer at the focal point of the first set of quadrupole lenses.

A beam-analyzing magnet system provides a resolution width of 0.1% or less. In order to utilize the analyzed beam to the maximum extent, a split-pole magnetic spectrograph of the Enge type has been ordered. Delivery is expected in 1968.

The cyclotron is in operation approximately 80 hours per week. On the average, the Physics Division uses 25—30% of the time.

a. Improvement of the 60-in. Scattering Chamber at the Cyclotron

J. L. Yntema

Preliminary sketches for redesign of the scattering chamber to permit automated control have been made. The data-handling system has been converted so that the readouts from both the Packard and the Victoreen 400-channel analyzers and the 4096-channel Packard analyzer are on computer-compatible magnetic tape.

b. Study of the ^{23}Na(^{3}He, d)^{24}Mg Reaction

R. C. Bearse and J. L. Yntema

The ^{23}Na(^{3}He, d)^{24}Mg reaction, initiated by the 35-MeV ^{3}He beam of the Argonne cyclotron, has been investigated by use of an E-dE/dx particle-identification system. The dE detector had a depletion

depth of 2mm; the 3-mm thickness of the E detector was obtained by combining two detectors with depletion depths of 1 mm and 2mm and adding their outputs. Targets of metallic sodium evaporated onto carbon backings were transferred to the scattering chamber via vacuum locks. The groups feeding the ground state and the first, fourth, fifth, and sixth excited states were resolved, but the second and third excited states and all higher than the sixth were not. The ground-state group is extremely weak and the group leading to the sixth excited state is even weaker. The angular distribution of each of these groups (Fig. 33) was taken in 2° steps for the angular range 11°—35°. All the strong groups show characteristic $\ell = 2$ angular distributions. The shapes of the angular distributions of weakly excited states are not those characteristic of direct reactions.

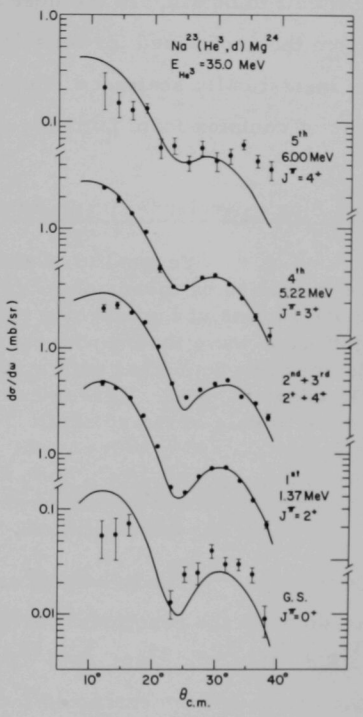

Fig. 33. Angular distributions extracted from the data. The solid lines are the predictions of the code JULIE for a pure $\ell = 2$ transition.

c. The $^{26}Mg(^3He, ^3He)^{26}Mg$ Reaction

J. L. Yntema and D. Dehnhard*

The angular distributions from 20° to 80° have been obtained for eight states. The analysis of the elastic scattering by means of a six-parameter search shows that a satisfactory fit to backward angles is

*University of Minnesota, Minneapolis, Minnesota.

difficult to obtain. In the best fits, the parameters differ drastically from those obtained for less deformed nuclei. The angular distributions of inelastically scattered ^{3}He particles have been fitted successfully by use of complex form factors.

d. Single-Nucleon-Pickup Reactions in the 2s-1d Shell

Several (d, t) and (d,^{3}He) reactions in the sd shell have been studied by means of (dE/dx)-E counter arrangements. The angular distributions of the outgoing particles have been analyzed in terms of distorted-wave theory with the JULIE code, and the spectroscopic factors are compared with a recent shell-model calculation by Glaudemans et al. Agreement is found for low-lying states of nuclei in the middle of the sd shell.

(i) Proton Hole States in ^{29}Al, ^{31}P, and ^{33}P

R. C. Bearse, D. H. Youngblood, and J. L. Yntema

The low-lying states in ^{29}Al, ^{31}P, and ^{33}P have been studied via the reactions ^{30}Si(d, ^{3}He)^{29}Al, ^{26}Mg(α, p)^{29}Al, ^{32}S(d, ^{3}He)^{31}P, ^{34}S(d, ^{3}He)^{33}P, and ^{30}Si(α, p)^{33}P. Spectroscopic factors have been extracted for the (d, ^{3}He) reactions leading to two final states in ^{29}Al, three in ^{31}P, and two in ^{33}P. In the ^{30}Si(d, ^{3}He)^{29}Al reaction, we observed $\ell = 2$ and $\ell = 0$ angular distributions from reactions leading to the ground state and first excited state, respectively. For the ^{34}S(d, ^{3}He)^{33}P reaction, we obtained an $\ell = 0$ distribution for the reaction to the ground state and an $\ell = 2$ distribution for the one to the second excited state.

(ii) Energy Levels of ^{36}S and ^{34}S from (d, ^{3}He) Reactions on ^{37}Cl and ^{35}Cl

N. G. Puttaswamy and J. L. Yntema

The excitation energies (MeV) and (in parentheses) the dominant ℓ value for proton pickup, the spin-parity J^π, and the

spectroscopic factor S in ^{36}S are:
0.0 (ℓ = 2, 0^+, S = 1.3),
3.31 (ℓ = 0, 2^+, S = 1.2), and
4.58 (ℓ = 0, 1^+ or 2^+, S = 1.4)
(Fig. 34); and in ^{34}S:
0.0 (ℓ = 2, 0^+, S = 1.0),
2.12 (ℓ = 0, 2^+, S = 0.3),
3.31 (ℓ = 0, 2^+, S = 1.0), and
4.09 (ℓ = 0, 1^+ or 2^+, S = 0.7).
In the above analysis, the results of (t, p) reactions on ^{34}S and ^{32}S have been used whenever a 2^+ assignment is made for an ℓ = 0 pickup. The states at 4.58 MeV in ^{36}S and 4.09 MeV in ^{34}S may be the 1^+ states predicted at 5.75 and 4.97 MeV, respectively, from shell-model calculations.

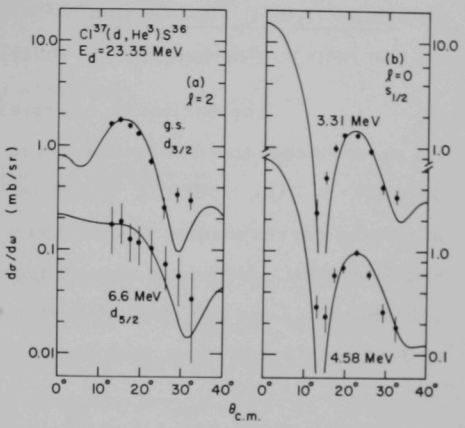

Fig. 34. Angular distributions of ^{3}He particles from the ^{37}Cl(d, ^{3}He)^{36}S reaction. The curves are DWBA predictions.

(iii) (d, t) Reactions on ^{37}Cl and ^{35}Cl

N. G. Puttaswamy and J. L. Yntema

Observation of tritons leading to all known levels below 2.38 MeV in ^{34}Cl indicates that they are all positive-parity states. The excitation energies (MeV) of the ^{36}Cl states and (in parentheses) the spectroscopic factors S_ℓ corresponding to the ℓ value of the neutron pickup are: 0.0 (S_2 = 1.0), 0.79 (S_2 = 1.4), 1.16 (S_0 = 0.03 and S_2 = 0.3), 1.60 (S_0 = 0.05 and S_2 = 0.3), 1.95 (S_0 = 0.1 and S_2 = 0.4), and 2.50 (S_0 = 0.1 and S_2 = 0.4). The values of S_0 and S_2 for the latter four states are uncertain by a factor of 2. There is evidence for two groups of tritons corresponding to excitation energies of 2.68 and 2.85 MeV in ^{36}Cl. The ℓ values are consistent with known spins for the states in ^{36}Cl.

(iv) $^{39}K(d, t)^{38}K$ Reaction

H. T. Fortune, N. G. Puttaswamy, and J. L. Yntema

The excitation energies (MeV) of the states in ^{38}K and (in parentheses) the dominant ℓ value for neutron pickup are: 0.0 (2), 0.46 (0), 1.7 (2), 2.41 (2), and 3.44 (0). We have found weak groups of tritons corresponding to excitation energies of 0.13, 2.64, 4.0, and 4.66 MeV. Previous results from the (^{3}He, α) reaction had shown only that $\ell = 2$ for the state at 0.46 MeV. The value $\ell = 0$ for the state at 3.44 MeV leads to an assignment of 1^+ or 2^+.

(v) Proton-Hole States in ^{38}Ar and ^{40}Ar from (d, ^{3}He) Reactions on ^{39}K and ^{41}K

N. G. Puttaswamy and J. L. Yntema

The results for the (d, ^{3}He) reaction on ^{39}K are in agreement with similar work at other deuteron energies. For the (d, ^{3}He) reaction on ^{41}K, the excitation energies (MeV) of the ^{40}Ar states and (in parentheses) the dominant ℓ value for proton pickup are: 0.0 (2), 1.45 (2), 3.22 (0), 3.53 (2), 4.36 (0), and 5.20 (0). There is evidence for two weak groups of ^{3}He particles corresponding to excitation energies of 2.5 and 4.6 MeV in ^{40}Ar. An $\ell = 0$ pickup restricts the spins and parities of the 3.22-, 4.36-, and 5.20-MeV states to 1^+ or 2^+. The 3.22-MeV state has previously been thought to be 4^+; but a 2^+ assignment now seems most likely. The state at 5.20 MeV has not been observed before.

e. (d, t) and (d, ^{3}He) Reactions on the Ca Isotopes

J. L. Yntema

A number of the results from the (d, t) reaction on ^{43}Ca disagree with earlier work done elsewhere at lower energies. In particular, the transition to the second 0^+ state in ^{42}Ca is observed.

Furthermore, the ratio of the spectroscopic factors of the transitions to the first and the second 2^+ states is much greater than unity and many levels just above the 6^+ state are observed.

f. The $^{40}Ca(d, \alpha)^{38}K$ and $^{48}Ca(d, \alpha)^{46}K$ Reactions

N. G. Puttaswamy and J. L. Yntema

Angular distributions for the (d, α) reactions are being analyzed with distorted-wave calculations. Theoretical angular distributions for "deuteron" pickup and for "proton-neutron" pickup (JULIE code) are found to be very sensitive to radial cutoff. To obtain a detailed comparison with theory, we are attempting to take data over the full angular range from 0° to 180°. The (d, α) reaction on ^{48}Ca shows the presence of a new state at 3.2 MeV in ^{46}K.

g. Nuclear Structure Near Z = 40

(i) The j Dependence Observed at Small Angles in the (d, ^{3}He) Reaction

H. Ohnuma and J. L. Yntema

The (d, ^{3}He) reaction on even-mass Mo isotopes was experimentally investigated with the 23-MeV deuteron beam from the Argonne cyclotron. The targets were isotopically enriched metallic foils, and the detection system consisted of surface-barrier Si counters. Experimentally, the $\ell = 1$ angular distributions have shallower minima around 20° for all the $p_{3/2}$ transitions than for the $p_{1/2}$ transitions (Fig. 35). This difference was observed over a wide range of Q values. The DWBA calculations correctly predicted the experimental effect, which was found to be caused by the spin-orbit term in the deuteron optical potential. No significant j dependence was experimentally observed nor theoretically predicted in the (d, t) reactions on Mo isotopes.

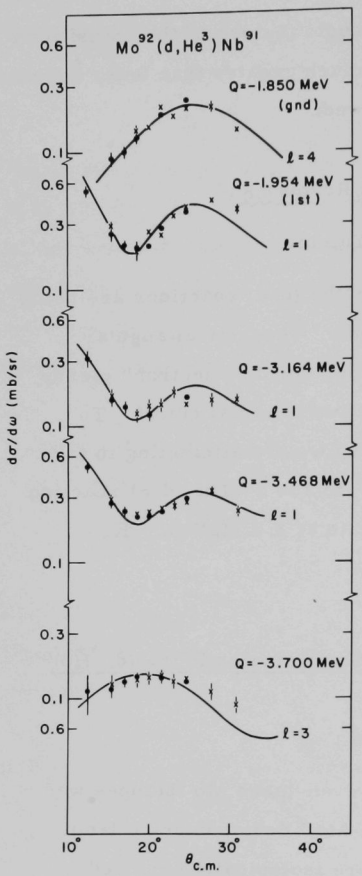

Fig. 35. The experimental angular distributions for the strong transitions in the ^{92}Mo(d,^{3}He)^{91}Nb reaction. The curves are the results of the distorted-wave calculculations. The quite pronounced difference between the depths of the minima for the ℓ = 1 transitions to the states labeled ℓ = 1 (3/2) and the corresponding depth in the curve labeled Q = -1.95 MeV has been shown to be a j-dependence effect. This permits the new assignment of spin $\frac{3}{2}$ to these states. The cross sections of the transition to the ground state is about 1.5 times the value that would be expected if the $p_{1/2}$ proton shell in ^{92}Mo were completely filled.

(ii) The (d, ^{3}He) Reaction on Mo Isotopes

H. Ohnuma and J. L. Yntema

The (d, ^{3}He) reaction on even-mass Mo isotopes was studied with the 23-MeV deuteron beam from the Argonne cyclotron. The resulting angular distributions of ^{3}He groups were compared with the DWBA calculations, and the ℓ values and spectroscopic factors of transitions were determined. Figure 35 shows the angular distributions, together with the calculated curves, for the strong transitions in the

^{92}Mo(d, ^{3}He)^{91}Nb reaction. In some cases j values were also determined on the basis of the j dependence of the ℓ = 1 angular distributions reported in Sec. (i). The results indicate that the ground-state proton configurations of even-mass Mo isotopes are approximately 65% $(p_{1/2})^2(g_{9/2})^2$ + 35% $(g_{9/2})^4$. This result agrees with the results of the ^{92}Mo(^{3}He, d) reaction and with the shell-model predictions. In contrast to the observation in the Zr isotopes, the proton configurations do not depend appreciably on neutron numbers.

(iii) The (d, t) Reaction on Mo Isotopes

H. Ohnuma and J. L. Yntema

The (d, t) reaction on even-mass Mo isotopes was studied with the 23-MeV deuteron beam from the Argonne cyclotron. The observed angular distributions of triton groups were analyzed by use of DWBA theory, and the ℓ values and spectroscopic factors of transitions were determined. In the ^{92}Mo(d, t) reaction, only three strong transitions were seen. They were assigned to be $g_{9/2}$, $p_{1/2}$, and $p_{3/2}$ neutron pickups. These assignments and the energies of these states suggest a close resemblance between the structures of ^{91}Mo and ^{89}Zr. In the heavier Mo isotopes, strong ℓ = 0 transitions as well as ℓ = 2 transitions were observed. This indicates the mixing of neutron configurations above the N = 50 closed shell.

h. Reaction Mechanisms and Structures of Light Nuclei

(i) ^{3}He-Induced Reactions in ^{12}C

H. T. Fortune and B. Zeidman

The reactions (^{3}He, d), (^{3}He, ^{3}He), (^{3}He, α), (^{3}He, t), and (^{3}He, ^{7}Be) have been investigated with the 35-MeV ^{3}He beam from the cyclotron. The last four reactions were measured simultaneously. These studies are intended to provide a clearer understanding of the optical model and of the mechanisms for the various reactions.

(ii) Single-Nucleon Transfers at N = 14

H. T. Fortune, G. C. Morrison, N. Williams, and B. Zeidman

The (d, ^{3}He), (d, t), (d, p), and (d, d') reactions on targets of ^{26}Mg, ^{27}Al, and ^{28}Si were simultaneously studied at E_d = 23.3 MeV. The purpose of the experiment is to provide a detailed comparison of spectroscopic factors at an energy at which all reactions have the identical incident channel. Where discrepancies in previous measurements had been noted, the present analysis yields a more precise determination of the vacancies in, and the filling of, the sd-shell orbitals for both protons and neutrons. The use of several targets with the same neutron number indicates the effect of the protons on the neutron orbits.

i. Elastic Scattering

T. H. Braid, T. W. Conlon,* and B. W. Ridley*

During the fall of 1967, the elastic scattering of ^{3}He and ^{4}He ions by ^{40}Ca and ^{58}Ni was studied at the Harwell Variable-Energy Cyclotron at a number of energies between 24 and 86 MeV. These data, together with data at other energies (previously reported by other experimenters, including two groups at Argonne) are being analyzed in terms of the optical model in order to study the energy dependence of the parameters of the potential. We have found that the ^{3}He scattering data are fitted very well above 30 MeV by a potential having a real depth V ≈ 175 MeV at 30 MeV and becoming ~75 keV shallower for each additional MeV of incident energy. This is a much smaller energy dependence than has been found in the elastic scattering of nucleons. Similar calculations are in progress for the α-particle data.

---

*AERE, Harwell, Berkshire, England.

The experimental work is being continued in an effort to extend the measurements of helium-ion scattering to large angles where the cross sections are very low, in the hope that such data will make possible a clearer distinction between different sets of parameters.

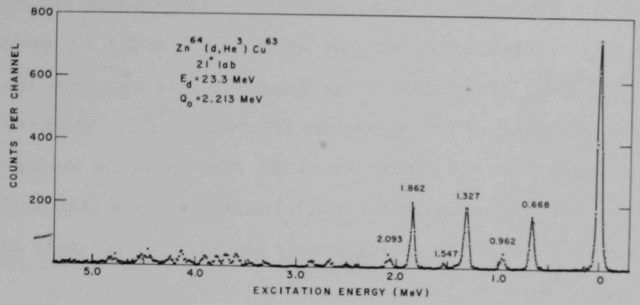

Fig. 36. The spectrum of the $^{64}Zn(d,^3He)^{63}Cu$ reaction at 21°(lab), obtained with a counter telescope mounted in the 18-in. scattering chamber at the cyclotron. The incident-deuteron energy was 23.3 MeV. Each channel is approximately 11.6 keV wide.

j. Nucleon-Transfer Reactions in fp-Shell Nuclei

(i) Proton Levels in fp-Shell Nuclei

B. Zeidman, T. H. Braid, and J. A. Nolen, Jr.

Proton levels in fp-shell nuclei have been investigated by means of the (d, ^{3}He) reaction at 23.3 MeV. Improvements in techniques now allow measurements with resolutions to 50 keV. An example of such data is shown in Fig. 36. Targets of ^{45}Sc, ^{51}V, $^{50, 52, 54}$Cr, $^{54, 56, 58}$Fe, $^{58, 60}$Ni, and $^{64, 66, 68, 70}$Zn have been bombarded and proton-hole states have been observed. There is evidence for a strong interaction between the 2p neutrons and the 2s-1d protons beyond N = 28.

(ii) $^{64, 66, 68, 70}$Zn(d, ^{3}He) Reactions at 23.3 MeV

B. Zeidman and J. A. Nolen, Jr.

The (d, ^{3}He) reactions induced by 23.3-MeV deuterons incident upon the stable even-mass Zn isotopes has been investigated.

The ^{3}He particles were detected and identified with a $\Delta E \cdot E$ counter telescope. The energy resolution width in the observed spectra was approximately 55 keV. Angular distributions were obtained over the angular range $12^{\circ} - 30^{\circ}$ for levels up to about 3 MeV excitation in the residual nuclei. Transitions between the low-lying levels all involve either $\ell = 1$ or $\ell = 3$ transfer. In this work, we find $Q = -5.60 \pm 0.03$ MeV for the ^{70}Zn(d, ^{3}He)^{69}Cu ground-state reaction; this provides the first accurate determination of the mass and levels of ^{69}Cu. We have obtained information on the structure of the odd-mass Cu isotopes from ^{59}Cu to ^{69}Cu. This allows a much more rigorous test of the various weak-coupling calculations which were originally done for the stable isotopes ^{63}Cu and ^{65}Cu.

k. Observation of Multinucleon-Transfer Reactions

J. A. Nolen, Jr., and B. Zeidman

The detection of reaction products from multinucleon-transfer reactions such as (^{3}He, ^{6}He), (^{3}He, ^{7}Be), etc. is quite difficult because the cross sections for these reactions are extremely low in comparison with that of the main reaction taking place. As a result, obscuring effects such as pile-up and reactions in the detectors produce yields comparable to the desired reactions. In order to overcome these problems, another laboratory has resorted to a multiple-counter telescope. Because of energy and range limitations, it is not possible for us to adopt this approach. Rather we are attempting to use a two-counter telescope which (in addition to the usual $\Delta E \cdot E$ information) yields the flight time between the two counters. Because of geometrical considerations and low cross sections, the flight path is limited to a few centimeters and flight times to a few nanoseconds. A timing system developed by the Electronics Division can measure these times to less than 160 psec. This device, which was developed

under the sponsorship of the Physics Division, has been reported by I. S. Sherman, R. G. Roddick, and A. J. Metz[1] of the Electronics Division. With this timing, mass identification from the time of flight will complement the particle identification from energy signals to substantially reduce background for the extremely-low-cross-section reactions.

[1]I. S. Sherman, R. G. Roddick, and A. J. Metz, IEEE Trans. Nucl. Sci. NS-15 (3), 500—508 (June 1968).

ℓ. Spectroscopy in Heavy Nuclei

(i) (^{3}He, d) Reaction on the Lead Isotopes[1]

Nelson Stein,* R. H. Siemssen,* and B. Zeidman

The (^{3}He, d) reaction on ^{206}Pb, ^{207}Pb, and ^{208}Pb has been studied with a 35-MeV beam from the Argonne cyclotron by use of a solid-state-detector particle-identification system. Angular distributions from ^{208}Pb were obtained from 20° to 100° with an energy resolution width of about 70 keV. The most prominent peaks in the spectra up to 4.5 MeV excitation in ^{209}Bi are at 0.0, 0.90, 1.61, 2.84, 3.14, 3.67, and 4.46 MeV. The first five states agree with the locations of the single-particle proton states identified from the ^{208}Pb(α, t) reaction. In particular, the state at 3.14 MeV (identified as the $3p_{3/2}$ level) is the most strongly excited state in the present experiment. This state does not appear in the previously published ^{208}Pb(^{3}He, d) results. The 3.67- and 4.46-MeV states are possible candidates for containing the $3p_{1/2}$ strength that has not been located previously. The collective E3 multiplet excited strongly by inelastic scattering is seen very weakly at 2.6 MeV in the present (^{3}He, d) spectra. This excitation was not observed in the previous (^{3}He, d) work but it does appear with significant strength in the (α, t) reaction.

[1]N. Stein, R. H. Siemssen, and B. Zeidman, Bull. Am. Phys. Soc. 12, 1066 (1967).

*Yale University, New Haven, Connecticut.

(ii) Reactions in Heavy Nuclei

A. F. Friedman* and B. Zeidman

A preliminary study of (^{3}He, d) reactions in rare earth nuclei indicated that better resolution was required than is available at the cyclotron. The experiment was therefore shifted to the tandem. However, the (α, t) reaction preferentially excites states of high spin which are weak in the (^{3}He, d) reaction. The initial study of some (α, t) and (^{3}He, d) reactions showed very different spectra. Accordingly, we plan to continue (α, t) studies with the split-pole spectrograph which will complement the (^{3}He, d) work at the tandem. The ^{205}Tl(α, t)^{206}Pb reaction was studied at E_α = 46 MeV to observe the particle-hole states of ^{206}Pb. In this case the resolution was adequate for the study. States at 5—7 MeV excitation were strongly excited and will be correlated with the single-particle states from studies of the (^{3}He, d) and (α, t) reactions on Pb. A preliminary study of (α,α') reactions shows that the octupole deformations in deformed nuclei and the 5^- excitations may be profitably examined. A program to study these excitations is being planned.

---

*Chemistry Division.

E. OTHER NUCLEAR EXPERIMENTS

Several experimental nuclear investigations in the Physics Division are not closely associated with any one of the major sources of neutrons or charged particles. These independent studies are collected for convenience in this section.

a. The ^{77}As Excited States Populated by Beta Decay

H. H. Bolotin and D. A. McClure

The low-lying ^{77}As excited states populated by the decay of 11-h ^{77}Ge were studied by singles and coincidence γ-ray spectroscopic techniques to enlarge a comprehensive systematic study of the nuclides in this mass region. Ge(Li) detectors were used exclusively. Activities were produced by thermal-neutron activation of enriched samples of ^{76}Ge in the rabbit facility at the CP-5 reactor. Two-parameter Ge(Li)-Ge(Li) coincidence spectra were obtained and stored in a 1024 $\times$ 1024 pulse-height matrix.

The previously proposed decay schemes were shown to be almost totally incorrect. However, the present studies have led to construction of a new level scheme that incorporates virtually all of the observed transitions. Some further analysis is in progress.

b. Argonne Six-Gap Beta-Ray Spectrometer

G. T. Wood

Measurements reported last year on the decay of 18-h ^{125}Xe have been repeated (with H. J. Sathoff). The new measurements include conversion-electron and positron spectra measured on the six-gap magnetic beta-ray spectrometer, gamma-ray spectra on a 15 cc Ge(Li) detector (loaned by G. Thomas), and gamma-gamma Ge(Li)-Ge(Li) coincidence data obtained in a 1000 $\times$ 1000-channel matrix (spectrometer loaned by H. H. Bolotin). The quality of the new magnetic-spectrometer data is considerably better than the previously reported set owing to

application of the magnetic field sweep technique and use of a double detector in which two photomultipliers in coincidence view the spectrometer detector crystal (to reduce the photomultiplier noise involved in the detection of low-energy electrons).

In addition to the double detector mentioned above, the developments on the beta-ray spectrometer have included the construction of an electronic interface for a small computer-based (4096-word 16-bit Varian Data Machines computer) data-acquisition system to collect and store beta-ray-spectrometer data obtained by the sweep technique and to simultaneously measure pulse-height spectra from a gamma-ray Ge(Li) detector viewing the beta-ray spectrometer source. The simultaneous measurement of electrons and gamma rays from the same source by this system will make possible improved accuracy in the determination of internal-conversion coefficients.

c. Perturbed Gamma-Gamma Angular Correlations in Magnetic Materials

G. T. Wood and S. B. Burson

Perturbed gamma-gamma angular-correlation studies have been continued on four gamma-gamma cascades following the decay of ^{152}Eu (13 y) which is incorporated as a dilute impurity in iron and nickel hosts. The source, produced in the Argonne CP-5 reactor, was implanted in the ferromagnetic host by use of the Argonne isotope separator. The large internal magnetic fields at the nuclei of the radioactive impurities are aligned by magnetizing the ferromagnetic host with a relatively small external field. In general, the strong internal magnetic fields that act on the radioactive impurity ions can be applied to the determination of the magnetic moments of short-lived nuclear states. In the present study, the emphasis has been placed on understanding the nature of the internal field acting at the nucleus.

In order to elucidate this question, an experimental method has been devised to maximize the information obtainable by angular correlation. In this method, the perturbed gamma-gamma correlation is measured for various orientations of the external magnetizing field relative to the plane of the counters. From the angular distributions measured, it is in principle possible to calculate all the attenuation coefficients that depend on the perturbing interaction and, in turn, determine the correlation. Although the number of non-zero attenuation coefficients can be as high as 19, it can be shown for the 1415-122-keV cascade that the perturbation may be expressed in terms of only five attentuation coefficients—regardless of the interaction (so long as the interaction is axially symetric). Measurements on ^{152}Eu implanted in iron have been made at five orientations of the magnetizing field (including transverse and longitudinal directions). From the five distributions the five attenuation coefficients have been evaluated. The second step of the calculation involves finding a choice of the perturbing interaction that fits the observed attenuation coefficients. The results clearly show that the interaction is not equivalent to a completely aligned magnetic field. Part of the lack of alignment is apparently due to incomplete magnetic saturation of the iron near the surface where the source is implanted. Although the electromagnet used for the measurements at five orientations was relatively weak, the internal magnetic fields are still not completely aligned at 10 kG at which the transverse-field measurements were repeated. Calculations are under way to determine what field distribution best fits the measured attenuation coefficients.

d. Pattern Recognition for Nuclear Events

C. Harrison,* D. Jacobsohn,* and G. R. Ringo

The mechanization of the procedure for identification of interesting events is a problem of increasing importance in nuclear and particle physics. It is particularly critical in the case of emulsions where it is desirable to scan large volumes of material with microscopes showing volumes of 10^{-8} cc or less in a view. Our approach to this problem uses a four-layer random-connection network similar in its general character to the Perceptron of F. Rosenblatt. It is intended to separate patterns presented in the form of 80-bit words into wanted and unwanted classes after a learning phase using a few hundred cases of each. The approach differs from the original Perceptron in that in the original the random connections were reinforced or weakened on the basis of the learning performance. In the Argonne version, many completely different sets of connections are tried and the most useful (in the learning phase) kept.

In the last year several tactics within this general strategy have been tested and a few of the more promising ones picked out for testing on a new general-purpose computer (IBM 360-75). By careful optimization of the program, these tests can be done as fast on this computer as on the small special-purpose unit built for this problem; and use of the large computer offers a great gain in flexibility.

The program for this work has been debugged and is running. The most promising scheme at present involves weighting of the patterns in the learning set to force the program to cover as much of the learning set as possible.

---

*Applied Mathematics Division.

e. Microscopic Location of ^{17}O, ^{18}O, and ^{15}N

G. R. Ringo and V. E. Krohn

A technique by which the tracer isotopes ^{17}O, ^{18}O, and ^{15}N could be located (possibly simultaneously) within a resolution diameter of 1 micron or better would have obvious value in biological research. We believe this could best be done by scanning a specimen with a focused beam of ions (e.g., Ne^{+}) to convert the tracer isotopes to ions which will be identified in a mass spectrometer with high resolution (a resolution of, say, 5000). The high-resolution mass spectrometer is available, but an ion beam with less than 1 μ diameter and more than 1pA current remains to be produced.

A duoplasmatron ion source and an ion-lens system have been obtained and the remainder of the ion-beam system is under construction.

II. MEDIUM-ENERGY PHYSICS

During the past few years the program in medium-energy physics has consisted of two distinct parts. One part has been a series of experiments on muonic x rays in collaboration with a group at the Carnegie-Mellon University cyclotron. The second part has been the development of detailed plans for the conversion of the 60-in. fixed-frequency cyclotron into a 71-in. variable-energy cyclotron.

Changed circumstances have made it necessary to redirect the program in medium-energy physics. Our participation in the muonic x-ray studies has been brought to a close during the past year. In the coming year the effort will be devoted to an investigation of the feasibility of other kinds of experiments with intermediate-energy projectiles. The design study of accelerators is also undergoing a substantial change. Since the design of the variable-energy cyclotron has been completed, the emphasis will now be on the investigation of new design concepts.

a. Study of Muonic x Rays

The study of muonic x rays in collaboration with members of the staff of the Carnegie Institute of Technology was terminated early in FY 68. However, we have continued to support the work to a modest extent by allowing Argonne equipment to remain at Carnegie and by providing a Ge(Li) γ-ray spectrometer. The work completed in the past year is reported below.

(i) Muonic x-Ray Spectra in Deformed Even-Even Heavy Nuclei

R. E. Coté, W. V. Prestwich, A. K. Gaigalas,* S. Raboy,* C. C. Trail,† R. A. Carrigan, Jr.,‡ P. D. Gupta,‡ R. B. Sutton,‡ M. N. Suzuki,‡ and A. C. Thompson‡

Muonic K and L x-ray spectra have been observed with a Ge(Li) detector for the deformed even-even nuclei ^{158}Gd, ^{160}Gd,

*New York State University, Binghamton, New York.

†Brooklyn College, Brooklyn, New York.

‡Carnegie-Mellon University, Pittsburgh, Pennsylvania.

^{232}Th, and ^{238}U. The data are well fitted by assuming the rotational model of the nucleus and a three-parameter modified Fermi function for the charge distribution. The values of the intrinsic quadrupole moment Q_0 found are in excellent agreement with those obtained from Coulomb-excitation measurements.

(ii) Observation of a Gamma Transition Induced in a Target Nucleus by Stopping Pions

R. A. Carrigan, Jr.,* P. D. Gupta,* R. B. Sutton,* M. N. Suzuki,* A. C. Thompson,* R. E. Coté, W. V. Prestwich, A. K. Gaigalas,† and S. Raboy†

Evidence is given for the excitation of the 482-keV state in a tantalum target by stopping pions. The yield relative to a pi-mesic x-ray transition is found to depend on target thickness. Several mechanisms for the excitation of the state are discussed. It appears that at least part of the excitation may be due to production of neutrons in the pion absorption process and the subsequent inelastic scattering of the neutrons elsewhere in the target.

*Carnegie-Mellon University, Pittsburgh, Pennsylvania.

†State University of New York, Binghamton, New York.

b. Design and Development of Devices

(i) Proposed Conversion of the 60-in. Cyclotron

J. J. Livingood, W. J. Ramler,* J. Aron,* R. Benaroya,* F. F. Cilyo,† K. W. Johnson,* K. T. Khoe,‡ T. E. Klippert,* J. A. Nixon,* G. W. Parker,* and W. Wesolowski*

Studies with the 28-in.-diameter, 3-sector model magnet—equipped with trimming and hill coils—show that a sector

*Chemistry Division.

†Electronics Division.

‡Particle Accelerator Division.

design has been attained that will produce the particle energies originally planned: 60-MeV H^+, 36-MeV D^+, 93-MeV $^3He^{2+}$, and 72-MeV $^4He^{2+}$.

This prediction, made by synthesizing isochronous fields with adequate flutter, is based on measured values of the fields produced by the main coils, the trim coils, and the hill coils.

The central region contains rotatable plugs with three radial slots, in one of which an axially mounted ion source can move so as to produce properly centered orbits for ions of different energies and charge-to-mass ratios. Plug dimensions have been adjusted so that the rotation does not disturb the flutter and so that one axial position is adequate for the full range of field values.

Calculations have been made to determine what tolerances in the shape and position of the spiral sectors can be permitted if undesired harmonic fields are to be kept within the correction capabilities of moderately powered valley coils.

The trimming, hill, and valley coils will be of round, coaxial mineral-insulated copper cable. A full-scale hill coil of this material has been formed without difficulty. Studies of appropriate brazing techniques are yet to be carried out.

Extraction studies with a computer, based on the measured magnetic field, have produced the design of a satisfactory electrostatic deflector for 60-MeV protons — the projectiles most difficult to remove. It is 120^o long, the second half embodying electrodes with hyperbolic cross section to produce radial focusing. Its position with respect to the sectors, and the location of the latter with respect to the magnet yokes, have been chosen to minimize the field that must be countered by a subsequent magnetic shielding channel that carries the ions through the fringing field out to the existing beam-transport system. By changing the applied potentials and the separation of the electrodes, a beam of 93-MeV $^3He^{2+}$ ions follows the same path. It is anticipated that other ions can be similarly accommodated.

A magnetic channel, designed to afford adequate shielding but not to disturb the still-circulating ions, will soon be tested in the model magnet.

A one-fifth-scale model dee and coaxial tuning system has been used to check calculations on frequency range and power requirements. It is capacitatively driven through a novel untuned line. Full-power, full-scale tests have been made on the flexible contact fingers that will be required, and a method has been worked out to retract and extend these pneumatically.

An active filter has been designed to stabilize the dee voltage. This is now being used on the present 60-in. cyclotron, where it reduces the peak-to-peak ripple on the dee voltage from a former value of 2% to 0.2%.

Most of the basic parameters of the machine have been determined, including the voltage, current, and stability of the many power supplies that will be needed.

(ii) A Review of Dispersive and Achromatic Passage of Charged Particles Through One, Two, or Three Magnets

J. J. Livingood

This has been considerably expanded and rewritten, and will be published (with a different title) as a book in the late autumn of 1968 by Academic Press.

III. THEORETICAL PHYSICS

The theoretical group consists of permanent staff members, postdoctoral research associates, and long- and short-term visiting scientists. Three of the permanent staff members hold joint appointments at neighboring universities, and others teach occasional courses. Members of the group also participate in research collaborations with university faculty members, some of whom serve as consultants to ANL. The group has also undertaken an important responsibility for postdoctoral training in nuclear theory, especially in phenomenological theory.

Although the largest concentration of theoretical effort is in nuclear physics, there is also theoretical research in superconductivity, statistical mechanics, hypernuclear structure, elementary-particle physics, applied mathematics, and the mathematical structure of quantum mechanics. There is also a systematic development of software facilities for the numerical computations needed in nuclear-structure calculations. This facility has by now become an important theoretical resource. Parts of it have successfully been transferred to other laboratories for the use of other groups, and that process is continuing.

The theoretical group maintains an active partnership in the experimental program of the Physics Division— through research collaborations, informal cooperative effort and mutual criticism, and also through joint seminars whose principal purpose is to facilitate the flow of ideas between theorists and experimentalists.

The largest theoretical research program continues to be the computer-based studies of nuclear structure via the nuclear shell model. There is also a major effort in nuclear many-body theory. The two programs are linked by some of their computational techniques. In addition, some of the many-body studies are directed toward the theoretical needs of the shell-model program. Examples of these and other research achievements are described briefly below.

a. The Nuclear Shell-Model Program

(i) The Shell-Model System

S. Cohen, D. Kurath, and J. M. Soper

The DELPHI (3600) Shell-Model System. The system of programs for doing shell-model calculations on the CDC 3600 is still being developed. The programs can now extract coefficients of fractional parentage and determine theoretical values for observable quantities such as multipole transition rates and log ft values for beta decay. Amplitudes for determining multipole-mixing coefficients can be obtained. The programs are still being extensively used for many problems, some of which are discussed below.

Additional programs to carry out calculations involving 2-particle coefficients of fractional parentage are now being added to the system. These programs will make it possible to perform studies involving (t, p) and (^{3}He, p) reactions.

The DELPHI (360) Shell-Model System. The entire nuclear shell-model system and its control program (DELPHI) are being rewritten for use on computers in the IBM-360 series. The programs are being simplified and made more efficient during the translation to the new machine. This new system of programs will be usable both at Argonne and at Harwell in computer environments which differ in available facilities.

For the most part, the logic of the older system is being maintained and present users of the older system should find little difficulty in adapting to the new system. The new system will also have a branch oriented towards the use of coefficients of fractional parentage as an intermediate step in the construction of energy matrices. Greatly increased capabilities for the system as a whole should result from this new branch.

(ii) The Effective Interactions in the sd Shell

The T = 0 Interaction[1] (S. Cohen, E. C. Halbert,* and S. P. Pandya). A simple model interaction for T = 0 two-nucleon states in sd-shell nuclei is described. All the two-body matrix elements are expressed in terms of seven radial matrix elements (which later effectively reduce to three) as in an earlier paper. The values of the parameters are obtained by making a least-squares fit to observed level energies in ^{18}F and ^{19}F, and are then used to calculate the level schemes of ^{20}F and ^{20}Ne. The parameters and the spectra obtained here are compared with those calculated from realistic nucleon-nucleon forces. Such simple interaction forms as are used here may be particularly valuable in assessing the sensitivity of shell-model results to the use of specific interactions, or to truncations of the basis space, or the like.

The T = 1 Interaction[2] (S. Cohen, R. D. Lawson, and S. P. Pandya). The effective interaction in T = 1 two-body states in the sd-shell is parameterized in terms of radial matrix elements of the effective potential in states of relative orbital angular momenta of two nucleons. Seven of these parameters are needed to define all the T = 1 matrix elements with the assumption of a central effective potential. The values of these parameters are determined by making a least-squares fit to sixteen observed level energies in the oxygen isotopes, and are then compared with values calculated from various realistic free nucleon-nucleon interactions. It is shown that a major effect of core excitation and the consequent renormalization of the two-body matrix elements, so forcefully pointed out by Kuo and Brown, consists of a strong modification of the contributions of the triplet-odd force.

---

*Oak Ridge National Laboratory, Oak Ridge, Tennessee.

[1] S. Cohen, E. C. Halbert, and S. P. Pandya, Nucl. Phys. A114(2), 353 (1968).

[2] S. Cohen, R. D. Lawson, and S. P. Pandya, Nucl. Phys. A114, 541 (1968).

Two-body matrix elements calculated with our parameters are also found to agree well with those determined by Glaudemans et al. from a least-squares fit to observed level schemes of nuclei with A = 29—40.

(iii) 1p-Shell Nuclei

S. Cohen and D. Kurath

The shell-model programs were used to study the sensitivity of electromagnetic transitions to the nuclear wave functions for the A = 8 and A = 12 states on which recent measurements have been reported. The 1p model is able to reproduce the observed values. A study was carried out for the boron isotopes, and again it was found that slight variations of the wave functions led to marked improvement in the similarity of calculated and observed transition rates.

A few simple cases of 2-nucleon transfer were calculated by use of the system plus an auxiliary SPEAKEASY* program. The results indicate that it would be beneficial to incorporate a program in the system to extract 2-nucleon fractional-parentage coefficients.

(iv) Shell-Model Calculations in a Deformed Basis

M. H. Macfarlane

A prominent feature of many nuclear spectra is the occurrence of rotational bands. In particular, such bands appear in the spectra of light nuclei, where the many-particle shell model is at its most successful. Now the shell model customarily starts from a spherical starting point and constructs its approximate nuclear wave functions by superposition of huge numbers of basic spherical structures. On the other hand, it is known that rotational band structure implies a nonspherical, deformed equilibrium shape for the nucleus in question and it is also known that members of a rotational band of states have the same intrinsic (i.e., particle) structure.

*Described in Sec. III.k.

These facts suggest that great simplifications might result were a shell-model description of light rotational nuclei to have a nonspherical starting point. Such deformed-shell-model calculations, of course, relinquish the great simplifications peculiar to computations in a spherical symmetry. The hope is that only a very few deformed shell-model states need be retained and that thereby an enormous truncation of the problem can be achieved.

Computer programs have been written to carry out the calculations outlined above; the deformed shell-model basis states with which these programs work have definite angular momentum, isobaric spin, and particle number. The first applications will be to an extended study of effective interactions in the isotopes of nickel and to even-even nuclei (^{20}Ne, ^{24}Mg) in the (1d, 2s) shell.

(v) Effects of Nuclear Deformation

D. Kurath

Quadrupole deformation of the nucleus explains the presence of strong E2 transitions. Such deformation can also have appreciable effects on other observable quantities. A microscopic picture of deformation effects in light nuclei can be obtained by analysis of the orbitals of odd nucleons in the field of a core with quadrupole deformation.

The magnetic octupole moments depend on which orbitals are occupied by the nucleons at the Fermi surface. If these orbitals have the same shape as the core, one expects enhancement of the M3 moment. In some cases these orbitals may have opposite shapes (i.e., oblate in a prolate field), in which case there should be suppression of the M3 moment.

Such an effect seems to be present in recent electron-scattering measurements of the M3 moments of ^{7}Li, ^{9}Be, ^{10}B, and ^{11}B. A similar effect should be present for forbidden beta decays between 0^{+} and 3^{+} states.

b. Theory of Stripping to Unbound States

C. M. Vincent, H. T. Fortune, and J. E. Monahan

The conventional distorted-wave Born-approximation theory of stripping does not apply to stripping to an unbound (resonant) state. Nevertheless the theory can be generalized to apply to this case, as suggested by Huby and Mines.[1] A paper discussing the justification of this theory has been submitted for publication.

For stripping to an unbound state, the wave function of the transferred particle oscillates at large radii instead of tending rapidly to zero as in the bound case. Consequently, the radial integrals of the theory converge extremely slowly. This difficulty has now been removed by using a complex contour for the radial integration. A computer program to evaluate the stripping angular distribution has been written and tested. This program is being used for the analysis of experimental data. The complex-contour technique will also be used in interpreting the divergent matrix elements of interactions between resonant states.

---

[1] R. Huby and J. R. Mines, Rev. Mod. Phys. 37, 406 (1965).

c. Average Properties of Atomic and Nuclear States, Transitions, and Cross Sections

The investigation of the statistical properties of the highly excited states of atoms and nuclei has continued with two main goals: (1) to define the limits of validity of Wigner's model, which has been very successful in the description of the "local" properties of the most complex systems, such as the distributions of level spacings in heavy nuclei, and (2) to formulate more advanced statistical theories which will reflect structural details of the systems, such as approximate constants of the motion and the energy dependence of the nuclear level density.

(i) Perturbation of the Statistical Properties of Nuclear States and Transitions by Interactions That Are Odd Under Time Reversal

N. Rosenzweig, J. E. Monahan, and M. L. Mehta

It is found that a rather small time-reveral-odd part in the nuclear Hamiltonian would produce an appreciable perturbation in the Porter-Thomas distribution of widths and also in the distribution of the spacings between energy levels.[1] A comparison between the experimentally determined variances for some published neutron widths and partial radiation widths and the calculated variance allows one to place an upper limit on the magnitude of the time-reversal-odd part. The shift of the spacing distribution is particularly large on a percentage basis in the region of small spacings. As a measure of the time-reversal-odd part of the wave function, the overlap $|(\psi, T\psi)|$ has been evaluated. All conclusions are based on a Monte Carlo calculation with random Hermitian matrices having a small imaginary part.

(ii) Distribution Laws for the Roots of a Random Antisymmetric Hermitian Matrix[2]

M. L. Mehta and N. Rosenzweig

In conjunction with the study of the perturbations of the statistical properties of nuclear spectra produced by interactions which are odd under time reversal, it was found that the case in which the odd part is very large can be treated analytically. While of no immediate physical interest, the precise results obtained serve as a check on the adequacy of the Monte Carlo calculations reported in Sec. (i). With the help of the theory of random matrices, analytical results are obtained for the distribution of widths, the level density, two-level cluster function, and the distribution of the spacing between adjacent energy levels.

[1] N. Rosenzweig, J. E. Monahan, and M. L. Mehta, Nucl. Phys. A109, 437 (1968).

[2] M. L. Mehta and N. Rosenzweig, Nucl. Phys. A109, 449 (1968).

(iii) Nuclear Level Density

N. Rosenzweig and P. B. Kahn*

The level density of a degenerate Fermi system is modified by the perturbation in the position of a single-particle level. To study this effect, miscellaneous exact relations between the level densities of the perturbed and unperturbed system are derived. For the special case of the perturbed uniform model, these connections become a set of recursion relations which lead to a complete solution of the problem. Results are also obtained in the saddle-point approximation, and these have a simple interpretation in terms of the usual Fermi occupation probabilities. If a single-particle level is deleted from the scheme, the resultant diminution in the level density persists indefinitely with increasing excitation energy. Information about the adequacy of the saddle-point approximation is obtained by comparison with some exact solutions.

*State University of New York, Stony Brook, New York.

d. Studies of Nuclear Matter

(i) The Ground State of Closed-Shell Nuclei and the Construction of the Shell-Model Hamiltonian

F. Coester

The nuclear-matter problem is the key to nuclear-structure theory in that it provides the formal framework for approximations to the ground states of closed-shell nuclei on the basis of so-called realistic potentials.

The effective Hamiltonian for the system consisting of a closed shell plus one particle (hole) can now be found by use of the known solution of the ground-state problem. The single-particle energies are distinct from those arising from the solution of the ground-state problem. The same general procedures apply to more than one particle outside a closed shell.

(ii) The Ground State of Nuclear Matter

F. Coester, S. Cohen, and James MacKenzie

We investigated the ground-state problem of nuclear matter as a mathematical problem both numerically and by methods of functional analysis. The Schrödinger equation implies a set of nonlinear equations for the correlated excitation amplitudes. It appears possible to prove the existence of a solution by a fixed-point theorem in an appropriate Banach space and to establish useful absolute error bounds on approximate solutions. For potentials with strong repulsion, the first approximation (Brueckner approximation) calls for the reaction matrix. We have developed a computer program that computes the reaction matrix by solving the integral equation in momentum space. The exclusion principle is treated exactly. For soft potentials for which the reaction matrix is well approximated by the first two terms of the perturbation series, the following question arises: Can the solution of the full many-body problem be approximated adequately by the Hartree-Fock approximation plus second-order perturbation corrections? In order to shed some light on that question, programs have been developed to compute all second- and third-order corrections to the Hartree-Fock approximation.

(iii) Accurate Solution of The Bethe-Goldstone Equation

A. Kallio and B. Day

The previously developed method of solution of the Bethe-Goldstone equation has been applied to ^{4}He and ^{16}O. The first-order binding energy and leading correction terms (second- and third-order diagrams) have been calculated. The correction terms are less than 1 MeV per particle, which indicates good convergence of the energy expansion. Also, the calculated binding energy of ^{4}He agrees to 1 MeV per particle with the result of an accurate variational calculation. Thus

it is believed that the present method will permit accurate calculation of binding energies in light nuclei.

The same method has been successfully used to solve the Bethe-Goldstone equation in infinite nuclear matter for both central and tensor forces. The method is slower but more accurate than the often-used reference-spectrum method. It also provides accurate two-body wavefunctions that are needed in three- and four-body calculations, which the reference-spectrum method does not do.

(iv) Four-Body Correlations in Nuclear Matter

B. Day

Numerical work on the four-hole-line diagrams is continuing, using wave functions and matrix elements calculated by the Kallio method reported in Sec. (iii). The result of these calculations will be useful (1) to check the convergence of the energy expansion for nuclear matter, and (2) to learn how much of the present discrepancy between theory and experiment is due to four-body terms.

e. Studies of Hypernuclei and the Interactions of Λ Particles

(i) Λ in Nuclear Matter; Effective Interactions

A. R. Bodmer and D. Rote*

The problem of a Λ in nuclear matter is an interesting many-body problem which is of considerable importance for hypernuclear physics. From studies of hypernuclei, quite good values of the binding energy (well depth) of a Λ in nuclear matter are now available. The limiting case of a Λ in nuclear matter has simplifying features as compared with finite hypernuclei, but at the same time furnishes a useful touchstone for many questions of importance for these. Examples

*University of Illinois at Chicago Circle, Chicago, Illinois.

of such questions which we are considering are the importance of interactions in p states, the effect and possible suppression of a ΛN tensor force, and the effect of the ΛN-ΣN coupling in nuclear matter.

This question of a possible suppression is closely related to the question of the equivalence of effective, purely central (s-state) ΛN interactions for the free ΛN case and for hypernuclei. An approach we have used is to compare effective s-state ΛN potentials for the free case with that for a Λ in nuclear matter by eliminating the $^3D_1$ state coupled in by the tensor force. It is already evident that for short-range tensor potentials, such as are relevant for the ΛN interaction, the effective s-state potentials (which are nonlocal) are very similar for nuclear matter and for the free ΛN case. Thus, it may be expected that for many purposes it is justified to use an effective s-state potential, which has been fitted to the Λp scattering data, also for a Λ in nuclear matter (and thus probably also more generally for finite hypernuclei) without explicit consideration of a tensor force. If such an equivalence holds, then it will considerably simplify hypernuclear spectroscopy. Quite similar considerations can be applied to the equivalence of the effect of the ΛN-ΣN coupling on the free ΛN interaction and on a Λ in nuclear matter.

The above investigation, which is part of a more comprehensive study of the problem of a Λ in nuclear matter, is based on the Brueckner-Goldstone-Bethe approach. At present we are calculating the ΛN K-matrix elements and the Λ well depth for a variety of two-body ΛN potentials with a hard core. The technique, which is due to Kallio and Day, is based on the reference-spectrum method. Some of the questions being studied are the goodness of a perturbation procedure in the attractive part of the interaction for potentials with varying hard-core radii and attractive parts but giving the same scattering length, the importance of p-state interactions, and the effect of changes of the Λ effective mass and/or of the reference spectrum for the nucleons.

Beyond the above investigations, an important fundamental problem is a good understanding of the convergence of the perturbation and, more particularly, of the K-matrix expansions. Of particular interest in this connection is the rearrangement energy for the Λ in nuclear matter (which results from the distortion of the nuclear matter by the Λ) and the question of the choice of single-particle potential for the Λ.

(ii) Theoretical Models of the ΛN and $\Lambda\Lambda$ Interactions

A. R. Bodmer and D. Rote*

Theoretical models of the ΛN and $\Lambda\Lambda$ interactions can provide a valuable guide to the form of interactions to use in studies of hypernuclear structure. Thus even rather qualitative information about the interaction may have very valuable implications for studies of hypernuclear structure. Conversely, the results of phenomenological hypernuclear analyses may give fundamental information about coupling constants, repulsive cores, etc.

A potential model is being studied which, for the ΛN interaction, includes both ΛN and ΣN channels ($\Lambda\Lambda$ and $\Sigma\Sigma$ channels for the $\Lambda\Lambda$ interactions). The ΛN-ΣN coupling is introduced explicitly because of its strength and because of the small mass difference between the Σ and Λ hyperons.

The main new aspect is the emphasis on the use of a matrix potential whose components are obtained from one-boson exchanges. Most of the emphasis, so far, has been on the lightest scalar and pseudoscalar mesons together with a hard core. Some consideration has also been given to vector mesons which lead to a repulsive core. One of the principal aims is to obtain at least a semi-quantitative understanding of the effects of the different exchanges, and considerable progress has been made.

* University of Illinois at Chicago Circle, Chicago, Illinois.

For use in hypernuclear-structure calculations, potentials with a reasonable range of strengths for the tensor component have been obtained. Characteristic, in this connection, of the tensor potential for the ΛN interaction (in contrast to that for the NN interaction) is its short range. It is to be emphasized that these theoretical studies of the interactions go hand in hand with the accompanying nuclear-structure studies.

(iii) Variational Studies of Bound Three-Body Systems

A. R. Bodmer and A. Mazza*

Variational wave functions of the product type, where (for an s state) each factor in the product is a trial function of the corresponding interparticle distance, are very commonly used for bound nuclear three-body systems. However, even the best product-type wave function is inadequate in certain important respects.

Thus considering the hypertriton ${}^{3}_{\Lambda}\mathrm{H}$ as an example, it is readily shown that the best product-type wave function cannot give the correct asymptotic behavior corresponding to the Λ-d separation; in particular, the optimum product wave function will not correspond to a free deuteron when the Λ particle is removed to infinity. The hypertriton may then be considered as illustrating a much more general problem, namely, that of the wave function for a system consisting of a core and an extra particle, where the core has dynamical properties. Of particular interest is the spatial extension of the core-particle wave function and the relation of this extension to the separation energy of the extra particle with respect to the core and to the core rearrangement energy (i.e., the increase in energy of the core resulting from its distortion by the extra particle). Qualitatively, the latter is expected to lead to a smaller extension of the core-particle wave function than is determined by the separation energy.

*University of Illinois at Chicago Circle, Chicago, Illinois.

For three-body systems these questions are being studied with the use of trial wave functions which are more flexible than the product type. In the case of ${}^{3}_{\Lambda}H$, for example, the wave function must, in particular, be sufficiently flexible to allow for a dependence of the deuteron (core) part of the wave function on the average Λ-deuteron separation.

These questions are also of importance in connection with attempts to determine the large-distance behavior of three-body wave functions by use of the appropriate empirical separation energy for ${}^{3}H$ and ${}^{3}He$, for which good wave functions are of considerable importance.

The work on the S' state in the hypertriton is being re-examined with the result that the S' state seems much less important than was originally concluded. Some other improvements in the variational calculations of ${}^{3}_{\Lambda}H$ are also being considered.

f. Equilibrium and Stability of Fluid Configurations

Carl E. Rosenkilde

Two problems have been examined as part of a continuing investigation of the application of the virial method to the equilibrium and stability of fluid configurations under the combined influence of various kinds of forces.

(i) Nuclear Liquid-Drop Model

In the standard form of the liquid-drop model, the attractive nuclear forces are usually represented by a constant surface tension. An earlier investigation of this model has been extended to include the effect of correcting the surface tension by a small amount which depends upon the curvature of the surface. The associated correction to the binding energy is proportional to $A^{1/3}$ and represents the diffuseness of the nuclear surface.

(ii) Cloud Electrification

One of the proposed mechanisms of cloud electrification during the formation of thunderstorms involves the disintegration of droplets which have become polarized by the prevailing electric field. The virial method has been extended to include an external electric field acting upon an incompressible dielectric fluid drop. Prolate spheroids of varying eccentricity are found to be good approximations to the exact equilibrium shapes. Criteria for the stability of these configurations with respect to second-harmonic deformations have been obtained as a function of the dielectric permeability.

g. Foundations of Quantum Mechanics *

(i) Locality in Field Theory

H. Ekstein

The usual statement of locality is that local observables commute if they belong to space-like positioned spacetime volumes. The present discussion rejects this as unacceptable because it does not express an operational statement. The alternative statement says (in loose language) that any observation in V_1 is compatible with any observation in V_2, if V_1 and V_2 are spacelike. It has been shown that the new and the conventional statement are not mathematically equivalent. It is hoped that a richer relativistic field theory will become possible with the new statement. The mathematical consequences of the proposed statement have been explored for finite-dimensional Hilbert spaces. A preliminary informal report entitled "Empirical Foundations of Non-relativistic Quantum Mechanics" has been distributed. The attempt to generalize the above-mentioned results for infinite-dimensional Hilbert spaces is continuing.

* This work was supported jointly by the High-Energy Physics and Low-Energy Nuclear Physics programs.

(ii) The Art of Educated Guessing in Quantum Mechanics

H. Ekstein

If the initial wave function or density matrix of a system is not known exactly (the usual situation) then, generally and strictly speaking, physics has no predictive power. The lacking knowledge must be supplemented by educated guessing, and this can be done either by common sense or in a systematic way. The theory of systematic guessing, sometimes called generalized statistical mechanics, is in an unsatisfactory state: (1) its basic assumptions seem unconvincing and arbitrary and (2) it gives divergent results even for some very simple cases, unless some more or less judicious tampering is performed. The present effort tends (a) to put the theory of physical conjecturing on a sounder basis and (b) to make it unambiguously applicable to the (realistic) case of infinite-dimensional Hilbert space. Because of certain mathematical difficulties encountered, work has been temporarily discontinued.

(iii) Presymmetry

H. Ekstein

Even in the presence of external fields, space-time symmetry implies nontrivial relations between observables at one time, i.e., kinematical relations. Symmetry operations at one time—translations, rotations, and (for Galilei symmetry) velocity shifts—can be performed on observation-producing and on state-producing instruments, regardless of the existence of an external field. Furthermore, it is possible to give an operational definition of every initial state intrinsically, i.e., regardless of the external field. The precise statement of this empirical fact explains, for example, why a particle in an external field has integral or half-integral eigenvalues of the spin, why a Hamiltonian exists even in the presence of a time-dependent

external field, and why (for Galilei symmetry) the cononical commutation relations are still valid, although the full space-time symmetry from which these results can be derived has been destroyed. It is pointed out that the rigorous validity of kinematical relations in spite of strong breaking of the underlying space-time symmetry is analogous to the rigorous validity of equal-time current commutation rules in spite of the breaking of the underlying U(3) symmetry. The final report on this part of the work has been published.[1]

In a continuation of this work, the theoretical scheme includes rigid-body accelerations (in addition to the Galilei group) in the presymmetry group—that is, the group of motions under which relations between measurement procedures remain invariant. From (hopefully) plausible operational assumptions, one derives (1) Newton's second law (roughly, the equations of motion of a particle in an external field are of second order) and (2) Einstein's equivalence principle. A paper is in preparation.

(iv) Causality in Quantum Mechanics

H. Ekstein and H. Mehlberg*

The philosophical aspects of this problem are reinvestigated in collaboration with H. Mehlberg. A paper is in preparation.

[1]H. Ekstein, Phys. Rev. 153, 1397 (1967).

*Department of Philosophy, University of Chicago, Chicago, Illinois.

h. Relation Between Measurement Theory and Symbolic Logic[1]

M. N. Hack

In recent years there has been a vigorous renewal of interest in the quantum theory of measurement. The crucial issue

[1]M. N. Hack, Nuovo Cimento 54B, 147 (1968).

appears to be the problem whether this theory casts doubt on customary conceptions of physical reality at the macroscopic level, i.e., an intrusion of the breakdown of naive realism for atomic and subatomic phenomena into the realm of large-scale observable phenomena. That the giving up in the present theory of customary concepts of naive realism cannot be circumscribed to the world of microscopic events has long been stressed by opponents of the orthodox interpretation, and particularly incisively by Schrödinger and Einstein. The question remains, however, whether this feature of quantum theory should be regarded as a defect, to be remedied in some future development of the theory, or rather whether it should properly be regarded as a correct indication of an aspect which might be featured even more prominently in the future theory. Arguments have been developed to explore the possibility of adopting the latter alternative.

i. Derivation of Newton's Law of Gravitation from General Relativity

Amnon Katz

A static situation of two objects held apart by a strut is considered within the framework of general relativity, and the gravitational attraction between the objects is inferred from the stress in the strut. In the Newtonian limit—the objects well separated and the field weak everywhere except in their immediate vicinity—Newton's law of gravitation is reproduced. This check goes well beyond verifications of the Newtonian limit based on considerations of "test particles," since arbitrarily strong self fields are not excluded for either object. It is also an explicit verification of the equality of active and passive gravitational masses.

j. Gravity-Induced Electric Field Near a Conductor

M. Peshkin

Recent experiments apparently show that a conductor which shields a test electron against external electric fields also shields the test electron against gravity. Two previous theoretical analyses differ. A perturbation-theoretic treatment of gravity agrees with the experiment, but a Thomas-Fermi treatment of the conduction electrons in the shield apparently disproves the perturbation-theoretic result. At Argonne, a careful analysis of the earlier theories has revealed that the answer in fact depends sensitively upon the surface properties of the conductor. Plausible assumptions about the surface can remove the discrepancy which arises in the simple Thomas-Fermi treatment, and restores agreement with the experimental result. A detailed report has been published.[1]

[1] M. Peshkin, Ann. Phys. (N. Y.) 46, 1 (1968).

k. An Improved Computer Language: Speakeasy II

S. Cohen and C. M. Vincent

A greatly improved version of SPEAKEASY (which was originally developed at Argonne in 1963) has been implemented for use on the IBM-360 computer system.

The aim of SPEAKEASY is to simplify the numerical solution of scientific problems by making it possible to write programs closely resembling the original mathematics. SPEAKEASY expressions can be written involving matrix multiplication, inversion, etc.; and any standard operations on matrices (such as diagonalization and evaluation of the determinant) may be included. Arrays of one and two dimensions can be manipulated with the same freedom, and all of the common functions are available.

```
                PROGRAM SPHEBESL
DOMAIN(COMPLEX); N=NUELS(RHO)
S=ARRAY(N,L+1:)+GRID(0,L,1)
L=ARRAY(N,L+1:)+L
COEFTS=1I**(S-L)*GAMMA(L+S+1)/(2**S*GAMMA(S+1)*GAMMA(L-S+1))
RIS=SUMROWS(COEFTS*RHO**(-S))
HPLUS=RIS*EXP(1I*RHO)/RHO
NBESL=REALPART(HPLUS)
JBESL=IMAGPART(HPLUS)
TABULATE(RHO,HPLUS,NBESL,JBESL)
VSCALE(MIN(JBESL),MAX(JBESL)); HSCALE(MIN(RHO),MAX(RHO))
GRAPH(NBESL,JBESL:RHO)
                END
```

Fig. 37. SPEAKEASY as a quick route from formulae to tables and graphs. Left (above): A SPEAKEASY program to compute, tabulate and graph spherical Bessel functions. The regular, irregular, and outgoing functions [j_ℓ, n_ℓ, and $h_\ell^{(+)}$, respectively] are calculated from the formulae

$$h_\ell^{(\pm)} = (R_\ell \pm iS_\ell)\ \frac{e^{\pm i\rho}}{\rho},$$

$$R_\ell \pm iS_\ell = \sum_{s=0}^{\ell} \frac{i^{s-\ell}}{2^s s!} \frac{(\ell+s)!}{(\ell-s)!} \rho^{-s},$$

$$n_\ell = \mathrm{Re}\ h_\ell^{(+)}, \quad j_\ell = \mathrm{Im}\ h_\ell^{(+)}.$$

In the program the symbol 1I stands for $i = \sqrt{-1}$. The computation is for any given array RHO of ρ values, and any value L of ℓ. Right (on facing page): The graphical output of this program for L = 3 and RHO a grid from 0.05 to 10 in steps of 0.05. The vertical scale is adapted to the regular function. Therefore, large and small values of the irregular function have been automatically truncated.

Calculations can be carried out on both real and complex numbers, and the operations of differentiaion and integration are built into the language.

Since a single SPEAKEASY statement can do the work of several FORTRAN statements, SPEAKEASY programs are more compact and easier to read. No FORMAT statements are required for printed SPEAKEASY output, and identification of printed variables by name is automatic. Output can very easily be graphed. Figure 37 shows a typical

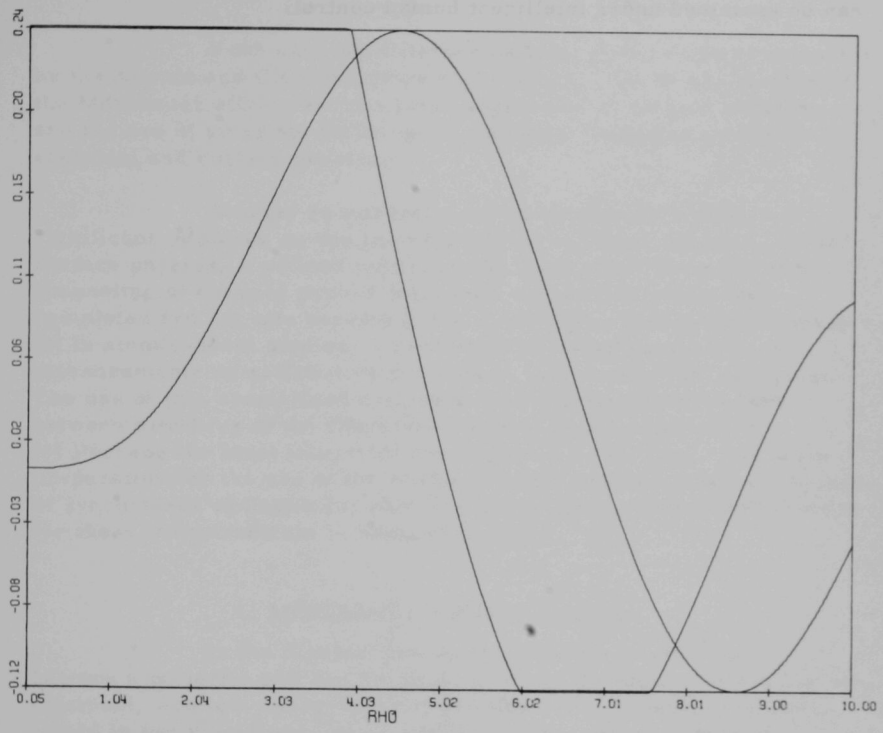

SPEAKEASY program, together with the source mathematics. There is a striking correspondence between the program and the mathematics. Thus SUMROWS corresponds to $\sum$ while GAMMA(L + S + 1) corresponds to $(\ell + s)! = \Gamma(\ell + s + 1)$.

Its programming ease makes SPEAKEASY suitable for on-line programming. SPEAKEASY II has been adapted for the 2250 display console. Rather complicated problems can be solved by typing a few SPEAKEASY statements at the console. Convenient means of storing and retrieving data have been devised, with the result that it is possible

to manipulate data generated by existing large programs. The graphical or numerical results can be displayed immediately on the console screen. Thus masses of intermediate data (ordinarily buried in piles of paper) can be examined under intelligent human control.

IV. EXPERIMENTAL ATOMIC PHYSICS

Four entirely different kinds of physics are supported by the Atomic and Classical Physics Program. These are studies of the Mössbauer effect, atomic-beam experiments, plasma physics, and the use of mass spectroscopy to investigate various problems in chemical and surface physics.

Several recent technical developments will have a significant influence on our future program in atomic physics. (a) In surface physics, a refined experimental system for the study of the channeling of charged particles through monocrystals has been completed and put into service at the 2-MeV Van de Graaff accelerator. (b) In atomic-beam studies, a new machine aimed exclusively at measurements on radioactive nuclides is now coming into operation. The use of this specialized system will be a collaborative effort between members of the Chemistry and the Physics Divisions. (c) Perhaps the most important development, in the long run, is the preparation for the use of the MURA electron storage ring as a source of synchrotron radiation for photoionization measurements; equipment for these measurements is being assembled.

1. MÖSSBAUER MEASUREMENTS

In the last few years, the Mössbauer effect has become a powerful tool for the study of many phenomena in solid-state, chemical, and low-energy nuclear physics. The experiments are aimed in two directions: (a) to yield accurate measurements of previously unobtainable nuclear properties (e.g., the quadrupole moments and magnetic moments of excited nuclear states) and (b) to make accurate determinations of the environment in which a nucleus is immersed (e.g., to determine the charge transfer from an iodine atom as it forms a chemical bond with chlorine). Recent Argonne experiments have been concerned with such diverse nuclear species ^{40}K, ^{57}Fe, ^{83}Kr, ^{119}Sn, ^{121}Sb, ^{127}I, ^{129}, ^{131}Xe, ^{133}Cs, ^{235}U, ^{191}, ^{193}Ir, and ^{237}Np, and others are being considered.

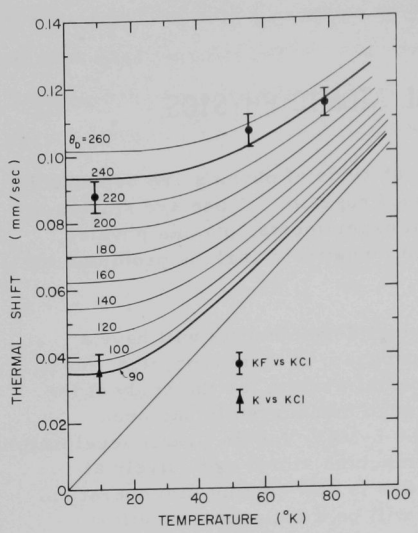

Fig. 38. Calculated thermal shifts and measured center shifts (isomer plus thermal) for K and KF. These data allow the calculation of an upper bound for $\delta\langle r^2\rangle/r^2$ in this nucleus.

a. Properties of Nuclear Excited States

(i) Studies with ^{40}K

S. L. Ruby and P. K. Tseng

^{40}K in a variety of chemical environments has been carefully studied by use of capture γ rays from the $^{39}K(n,\gamma)^{40}K$ reaction. For this nucleus, the four low-lying levels come from various couplings of the same single-particle states; if this were completely true, then $\delta\langle r^2\rangle/r^2$ should be zero. Figure 38 shows the experimental shifts for potassium in the metal and in a chloride. It is shown in the report[1] that these shifts are virtually entirely due to the second-order Doppler shifts arising from thermal vibrations. Analysis leads to $\delta\langle r^2\rangle/r^2 < 5\times10^{-4}$, in agreement with the simple shell model. The published results[1] show that useful lattice-dynamical information can be obtained with Mössbauer studies on potassium.

(ii) Magnetic Moment of the First Excited State in ^{83}Kr by the Mössbauer Effect

G. J. Perlow, M. A. Grace, and L. E. Campbell

The ground state of ^{83}Kr has $J^\pi = \frac{9}{2}^+$. Its first excited state at 9.3 keV has $J^\pi = \frac{7}{2}^+$. The simplest shell-model configuration

[1] P. K. Tseng, S. L. Ruby, and D. H. Vincent, Phys. Rev. 172, 249 (1968).

involved is three $g_{9/2}$ neutron holes coupling to $\frac{9}{2}^+$ for the ground state and to $\frac{7}{2}^+$ for the excited state. A consequence of this assignment is that the g values should be identical for the two states. In order to test this shell-model assignment, the magnetic moment of the first excited state is being measured by use of the Mössbauer effect in ^{83}Kr and absorbers consisting of solid krypton and krypton clathrate placed in a superconducting magnet. Results so far indicate that the ratio of the g values is approximately 1.25. A careful computer analysis of the data is once again necessary in order to extract the value of the excited-state moment.

(iii) Magnetic Moment of the First Excited State in ^{133}Cs by the Mössbauer Effect[1]

L. E. Campbell and G. J. Perlow

The Zeeman splitting of the 81-keV first excited state of ^{133}Cs in a magnetic field of approximately 78 kG has been observed by means of the Mössbauer effect. The field at the nucleus was produced by placing the diamagnetic cesium compounds CsF, CsCl, and CsI into a superconducting magnet. Because the total magnetic splitting produced was not much larger than the width of each individual level, the resulting absorption spectra were carefully computer-fitted in order to obtain the best value for the magnetic moment of the excited state. The results obtained with the different absorbers agreed within the statistical errors and give a most probable value $\mu_{ex} = +3.44 \pm 0.02$ mm. This value is consistent with the ground-state moment and the simplest shell-model configuration $(j^n)_j$ when core polarization is taken into account by a reduction in the intrinsic moment of the unpaired nucleon.

[1] L. E. Campbell and G. J. Perlow, Nucl. Phys. A109, 59 (1968).

(iv) Mössbauer Studies with ^{191}Ir and ^{193}Ir

D. N. Olson and G. J. Perlow

The isotopes of iridium with mass numbers 191 and 193 have very similar nuclear properties, exhibiting rotational spectra characteristic of deformed nuclei. Two levels in each of these isotopes are suitable for Mössbauer studies, although the 82-keV level in ^{191}Ir and the 140-keV level in ^{193}Ir had not been observed prior to the commencement of these measurements. A report on these is being prepared, and further study of the magnetic moments and E2-M1 mixing is under way. The 73-keV transition in ^{193}Ir is being used to study compounds of this interesting transition metal.

(v) Isomer Shifts and Hyperfine Splittings of the 59.6-keV Resonance in ^{237}Np

B. D. Dunlap,* G. M. Kalvius,* S. L. Ruby, M. B. Brodsky,† and D. Cohen‡

The isomeric shifts of the 59.6-keV transition of ^{237}Np in the 4+, 5+, and 6+ charge states were observed. Coupled with results from an atomic self-consistent-field calculation, the change in nuclear charge radius and in nuclear deformation was found to be $\Delta\langle r^2\rangle/r^2 = -2.5 \times 10^{-4}$ and $\Delta\beta/\beta_0 = -5 \times 10^{-3}$. This result is discussed in the light of the collective nuclear model. Magnetic and electric hyperfine interactions have been found for several compounds and intermetallics. The values for the ratio of nuclear moments are confirmed to be $g^*/g = +0.533 \pm 0.005$ and $Q^*_0/Q_0 \approx +1$. The temperature dependence of the hyperfine splitting of several compounds was investigated. The results have been published.[1]

*Solid State Science Division.

†Metallurgy Division.

‡Chemistry Division.

[1] B. D. Dunlap, G. M. Kalvius, S. L. Ruby, M. B. Brodsky, and D. Cohen, in Hyperfine Structure and Nuclear Radiations, edited by E. Matthias and D. A. Shirley (North-Holland Publishing Co., Amsterdam, 1968), p. 84; Phys. Rev. 171, 316 (1968).

b. Studies of Chemical Environment and Electronic Configurations

(i) Mössbauer-Effect Studies of the Formation of Xenon Bromides in Beta Decay[1]

G. J. Perlow and Hiroyuki Yoshida

The reaction $^{129}IBr_2 \xrightarrow{\beta^-} {}^{129}XeBr_2$ has been observed for a pure sample of the potassium salt by use of the Mössbauer effect of the 39.58-keV gamma ray of ^{129}Xe. With the assumption of p_σ bonding, the quadrupole splitting leads to a value of 0.41 electron transferred to each Br. This is to be compared with 0.52 to each Cl in $XeCl_2$ and 0.72 to each F in XeF_2. An impure $KIBr_2$ source shows a qualitatively different velocity spectrum—either due to a distribution of unknown xenon halides or to a molecular rearrangement observed in the act of occurring. If the latter explanation is correct, the line width gives a mean life $\tau_m \approx 3.5 \times 10^{-10}$ sec for the rearrangement. A source of $CsIBr_2$ gives a broad singlet spectrum with no trace of $XeBr_2$. The line represents either atomic xenon or a cubic rearrangement product such as $XeBr_6^{-4}$ or $XeBr_4^{-2}$. Evidence from data on the recoilless fraction and isomer shifts somewhat favors atomic xenon as the product but is not completely conclusive.

(ii) Tin Ions in Ice[2]

S. L. Ruby, P. K. Tseng, Hwa-Sheng Cheng,* and I. Pelah†

Tin ions dissolved in H_2O and then frozen can be studied by the Mössbauer effect. We have found that the dependence of the isomer shifts upon the concentration of added HX (X = F, Cl, Br, or I) suggests that the distribution of complex ions formed in the solution

[1] G. J. Perlow and H. Yoshida, J. Chem Phys. (in press).

[2] S. L. Ruby, P. K. Tseng, H.-S. Cheng, and N. C. Li, Chem. Phys. Letters 2, 39 (1968).

* Tsing-Hua University, Taipei, Taiwan.

† Solid State Science Division.

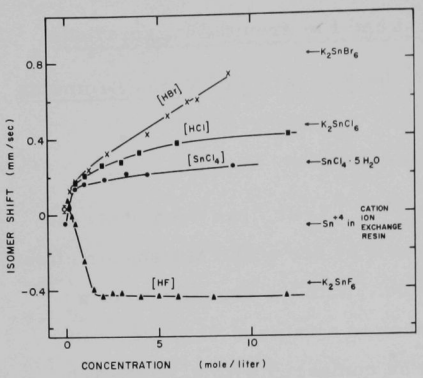

Fig. 39. Curves showing the variation of the isomer shift as a function of the concentrations of the indicated solvents. The labels [HBr], [HCl] and [HF] indicate that the isomer shift was measured with 0.22-molar $SnCl_4$ mixed with increasing concentrations of these solutions. The curve labeled [$SnCl_4$] was obtained by varying the concentration of $SnCl_4$ in pure water.

may be trapped by quick freezing. Some results are shown in Fig. 39. This may provide a new method of studying equilibrium constants.

The thermal vibrations of the Sn atoms in such ice, when studied as a function of temperature, are quite anomalous. In particular, there is a rapid increase in $\langle x^2 \rangle$ from about 170—190°K, and only a slow increase after that. Within the same temperature range, the conductivity of the ice increases by 10^2—10^3 times. The tin atoms do not appear to be mobile. We anticipate learning about the motion of ions in ice.

(iii) Mössbauer Investigation of Iron in Ordinary Chondrites[1]

E. L. Sprenkel-Segel

The recoilless resonant interaction of 14.4-keV gamma rays in ^{57}Fe was used for the investigation of iron minerals in the ordinary chondrites. The absorption spectra are composites of the 2-line patterns of olivine $(Mg, Fe)_2SiO_4$ and pyroxene $(Mg, Fe)SiO_3$ and the 6-line patterns of troilite FeS and kamacite (a nickel-iron alloy with body-centered cubic structure). With the exception of some

[1] E. L. Sprenkel-Segel, in Proceedings of the International Atomic Energy Agency Symposium on Meteorite Research, Vienna, 7—13 August 1968 (in press).

terrestrially weathered meteorites, all the ordinary chondrites have spectra of similar general appearance. The chief variant between the hypersthene and bronzite chondrites is the ratio of olivine iron to pyroxene iron. For the equilibrated bronzite chondrites, the mean value is 1.6; for the equilibrated hypersthene chondrites, the values cluster about 2.2.

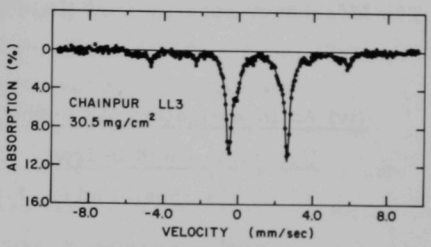

Fig. 40. Mössbauer absorption spectrum of the Chainpur unequilibrated meteorite. The most intense doublet corresponds to resonant absorption by ^{57}Fe in olivine; the inner (less intense) doublet corresponds to pyroxene absorption. This meteorite has been the subject of several Science articles indicating its primitive nature and has been suggested as an example of the precursory material of the equilibrated ordinary chondrites, the largest group of meteorites.

The absorption spectra of the unequilibrated chondrites Tieschitz, Bremervorde, Clovis No. 1, Hallingeberg, Barratta, and Chainpur have been measured at 77° and 300°K. The spectra (Fig. 40) appear to indicate very large ratios of olivine to pyroxene iron. In certain meteorites, however, some of the pyroxene iron resides in a nonequivalent lattice site such that the corresponding absorption is in the same region of the spectrum as the absorption by ^{57}Fe in olivine. When allowance is made for this effect, the olivine/pyroxene ratios become more similar to the ratios for the equilibrated ordinary chondrites.

It has been suggested that the equilibrated chondrites have been produced from unequilibrated material by thermal metamorphosis. However, the average iron contents for olivine and pyroxene in unequilibrated chondrites are much lower than the corresponding contents of the equilibrated chondrites (an exception is the bronzite olivine). Magnetite has been suggested as the source to raise the iron content of

the silicate system to the level observed for the equilibrated chondrites. The Mössbauer spectra show little or no magnetite, however, and the required amounts of iron are not present.

(iv) An Investigation of Conduction-Electron Contributions to the Hyperfine Field in Iron

L. E. Campbell and G. J. Perlow

The hyperfine field in iron is being measured as a function of external magnetic field by use of the Mössbauer effect and a superconducting magnet. Once the magnetization arising from localized moments is saturated, any increase in external field should appear directly at the nucleus — modified only by paramagnetic contributions from the conduction electrons. Thus if the slope of the plot of the hyperfine field as a function of the external field deviates from -1 in the high-field region, the amount of deviation will be a reflection of the paramagnetism due to the conduction electrons. Although the initial experiments did not quite have the necessary sensitivity, they suggested that reasonable modifications would make the measurement feasible. Such modifications are now being planned.

(v) Studies with ^{121}Sb

In Alloys with Sn (S. L. Ruby and Clyde W. Kimball*). Alloys of Sn and Sb have been made; it is possible to put about 8% of each into the other, but higher concentrations result in two-phase material. The isomer shifts have been studied as a function of concentration. The results indicate that beyond 4 electrons/atom, added electrons go almost completely into other than s-like wave functions centered on the tin nucleus.

---

*Metallurgy Division.

In Ferrites (S. L. Ruby and Billy Joe Evans†). Antimony has been substituted into several ferrites, and the Mössbauer effect has been used to examine the magnetic field the iron atoms produce at the site of this diamagnetic ion—even though an oxygen atom separates them. Transferred hyperfine fields have been studied in metals (e.g., Sb dissolved in Fe metal) but their magnitudes are not yet understood. Several authors lay much stress on conduction electrons. It is therefore of interest to consider insulators such as the ferrites in which the density of conduction electrons approaches zero. Despite the nonmagnetic oxygen atoms between the Fe and the Sb, the transferred field is even larger than for Sb dissolved in Fe metal.

(vi) Studies of Xenon Chlorides and Other Xenon Compounds by the Mössbauer Effect in ^{129}Xe[1]

G. J. Perlow and M. R. Perlow

The compounds $XeCl_2$ and $XeCl_4$ have been made in the beta decay of ICl_2^- and ICl_4^- containing radioactive ^{129}I. The electric-quadrupole interaction in the 39.6-keV excited state of the ^{129}Xe nucleus was employed to study these substances by the Mössbauer effect. The decay products were compared with XeF_2 and XeF_4 and with the parent ions. It was shown that the decays $ICl_2^- \rightarrow XeCl_2$ and $ICl_4^- \rightarrow XeCl_4$ both result in the recall of 0.2 electrons per bond from each ligand to the central atom. In the xenon halides the charges per fluorine are -0.72 and per chlorine are -0.5. The assumption of pure p_σ bonding in the xenon halides was tested by the isomer shifts. With its aid the shifts were calibrated by the quadrupole couplings. A shielding constant obtained from Hartree-Fock calculations by Wilson was then used to

†University of Chicago.

[1] G.J. Perlow and M. R. Perlow, J. Chem. Phys. 48, 955 (1968).

relate p-electron to s-electron transfer, which was next employed to examine the charges on the xenon atom in XeO_4 and XeO_6^{-4}. The former was prepared in beta decay, the latter equivalently either in beta decay or in bulk. It was shown that directed sp^3d^2 hybrid bonds for XeO_6^{-4} are inconsistent with the measured isomer shift. The recoilless fractions and linewidths were determined for a number of xenon compounds.

(vii) Studies of Cesium-Graphite Compounds

G. J. Perlow, G. L. Montet,* L. E. Campbell, and A. J. F. Boyle

In the continuing Mössbauer experiments on the cesium-graphite compound CsC_8, the absorbers are made from pyrolytic graphite with the c axis of the absorber oriented at a variety of angles with respect to the gamma-ray direction. These experiments are designed to demonstrate the very large anisotropy of the recoilless fraction in this compound. These spectra also exhibit the only clear case of quadrupole splitting in a cesium compound. They are being studied with an eye toward a possible measurement of the quadrupole moment of the first excited state in ^{133}Cs. In addition, data taken with an applied magnetic field are being analyzed for possible paramagnetic contributions to the field at the nucleus. Such contributions would throw light on the electronic structure of the cesium atom.

(viii) The Hyperfine Field at Cesium Nuclei in Iron

G. J. Perlow and L. E. Campbell

^{133}Ba decays by K capture to excited states of ^{133}Cs in which the Mössbauer effect may be observed. A Mössbauer source was prepared by implanting ^{133}Ba in iron foil, and absorption spectra have been taken in conjunction with a single-line absorber. The effects

*Solid State Science Division.

on the spectra obtained after subsequent annealing of the source were also observed. The experiments indicate that some of the cesium nuclei experience fields of 100—200 kG (considerably less than expected by current theories) while others experience virtually no field at all. This may be caused by too high a concentration of Ba atoms in the active portion of the foil. After annealing, all evidence of hyperfine fields disappears. It seems likely that the barium has become oxidized in the annealing process.

(ix) The Effect of Radio-Frequency Fields on the Mössbauer Effect in Magnetic ^{57}Co Sources[1]

G. J. Perlow

In an extension of experiments by E. C. Avery, C. Littlejohn, G. J. Perlow, and B. Smaller,[2] work was done to

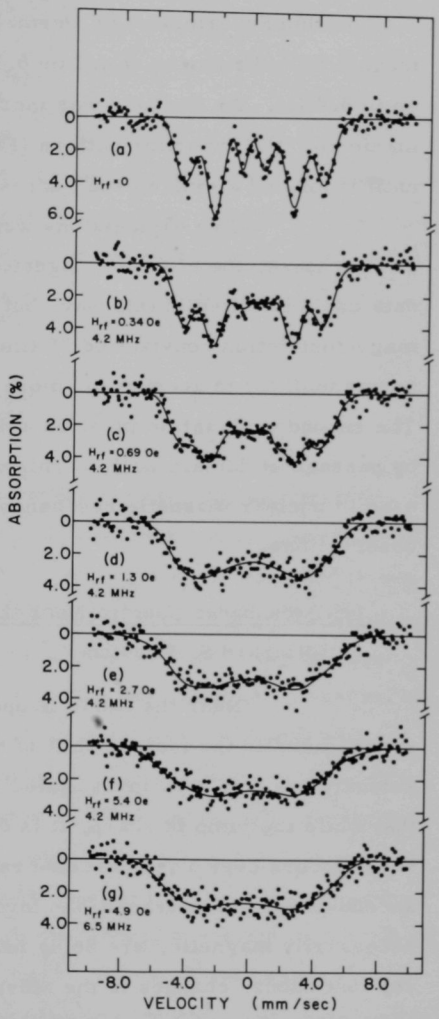

Fig. 41. The effect of the rf magnetic field. In runs (a)—(f), the field amplitude was increased from 0 to 5.8 Oe at 4.2 MHz. Run (g) was at 4.9 Oe and 6.5 MHz. The source was ^{57}Co diffused into Supermalloy; the absorber was sodium ferrocyanide.

[1] G. J. Perlow, Phys. Rev. 172, 319 (1968).

[2] Reported by G. J. Perlow, Allerton Park Conference Report, University of Illinois, 1960.

investigate the off-resonance effects described there. Sources of ^{57}Co in thin Supermalloy or Permalloy foils were placed in an rf magnetic field rotating at 4.2 or 6.5 MHz and having an amplitude of up to 5.4 Oe. As the field was increased from low values toward the maximum, the hyperfine pattern (Fig. 41) was observed to broaden until it formed a single broad unresolved band.

Two explanations were tested by computation. In the first of these, the effect of magnetostriction was considered. The data could be fitted in this way, but the fit required that the magnetostriction constant be 25 times its bulk value. It therefore seems unlikely to account for more than a small part of the effect. The second explanation involves a disturbance of the radiating nuclei by passage of domain walls. This was treated by theoretical techniques used in nuclear magnetic resonance and could be made to fit the observations.

(x) Mössbauer Spectra Near the Magnetic Curie Temperature

Richard S. Preston

Near the Curie temperature in iron there is a rather sudden jump in the isomer shift of the Mössbauer spectrum. This anomaly has now been investigated in detail and it has become clear that while the jump is sharp, it is definitely not a discontinuity. That is, it occurs over a temperature range of about 0.3^{o} at $1040^{o}K$. Other second-order phase transitions involving different kinds of order, not necessarily magnetic, are being investigated to see whether abrupt, yet continuous, changes in the Mössbauer spectrum are characteristic of second-order phase transitions generally. A change in the isomer shift has been observed at the Curie temperature of a 60-40 NiFe alloy. It is similar to the change in the isomer shift in pure iron.

c. Mössbauer Techniques and Equipment

(i) Studies with Uranium

S. L. Ruby and G. M. Kalvius*

In addition to work on ^{237}Np, we have made several more attempts to use Mössbauer techniques to study uranium. Our attempts to use Coulomb excitation by Van de Graaff accelerators have yielded unsatisfactory results. Hence we are now attempting to use α particles from the decay of ^{240}Pu and ^{242}Pu to produce the 45-keV gamma rays needed in a study of ^{236}U and ^{238}U.

(ii) Improved Mössbauer Spectrometer

Richard S. Preston

A new procedure has been developed for accumulating a Mössbauer spectrum in the multichannel analyzer. It is superficially similar to an older procedure in which the analyzer is operated in the "pulse-height" mode and the horizontal scale of the stored spectrum is a linear function of velocity, so that irregularities in the spectrum caused by nonlinearity of the actual velocity waveform can be corrected with the help of a dummy spectrum accumulated concurrently with the Mössbauer spectrum. The new procedure differs from the old in that (1) the analyzer is operated in the faster "time" mode, (2) concurrent accumulation of a dummy spectrum causes negligible interference with the accumulation of the real Mössbauer spectrum, and (3) there are no appreciable statistical fluctuations in the dummy spectrum to contribute to the statistical fluctuations of the final, corrected spectrum. It represents an improvement over the standard "time" mode of operation in that the horizontal scale is linear in velocity, and that careful control of the actual velocity waveform is not necessary.

---

*Solid State Science Division.

(iii) Computer Techniques for Use with Mössbauer Spectrometers

New digital computer techniques have been introduced to improve both the taking and the analysis of data.

On-Line Data Collection from Spectrometers (R. H. Vonderohe,* R. J. Pecina,† J. A. Wiesmes,† and D. N. Olson). A small general-purpose digital computer is now being used to acquire data from three Mössbauer spectrometers simultaneously. The spectrometers are interfaced to the computer so as to permit channels to be accumulated in the core memory of the computer without action by the central processing unit (CPU). In this manner the CPU is able to perform the various tasks of data preprocessing before outputting for final processing on a larger computer, to control the actual output and non-real-time data input as well as program input functions, and to control the oscilloscope display with the associated parameter variables. In addition, the computer can perform other programmable tasks without interfering with the data-collection function.

Data Analysis (R. S. Preston, S. L. Ruby, and B. J. Zabransky). New computer programs have been developed for the analysis of Mössbauer spectra exhibiting the effects of combined magnetic-dipole and electric-quadrupole interactions with the nucleus. Least-squares fitting is now done directly by adjusting the parameters of the interaction for best fit to the data, rather than by the old two-step process which included a considerable amount of human trial and error.

---

*Applied Mathematics Division.

†Electronics Division.

2. ATOMIC-BEAM RESEARCH

a. Investigations of Stable Isotopes

W. J. Childs and L. S. Goodman

The previous report described the results of a series of experiments that measured the hyperfine structure of several atomic levels in each of two electronic configurations of ^{51}V. The present form of the theory of the hyperfine interaction (with the appropriate adjustable parameters) was found to be adequate for understanding the observations in the $3d^3 4s^2\ ^4F$ term. During the past year, similar studies have been made in ^{59}Co; in particular, the $3d^7 4s^2\ ^4F$ term has been studied. The situation differs from the conjugate case in ^{51}V principally in that (1) the departure from the LS limit is much more severe for Co, and (2) the electric-quadrupole interaction is much stronger for Co, and can thus be measured with relatively much higher precision. Thus a more demanding test can be made of the theory for ^{59}Co than for ^{51}V. Although agreement between theory and experiment is still remarkably good, certain differences were found. Measurements were also made for the $3d^8 4s\ ^4F$ term of ^{59}Co. A paper describing the results and their interpretation has been accepted for publication in the Physical Review.

The theory of the hyperfine interaction of an atom in its nuclear ground state makes definite predictions of the variation of the interaction constants between different metastable atomic states. The theory can best be tested in an atom that has many atomic levels of the same configuration lying low enough to be populated in an atomic beam. Measurements are currently being made on levels of the $5d^2 6s$ configuration of ^{139}La. Of the 16 theoretical levels, 15 have been identified from optical spectra, and hfs data have already been obtained on eleven of these. It is hoped that high-precision measurements can ultimately be made for all 15 levels. When the work is complete,

rather sophisticated tests of the theory can be made; and in addition, the appropriate radial integrals, which are treated as adjustable parameters, can be evaluated.

A number of improvements have been made in the atomic-beam laboratory, particularly in regard to electronic equipment. The sweeping system for the rf has been completely linearized by the use of a Hewlett-Packard frequency synthesizer. The output is swept through a range of any width up to 1 Mc/sec at 30 Mc/sec in conjunction with the multichannel scaler. The 30-Mc/sec output is then mixed with crystal-stabilized sources to provide a swept output at any desired frequency.

Our ability to produce and measure both frequency and power level at microwave frequencies have also been improved substantially. We now have available 1 W of swept, phase-locked, rf power through 8 Gc/sec.

b. Investigations of Radioactive Isotopes

J. A. Dalman, H. Diamond,* L. S. Goodman, and H. E. Stanton

A new atomic-beam apparatus for measurements on radioactive isotopes (especially transuranic species) has been installed in the "hot wing" of the Chemistry Building. Resonances in some stable isotopes have been observed and the machine parameters have been optimized. After some minor modifications of the vacuum system, measurements on radioactive atoms will begin.

The frequencies measured in these experiments depend on both nuclear and atomic properties and on their interaction. The analysis therefore yields not only nuclear parameters (spins and magnetic-dipole and electric-quadrupole moments) but also such atomic quantities as the hyperfine-interaction constants, the value of

---

*Chemistry Division.

$\langle 1/r_e^3 \rangle_{av}$, an identification of the electronic angular momentum J of the atomic ground state, and the values of g_j.

Argonne is an especially good place to carry out this kind of research. Source preparation requires expertness on the very frontiers of actinide radiochemistry, and this joint effort of the Physics and Chemistry Divisions relies strongly on the heavy-element chemistry group.

3. HIGH-FREQUENCY PLASMAS

The central purpose of this research is to advance the understanding of the basic properties of low-pressure gaseous discharges and plasmas produced by high-frequency fields. The two lines of experimental and theoretical investigation being pursued are studies of plasmas produced (1) in the approximately uniform rf electric field between plane parallel electrodes and (2) in the nonuniform standing-wave fields in resonant cavities.

a. Plasmas in Uniform Electric Fields

A. J. Hatch and M. Hasan

The main goal of this work is to elucidate the basic mechanisms involved in high-frequency plasmoids and other resonant discharge modes that occur at pressures in the vicinity of the collision-frequency transition ($\sim 10^{-5}$—1 Torr). Our approach has been to measure the complex impedance Z_p (or admittance) by a substitution method and to correlate the results with a slab-model theory. Two papers describing this work were presented at the 8th International Conference on Phenomena in Ionized Gases, Vienna, 27 August—2 September 1967. However, because of the highly nonlinear nature of the plasmas, these earlier results leave significant aspects of the various phenomena unexplained. Therefore, we have recently modified the substitution method of measurement (in which the exciting circuit is retuned with the discharge present) so that Z_p is measured as a function of any tuned or detuned condition of the circuit. This is

in essence a slotted-line type of measurement which is done at our relatively low operating frequency of 45 MHz by measuring the feed-line potential at four positions spaced at intervals of one-eighth of a wavelength. The results are expected to give values of Z_p that can be correlated with observed mode changes during the retuning process and thus reveal more about the nonlinear nature of the various plasma modes.

b. Plasmas in Nonuniform Cavity Fields

A. J. Hatch, S. Halverson,* and W. E. Smith†

The main goals of this work are to elucidate the basic phenomena and mechanisms of plasmas produced in the standing-wave fields of resonant cavities and to study the time-averaged drift forces on plasmas in such fields with special attention to their confinement properties. Two significant advances—one theoretical, the other experimental—have been made during the past year.

The experimental advance has been the development of a frequency-shifting method of exciting a plasma in the cavity while maintaining the essential field structure of the exciting normal mode. The excitation frequency has been shifted by as much as 10% above the empty-cavity frequency (unloaded $Q \approx 4000$) with a resultant ten-fold increase in plasma density, all at a constant input power ($\sim$35 W) to the cavity with its impedance-matching network. The significance of this method of increasing plasma density can be appreciated by noting that to have obtained the same increase by increasing power without shifting frequency would have required a 100-fold increase in power.

The theoretical advance has been the derivation of expressions for the electric and magnetic rf polarizability of a plasma sphere as a function of plasma density. From these expressions the

*Electronics Division.

†Applied Mathematics Division.

low- and high-density limiting potential functions for confinement have been retrieved and the transition behavior at intermediate densities has been determined.

Two papers describing both of these advances were presented at an International Colloquium on the Interaction of High-Frequency Fields with Plasmas, Saclay, France, January 1968, and will be published in the proceedings of the colloquium.

4. MASS-SPECTROMETRIC INVESTIGATIONS

The mass-spectrometric investigations employ seven instruments, each designed for one or more specific fields of activity. Mass spectrometer MA-15B is used primarily in the study of the molecular composition of high-temperature vapors but is also used together with MA-18 for gas-phase molecular reactions and dissociations. Extensive studies of photodissociation in complex molecular species are carried out on MA-24, which is provided with a vacuum ultraviolet monochromator. The spectrometer MA-17 is equipped with an energy analyzer and is being used to study the kinetic energy liberated in molecular reactions and fragmentations. Two additional instruments, MA-25 and MA-27, are in use in molecular and ionic sputtering experiments and similar investigations involving surface properties and reactions. The portable mass spectrometer (MA-28) is used at various accelerators in studies of the phenomena involved in ion bombardment of polycrystalline and monocrystalline foils and thick targets. An old instrument MA-16A is at present on a stand-by basis.

The main emphasis of these investigations is on providing fundamental information on the thermodynamics and kinetics of chemical reactions, the interaction of radiation with matter, desorption kinetics, the interactions of energetic ions bombarding crystal surfaces, molecular structure, and similar aspects of the properties of matter.

a. Ionization and Fragmentation of Gas Molecules

J. Berkowitz, W. A. Chupka, W. Jivery, and T. A. Walter

(i) Photoionization Studies of Small Molecules

Photoionization cross sections as a function of photon energy have been measured for parent and most fragment ions with

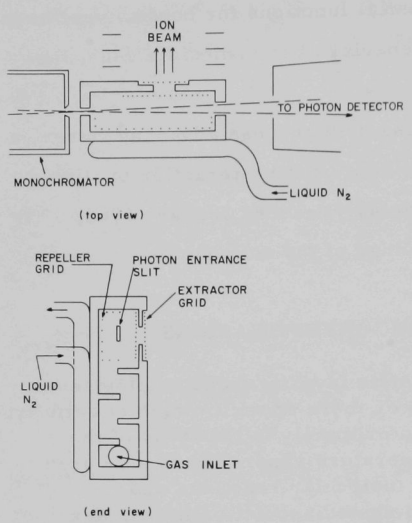

Fig. 42. Liquid-nitrogen-cooled photoionization chamber. The use of repeller and extractor grids that could be warmed to evaporate any condensed insulating deposits ensured freedom from erratic behavior caused by the charging of surfaces inside the chamber.

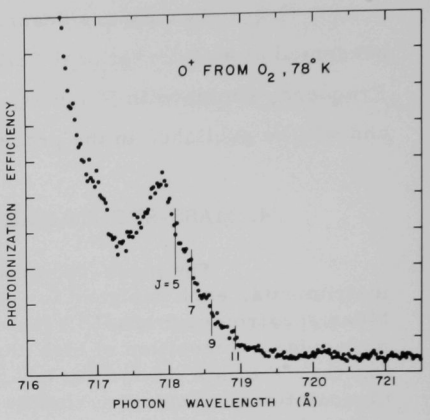

Fig. 43. Photoionization efficiency at the threshold for the process $O_2 + h\nu \rightarrow O^+ + O^-$, obtained with the photoionization chamber shown in Fig. 42. Similar data taken at room temperature show a much broader Boltzmann distribution of rotational states. This broader distribution leads to a more complicated structure which cannot be analyzed reliably.

improved resolution (to ca. 0.12 Å) and at temperatures down to 78°K (Fig. 42) for O_2, N_2, CH_4, C_2H_4, CF_4, and C_2F_4. The cross section for production of $O^+ + O^-$ from O_2 at 78°K (Fig. 43) has shown partially-resolved rotational fine structure at threshold. Preliminary analysis of the data has yielded the value 1.456 ± 0.004 eV for the electron affinity of the O atom. The controversial ionization potential of CH_4 has been unambiguously determined to be 12.60 ± 0.01 eV. A study of vibrational structure near the ionization threshold shows that the predominant excitation of the CH_4^+ ion is to a normal vibration of wave number 1085 cm^{-1}. This value is consistent with a theoretical prediction that the ground state of

the CH_4^+ ion has C_{3v} symmetry as a result of the Jahn-Teller effect. More accurate values of some bond energies of polyatomic molecules were obtained by carrying out photoionization measurements at lower temperatures in order to minimize the effects of thermal vibrational and rotational energy.

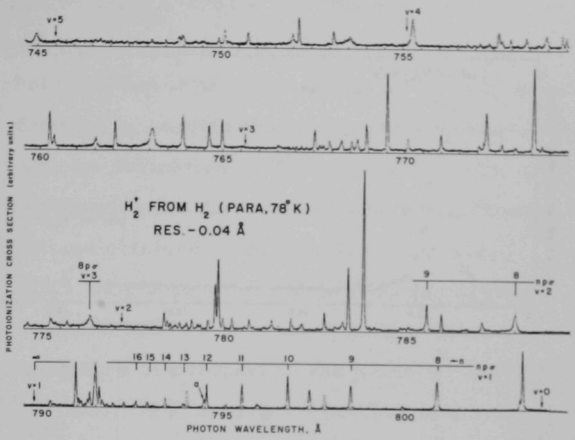

Fig. 44. Relative photoionization cross section of para H_2 at 78°K, measured with a resolution width of 0.04 Å. Some of the autoionized members of the Rydberg series converging to the v = 1 and v = 2 states of the H_2^+ ion are indicated. Lower limits on the lifetimes can be estimated from the line widths.

(ii) Photoionization of the Hydrogen Molecule

Further analysis of the autoionization fine structure in the ionization threshold region of H_2 has shown that at least most of the autoionizing states are vibrationally-excited Rydberg states that converge to vibrationally-excited states of the H_2^+ ion. Especially enlightening is the photoionization-efficiency curve (Fig. 44) of para-H_2 taken at 78°K. States of principal quantum number $\gtrsim 8$ have lifetimes greater than 10^{-12} sec—contrary to the earlier theoretical calculations of Berry but in agreement with recent estimates of Bardsley. Analysis of the data also shows that as the principal quantum number n increases, the R(0) lines of the Π system of Rydberg states diminish in intensity while the R(0) lines of the Σ system and the Q(1) lines of the Π system remain intense. This is very probably a result of the transition of the coupling from Hund's case (b) to his case (d) as n increases, together with the preference for ionization to occur without change in rotational quantum number.

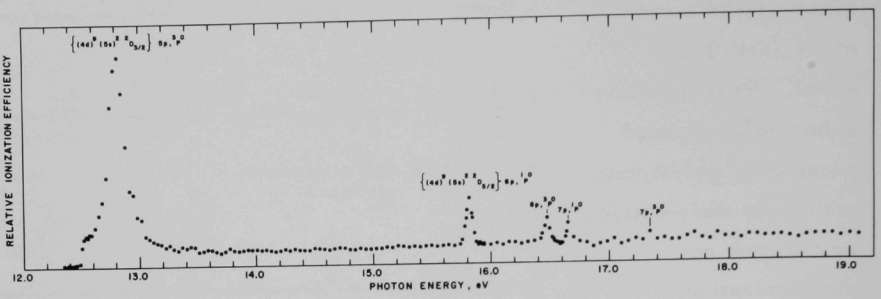

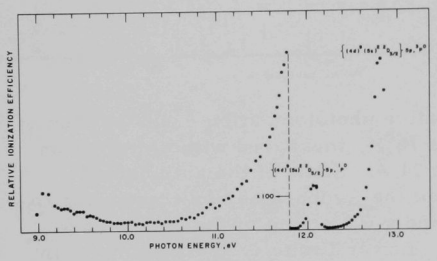

Fig. 45. Ionization-efficiency curves of cadmium vapour. Below: The region of the hydrogen many-line spectrum. The dispersion was 8.3 Å/mm, the width of the entrance slit was 1000 microns, and that of the exit slit was 300 microns. Above: The region of the helium continuum. The dispersion and exit slit were as in the lower curve, but the entrance slit was narrowed to a width of 300 microns. The upper curve is matched to the lower in the region of overlap.

b. Photoionization of High-Temperature Vapors

J. Berkowitz, W. Jivery, and T. A. Walter

The vapors of Cd and Hg have been investigated, and were shown to have very intense autoionization peaks and relatively weak continua (Fig. 45). The peaks correspond to excitations of inner d electrons of the neutral atoms. Oscillator strengths have been measured for the autoionization peaks in Cd.

Photoionization-efficiency curves of sulfur molecular species generated by various solids have been measured. The ionization potentials (in eV) deduced are 9.36 ± 0.02 for S_2, 9.68 ± 0.03 for S_3,

8.60 ± 0.05 for S_5, 9.00 ± 0.03 for S_6, 8.67 ± 0.03 for S_7, and 9.04 ± 0.03 for S_8. No evidence for structures other than rings has been obtained. The threshold for dissociative ionization of S_8 is in very good agreement with that deduced by earlier thermodynamic measurements.

The thresholds for formation of Tl^+ from TlF, TlCl, and TlBr have been utilized to determine the dissociation energies of these diatomic molecules. The values obtained (4.57 ± 0.02 eV for TlF, 3.82 ± 0.02 eV for TlCl, and 3.42 ± 0.02 eV for TlBr) are in excellent agreement with some recent thermochemical data. The TlF value provides confirmation for existence of barriers in the potential energy curves of its $^3\Pi_{0+}$ and $^3\Pi_1$ states. The ion pairs from TlF and TlCl are formed with considerable kinetic energy, probably by a predissociative mechanism.

c. Chemi-Ionization by Photon Absorption

J. Berkowitz, W. A. Chupka, W. Jivery, and T. A. Walter

The production of H_3^+ ions by the reaction of H_2 with electronically excited H atoms and H_2 molecules was studied further by measuring the photoionization cross section for production of H_3^+ from para hydrogen at $78^\circ K$, with resolution to 0.12 Å from 848 to 810 Å. The data are being analyzed to determine the identity of the excited states of H_2 which react to form H_3^+.

The only chemi-ionization reactions of an excited polyatomic molecule reported in the literature are

$$C_2H_2^* + C_2H_2 \begin{cases} \rightarrow C_4H_3^+ + H + e^-, \\ \rightarrow C_4H_2^+ + H_2 + e^-. \end{cases}$$

We have attempted to observe these reactions but the results were negative and indicate strongly that the published results are in error.

Our negative results support the view that chemi-ionization reactions by excited polyatomic molecules occur rarely if at all, probably because of the severe competition from predissociation of the excited molecule.

Attempts to observe chemi-ionization reactions in gaseous ethylene and acetone below their respective ionization energies yielded negative results. In the case of acetone, a small amount of ionization was found to occur just below (by ca. 1—2 Å) the ionization threshold. Part of this is due to "hot bands" but some was proportional to the square of the gas pressure, and was probably due to collision-induced ionization of molecules in electronically excited states just below the ionization threshold. The ions so produced were parent ions.

d. Study of Fragmentation Processes

H. E. Stanton

Developments of the mass spectrometer used to study fragmentation processes in molecules have proceeded slowly and with low priority. An electronic circuit to sweep the kinetic energies has been designed and built and is ready for installation. The pulse-height analyzer has become available recently and a suitable interface to adapt it to the spectrometer is being studied.

The theoretical developments have run into computational difficulties and are also proceeding with reduced emphasis because of involvement in other more urgent work. The aims of the investigation continue to appear to be worth while and are being pursued as actively as time permits.

e. Studies of Negative-Ion Formation with the New High-Resolution Mass Spectrometer (MA-28)

M. Kaminsky and P. Williams

The Argonne-built pulsed-molecular-beam mass spectrometer (MA-25) has been used to study the mean residence times

τ_i of alkali ions on atomically clean surfaces of polycrystalline tungsten. In the earlier phases of this study, it was observed that (contrary to earlier reports from other authors) the values of τ_i did depend on the composition of the incident beam. (For example, changing from alkali metal sources to alkali chloride sources resulted in a significant change in τ_i.) The results indicated strong processes of adsorption and absorption of chlorine on the tungsten substrate with the possible formation of tungsten chloride compounds.

To check this hypothesis, a search for negative ion species formed during the bombardment of heated polycrystalline tungsten surfaces by a KCl beam was started. The first results indicate that the dominant negative ion species is Cl^-; no negative molecular chlorine ions Cl_2^- could be observed. With the high sensitivity of the machine, it could be established that any Cl_2^- ion current could not be more than 1×10^{-6} of the Cl^- ion current. Other negative ion species (e.g., CN^- and $C_2H_2^-$) formed by surface ionization could be observed, but not a stable negative ion of a tungsten chloride compound (e.g., WCl_6^-). We intend to search for neutral species of tungsten chloride.

A very important preliminary result is the observation (using a simple shutter device with instrument MA-28) that the lifetime of negative chlorine ions on surfaces is approximately two orders of magnitude longer than for positive ions under corresponding conditions. No lifetime data on negative ions have ever been reported in the literature. We intend to check these preliminary results with the more suitable machine MA-25.

Another important result was the observation that under certain well-reproducible operating conditions in the ion source, two processes (electron attachment and surface ionization) contributed to the negative-ion formation. A surprisingly large number of negative ions (approximately 2—3 orders of magnitude higher than could be

expected from surface ionization alone) was observed if a resonance condition for optimum electron attachment was achieved. (Resonance energies for the formation of certain negative ion species were found to be as sharp as ±0.5 eV.) This mode of source operation will be studied for further application as an ion source for the Physics Division tandem Van de Graaff accelerator.

f. The Effect of Ion Channeling on the Energy Losses of Energetic Protons in Silver, Gold, Tungsten, and Tantalum Monocrystals of Various Crystallographic Orientations

M. Kaminsky

In earlier experiments we reported that the crystallographic orientation affects the yields from such secondary phenomena as back sputtering, secondary-ion emission, and secondary-electron emission from metal monocrystals (e.g., Cu or Ag) under the impact of light ions (e.g., H^+ or D^+) in the energy range from 0.2 to 2.0 MeV. The yield data suggested a close relationship between the production of secondary particles and the characteristic energy loss of the incident ion traveling along certain crystallographic directions within a critical region of the monocrystalline target.

Since there were no reliable data available for the rate at which light ions (e.g., H^+ or D^+) with energies in the region of interest (0.2—2.0 MeV) lose energy in the metal monocrystals, last year we started to study how the crystallographic orientation affected the energy loss of protons directed along the [111], [100], and [110] directions of Cu monocrystals. These measurements were now extended to monocrystals of Ag ([111], [100], and [110] directions), Au ([100] direction), W ([111] direction), and Ta ([111] direction) for the energy range from 750 keV to 2.0 MeV. Over an area four times that actually struck by the beam, each foil thickness varied $\lesssim$ 3%.

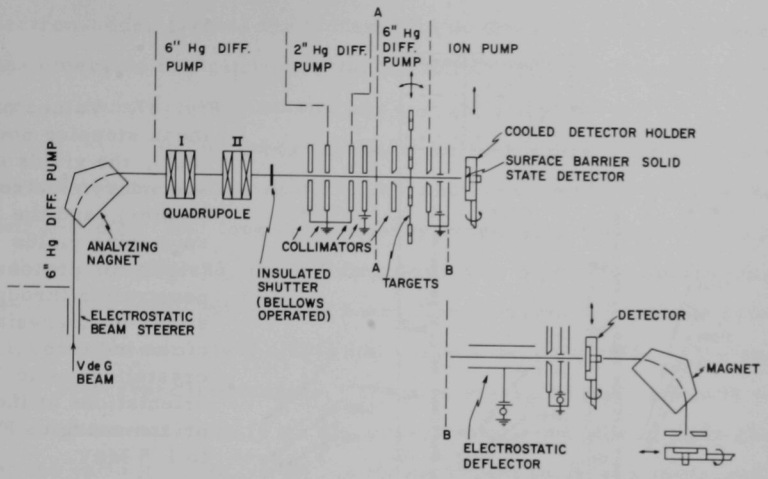

Fig. 46. Experimental arrangement: (upper diagram) as used to measure characteristic energy losses of ions in metal monocrystals and (at right below) as used to measure the distribution of charge states of ions penetrating through polycrystalline or monocrystalline metal foils.

The angular spread of the incident proton beam was $< 0.01^{\circ}$ and the angle of incidence was defined to $< 0.1^{\circ}$. The emerging particles (H^+ or D^+) were collimated before being analyzed with a surface-barrier solid-state detector, as shown in the upper portion of Fig. 46.

Whenever the proton beam was incident in one of the low-index directions (e.g., [111]), we observed that the energy spectrum of the emergent particles consisted of two well-separated peaks. The low-energy peak was characteristic of the normal energy loss E_n expected for polycrystalline targets, while the high-energy peak (with average energy E_c) is probably due to channeled protons. If the proton beam was incident parallel to the [111], [100], or [110] directions of the Ag monocrystal, the value of $(dE/dx)_{av}$ for peak E_c decreased in the order [111] > [100] > [110]. This is the same order we observed earlier in the yields of sputtered particles, of secondary ions, and of secondary electrons. The curves are shown in Fig. 47. It appears that the new stopping-power data will provide a more quantitative theoretical description of the secondary phenomena mentioned.

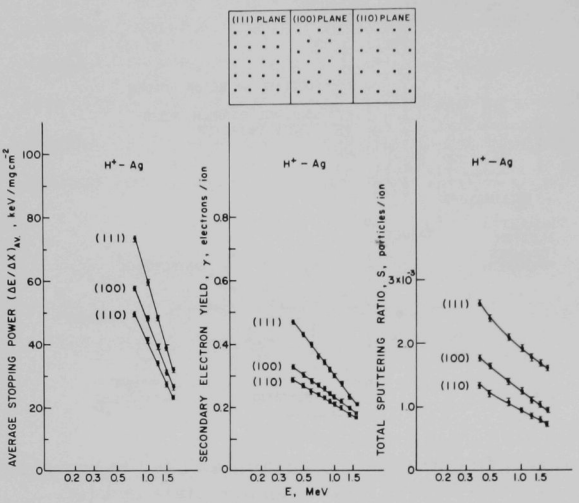

Fig. 47. Values of the mean stopping power (left), the yields of secondary electrons (center), and the sputtering yields (right) for protons penetrating through silver monocrystals of the indicated crystallographic orientations at incident proton energies E up to 1.5 MeV.

g. The Effect of Channeling on the Charge-Changing Collisions of Energetic $^3He^+$ Ions Penetrating Through Au(100) Monocrystals

M. Kaminsky

A new program of measuring the distribution of the charge states of energetic ions penetrating through polycrystalline or monocrystalline metal foils was started. The new portable high-resolution mass spectrometer (MA-28) was used in conjunction with the 2-MeV Van de Graaff and its associated beam-handling equipment.

In the past, most studies of charge-changing collisions were conducted in gaseous targets and in a few polycrystalline solid targets. For light ions penetrating through metal monocrystal foils, information is completely lacking. However, such studies in monocrystal foils promise to yield more information on the way in which the electron density distribution in the "lattice channels" affects the processes of electron capture and electron loss by the penetrating ions. In addition, such information may prove useful in the operation of electron-stripping and

electron-adder targets for tandem Van de Graaffs, since it appears that ions emerging from monocrystalline foils have a much larger emittance (i.e., a much larger intensity per unit solid angle).

In our experiments, a Au(100) foil (0.9 mg cm^{-2} thick) and two polycrystalline Au foils (0.8 and 1.98 mg cm^{-2} thick) were bombarded by $^3He^+$ ions in the energy range from 600 keV to 2.0 MeV. In these experiments, the incident beam was highly collimated (angular spread less than 0.01^o). The beam direction was 0.5^o off the [100] axis in the case of the Au(100) foil and was perpendicular to the surface of the polycrystalline targets. The ions emerging from the foils were analyzed magnetically (Fig. 46, lower right) according to their charges, and the ratio $R = {}^3He^{++}/{}^3He^+$ in the emergent beam was measured for different primary $^3He^+$ energies in the range from 600 keV to 2.0 MeV. For the two polycrystalline targets, it was found that the ratio R varied from approximately 0.3 to 40 as the average energy of the emergent beam (not primary ion energy!) varied from 300 keV to 1 MeV. When the monocrystalline foil was bombarded, the energy spectrum of the emergent beam consisted of two well-separated peaks. The low-energy peak was characteristic of the normal energy loss expected for polycrystalline targets. The ratio R was determined for this peak. After normalization for the same energy of the emergent beam, it was found that the values of R for this normal peak were nearly identical to those obtained from the polycrystalline foils.

For the high-energy peak, which is due to channeled He ions, the first preliminary measurements of R reveal very interesting results. It is found that the ratio R after normalization for the same emergent beam energy is only about 1/2 to 1/3 of the value of R for the low-energy peak at the same energy, as shown in Fig. 48. The result indicates that the electron stripping probability is reduced if the penetrating ion moves in (and escapes from) regions of lower electron density (as for instance in the center of lattice channels).

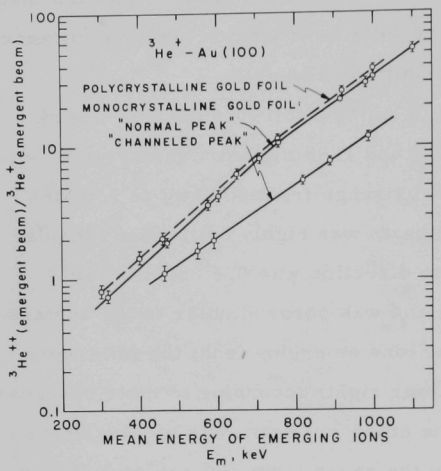

Fig. 48. The ratio $R = {}^3He^{++}/{}^3He^+$, both measured in the emergent beam, as a function of the mean energy of the emerging ions. The curves are for $^3He^+$ ions incident normal to the surface of an Au(100) foil or of a polycrystalline Au foil.

These experiments will be continued for different target materials and different crystallographic orientations. Studies of the effect of channeling on the electron capture processes will be started as soon as thinner monocrystalline metal films (100—500 $\mu g\ cm^{-3}$ thick) can be produced.

h. Production of Thin Monocrystalline Metal Foils and Monocrystalline Tungsten Filaments

M. Kaminsky and G. Goodwin

New programs of producing thin monocrystalline metal foils (5—0.05 μ thick) and thin monocrystalline tungsten wires have been initiated to provide targets for the measurements mentioned in Secs. IV. 4e—g.

In one method, we started with 0.018-in. monocrystalline metal sheets and thinned them by eloxing (done in Metallurgy) to the lowest possible limit (at present 0.0008 in.). These foils were then thinned further by electropolishing and etching. In this way, foils as thin as ~0.0001 in. could be prepared with reasonable usable areas

($\sim$4 mm^2) and a high degree of monocrystallinity. It appears, however, that this method will not permit us to obtain much thinner foils.

Therefore the ultrahigh-vacuum bell jar is being prepared for growing thin monocrystalline metal films epitaxially. Additional equipment will be needed (such as an electron gun and power supplies, a film-thickness monitor, a unit to control the deposition rate, and a multi-beam interferometer) to grow and characterize the thin films.

With the aid of our new ultrahigh-vacuum bell jar, we succeeded in growing monocrystalline tungsten wire with a "hot-zone strain-annealing" technique. These tungsten wires have diameters of 0.003 in., 0.005 in., or 0.008 in.; the length of $\sim$20 cm is occupied by several monocrystalline regions $\sim$2—3 cm long. These wires are used in the experiments mentioned in Sec. IV. 4e.

i. Operation of the 2-MeV Van de Graaff Accelerator

Jack R. Wallace

The 2-MeV Van de Graaff accelerator has operated 1345 hours from 1 April 1967 to 31 March 1968. It is operated 40 hours per week.

Considerable time was spent in realigning the beam-transport tubes and their associated components to improve the beam focusing at the target. To facilitate servicing of the power supply for the analyzing magnet, we have obtained new schematic diagrams from High Voltage Engineering. These include suggested improvements that will up-date the circuits.

V. PUBLICATIONS FROM 1 APRIL 1967 THROUGH 31 MARCH 1968

The papers listed here are those whose publication was noted by the reporting unit of the Laboratory in the 1-year period stated above. The dates on the journals therefore often precede this period, and some dated within the period will be listed subsequently. The list of "papers and books," which also includes letters and notes, is classified by topic; the arrangement is approximately that followed in the Table of Contents of this Annual Review. The "reports at meetings" include abstracts, summaries, and full texts in volumes of proceedings; they are listed chronologically.

A. PUBLISHED PAPERS AND BOOKS

1. MEASUREMENT OF THE POLARIZATION OF THERMAL NEUTRON BEAMS OF MIXED VELOCITIES
   S. H. Barkan, E. Bieber, M. T. Burgy, S. Ketudat, V. E. Krohn, P. Rice-Evans, and G. R. Ringo
   Rev. Sci. Instr. 39, 101-104 (January 1968)

2. PRECISION DETERMINATION OF THE C^{12}-C^{13} NEUTRON SEPARATION ENERGY
   W. V. Prestwich, R. E. Coté, and G. E. Thomas
   Phys. Rev. 161, 1080-1082 (20 September 1967)

3. TOTAL NEUTRON CROSS SECTION OF LANTHANUM
   Hla Shwe, R. E. Coté, and W. V. Prestwich
   Phys. Rev. 159, 1050-1056 (20 July 1967)

4. SPECTRUM OF HIGH-ENERGY GAMMA RAYS FOLLOWING THERMAL-NEUTRON CAPTURE BY Er^{166}
   W. V. Prestwich and R. E. Coté
   Phys. Rev. 162, 1112-1118 (20 October 1967)

5. GAMMA-RAY SPECTRA OF Co^{60} AND Mn^{56} FOLLOWING RESONANCE-NEUTRON CAPTURE IN Co^{59} AND Mn^{55}
   W. V. Prestwich and R. E. Coté
   Phys. Rev. 155, 1223-1229 (20 March 1967)

6. RESONANCE NEUTRON CAPTURE IN THE EVEN-A ISOTOPES OF TUNGSTEN
   W. V. Prestwich and R. E. Coté
   Phys. Rev. 160, 1038-1042 (20 August 1967)

7. HIGH-SENSITIVITY NEUTRON-CAPTURE GAMMA-RAY FACILITY
   G. E. Thomas, D. E. Blatchley, and L. M. Bollinger
   Nucl. Instr. Methods 56(2), 325-337 (1967)

8. AVERAGE WIDTHS FOR HIGH-ENERGY RADIATIVE TRANSITIONS
   L. M. Bollinger and G. E. Thomas
   Phys. Rev. Letters 18, 1143-1147 (19 June 1967)

9. ENERGY DEPENDENCE OF HIGH-ENERGY K CONVERSION COEFFICIENTS
   R. K. Smither
   Phys. Letters 25B(2), 128-129 (August 1967)

10. LOW-LYING EXCITED STATES OF Ag^{108} AND Ag^{110} POPULATED IN THERMAL-NEUTRON-CAPTURE REACTIONS
    H. H. Bolotin and A. I. Namenson
    Phys. Rev. 157, 1131-1136 (20 May 1967)

11. THERMAL-NEUTRON-CAPTURE GAMMA-RAY STUDIES OF THE EXCITED STATES OF ODD-A HAFNIUM ISOTOPES
    A. I. Namenson and H. H. Bolotin
    Phys. Rev. 158, 1206-1213 (20 June 1967)

12. LIFETIME OF THE 1.042-MeV STATE IN ^{18}F
    A. E. Blaugrund, D. H. Youngblood, G. C. Morrison and R. E. Segel
    Phys. Rev. 158, 893-897 (20 June 1967)

13. SPEED OF THE $\Delta J = 1$, $\Delta T = 1$ M1 TRANSITION IN Al^{28}
    D. H. Youngblood, R. C. Bearse, N. Williams, A. E. Blaugrund, and R. E. Segel
    Phys. Rev. 164, 1370-1374 (20 December 1967)

14. LIFETIMES OF THE FIRST TWO LEVELS IN ^{30}P
    E. F. Kennedy, D. H. Youngblood, and A. E. Blaugrund
    Phys. Rev. 158, 897-900 (20 June 1967)

15. LIFETIMES OF THE FIRST AND THE THIRD EXCITED STATES OF Ca^{41}
P. P. Singh, R. E. Segel, R. H. Siemssen, S. Baker, and A. E. Blaugrund
Phys. Rev. 158, 1063-1068 (20 June 1967)

16. RADIATIVE-CAPTURE STUDIES OF THE GIANT DIPOLE RESONANCE
Ralph E. Segel
Science 158, 723-730 (10 November 1967)

17. RADIATIVE CAPTURE BY ^{19}F: THE GIANT DIPOLE RESONANCES IN ^{20}Ne
R. E. Segel, Z. Vager, L. Meyer-Schützmeister, P. P. Singh, and R. G. Allas
Nucl. Phys. A93(1), 31-48 (1967)

18. THE GIANT DIPOLE RESONANCE EXCITED BY α CAPTURE
L. Meyer-Schützmeister, Z. Vager, R. E. Segel, and P. P. Singh
Nucl. Phys. A108(1), 180-208 (1968)

19. STUDY OF THE (d, p) REACTION IN THE 1p SHELL
J. P. Schiffer, G. C. Morrison, R. H. Siemssen, and B. Zeidman
Phys. Rev. 164, 1274-1284 (20 December 1967)

20. HEAVY-PARTICLE EMISSION FROM THE REACTIONS $^{19}F + d$ AND $^{19}F + {}^3He$
D. Dehnhard, D. S. Gemmell, and Z. Vager
Nucl. Phys. A104, 202 (1967)

21. THE REACTION $^{25}Mg(^3He, d)^{26}Al$ AT 12 MEV
A. Weidinger,* R. H. Siemssen,* G. C. Morrison, and B. Zeidman
Nucl. Phys. A108(3), 547-560 (1968)

22. PROTON HOLE STATES IN ^{29}Al, ^{31}P, AND ^{33}P
R. C. Bearse, D. H. Youngblood, and J. L. Yntema
Phys. Rev. 167, 1043-1048 (20 March 1968)

---

*Yale University, New Haven, Connecticut.

23. COMPLETE $(f_{7/2})^2$ SPECTRUM OF Sc^{42}
J. J. Schwartz,* D. Cline,* H. E. Gove,* R. Sherr,†
T. S. Bhatia,† and R. H. Siemssen
Phys. Rev. Letters 19, 1482-1484 (25 December 1967)
Erratum: Phys. Rev. Letters 20, 175
(22 January 1968)

24. LEVEL STRUCTURE AND DECAY SCHEME OF Sc^{43}
J. J. Schwartz,* W. P. Alford,* T. H. Braid, and
L. Meyer-Schützmeister
Phys. Rev. 155, 1191-1194 (20 March 1967)

25. ENERGY LEVELS OF Fe^{59} FROM THE $Fe^{58}(d, p)Fe^{59}$ REACTION
E. D. Klema, L. L. Lee, Jr., and J. P. Schiffer
Phys. Rev. 161, 1134-1136 (20 September 1967)

26. STUDY OF THE (d, p) REACTIONS ON $Zn^{64,66,68,70}$
D. von Ehrenstein and J. P. Schiffer
Phys. Rev. 164, 1374-1385 (20 December 1967)

27. STRUCTURE OF PARTICLE-HOLE STATES IN Ba^{138}
G. C. Morrison, N. Williams, J. A. Nolen, Jr., and
D. von Ehrenstein
Phys. Rev. Letters 19, 592-594 (4 September 1967)

28. A STUDY OF ENERGY LEVELS IN ODD-MASS YTTERBIUM ISOTOPES BY MEANS OF (d, p) AND (d, t) REACTIONS
D. G. Burke,‡ B. Zeidman, B. Elbek,‡ B. Herskind,‡
and M. Olesen‡
Kgl. Danske Videnskab. Selskab, Mat.-Fys.
Medd. 35, No. 2, 1-53 (1966)

29. ABSOLUTE SPECTROSCOPIC FACTORS FOR (d, p) REACTIONS ON HEAVY DEFORMED NUCLEI
R. H. Siemssen and J. R. Erskine
Phys. Rev. Letters 19, 90-94 (10 July 1967)

---

*University of Rochester, Rochester, New York.

†Princeton University, Princeton, New Jersey.

‡Institute for Theoretical Physics, Copenhagen.

30. ELASTIC SCATTERING OF 6—12-MEV DEUTERONS BY ^{48}Ti
R. H. Siemssen and C. Mayer-Böricke
Nucl. Phys. A96(3), 505-512 (1967)

31. COULOMB DISPLACEMENT ENERGIES OF Ca-Sc ISOBARIC PAIRS
J.A. Nolen, Jr., J. P. Schiffer, N. Williams, and D. von Ehrenstein
Phys. Rev. Letters 18, 1140-1143 (19 June 1967)

32. COULOMB EXCITATION OF LOW-LYING EXCITED STATES IN Sc^{45}
A. E. Blaugrund, R. E. Holland, and F. J. Lynch
Phys. Rev. 159, 926-930 (20 July 1967)

33. THE $Mg^{25}(He^3, \alpha)$ REACTION AT E(He^3) = 33.0 MeV
D. Dehnhard and C. Mayer-Böricke
Nucl. Phys. A97(1), 164-176 (1967)

34. NEUTRON-PICKUP REACTIONS ON Mg^{26}
D. Dehnhard and J. L. Yntema
Phys. Rev. 160, 964-972 (20 August 1967)

35. EVIDENCE FOR TARGET-EXCITATION EFFECTS IN A SINGLE-PARTICLE-TRANSFER REACTION
D. Dehnhard and J. L. Yntema
Phys. Rev. 155, 1261-1263 (20 March 1967)

36. NEUTRON PICKUP REACTIONS ON Si^{30}
D. Dehnhard and J. L. Yntema
Phys. Rev. 163, 1198-1203 (20 November 1967)

37. SCATTERING OF 43-MeV ALPHA PARTICLES BY THE TITANIUM ISOTOPES
J. L. Yntema and G. R. Satchler*
Phys. Rev. 161, 1137-1147 (20 September 1967)

38. J DEPENDENCE FOR ℓ =1 NUCLEON TRANSFER
J. L. Yntema and H. Ohnuma
Phys Rev. Letters 19, 1341-1343 (4 December 1967)

---

*Oak Ridge National Laboratory, Oak Ridge, Tennessee.

39. DELAYED PROTONS FOLLOWING He^3 REACTIONS WITH OXYGEN, SILICON, AND SULFUR TARGETS
R. W. Fink,* T. H. Braid, and A. M. Friedman (Chemistry)
Arkiv Fysik 36, 471-475 (1967)

40. DECAY OF Cu^{61} AND ENERGY LEVELS IN Ni^{61}
H. H. Bolotin and H. J. Fischbeck
Phys. Rev. 158, 1069-1072 (20 June 1967)

41. ENERGY LEVELS OF $_{68}Er^{166}$ AND $_{69}Tm^{166}$ (7.7 h) EXCITED IN THE DECAY OF $_{67}Ho^{166}$ (26.7 h), Ho^{166m} (1.2×10^3 yr), AND $_{70}Yb^{166}$ (57 h)
S. B. Burson, P. F. A. Goudsmit,† and J. Konijn†
Phys. Rev. 158, 1161-1181 (20 June 1967)

42. A SHELL-MODEL STUDY OF THE ISOTOPES OF O, F, AND Ne
A. Arima, S. Cohen, R. D. Lawson, and M. H. Macfarlane
Nucl. Phys. A108, 94-112 (1968)

43. SHELL MODEL OF THE NICKEL ISOTOPES
S. Cohen, R. D. Lawson, M. H. Macfarlane, S. P. Pandya, and Michitoshi Soga
Phys. Rev. 160, 903-915 (20 August 1967)

44. M2 TRANSITIONS IN NUCLEI
Dieter Kurath and R. D. Lawson
Phys. Rev. 161, 915-924 (20 September 1967)

45. SPECTROSCOPIC FACTORS FOR THE 1p SHELL
S. Cohen and D. Kurath
Nucl. Phys. A101(1), 1-16 (1967)

46. RELATIVE PHASES OF E2 AND M1 MATRIX ELEMENTS IN 1p-SHELL NUCLEI
A. R. Poletti,‡ E. K. Warburton,‡ and Dieter Kurath
Phys. Rev. 155, 1096-1104 (20 March 1967)

---

*Georgia Institute of Technology, Atlanta, Georgia.

†Instituut voor Kernphysisch Onderzoek, Amsterdam, Holland.

‡Brookhaven National Laboratory, Upton, L.I., New York.

47. INELASTIC ALPHA SCATTERING AND ASSOCIATED GAMMA RADIATION. III
David R. Inglis
Phys. Rev. 157, 873-878 (20 May 1967)

48. REVIEW OF "G. E. BROWN, UNIFIED THEORY OF NUCLEAR MODELS AND FORCES," 2nd ed. (North Holland Publishing Co., Amsterdam, 1967).
D. R. Inglis
Science 159 (No. 3810), 73 (5 January 1968)

49. EVAPORATIVE DATA ON INTERMEDIATE RESONANCES IN NUCLEAR REACTIONS
Donald W. Lang
Nucl. Phys. A96(2), 273-278 (April 1967)

50. PERTURBATION OF THE STATISTICAL PROPERTIES OF NUCLEAR STATES AND TRANSITIONS BY INTERACTIONS THAT ARE ODD UNDER TIME REVERSAL
N. Rosenzweig, J. E. Monahan, and M. L. Mehta
Nucl. Phys. A109(2), 437-448 (26 February 1968)

51. DISTRIBUTION LAWS FOR THE ROOTS OF A RANDOM ANTISYMMETRIC HERMITIAN MATRIX
M. L. Mehta and N. Rosenzweig
Nucl. Phys. A109(2), 449-456 (26 February 1968)

52. CURRENT ALGEBRAS AND CONFIGURATION MIXING
F. Coester
Phys. Rev. 155, 1647-1648 (25 March 1967)

53. CURRENT ALGEBRAS AT INFINITE MOMENTUM
F. Coester and G. Roepstorff
Phys. Rev. 155, 1583-1590 (25 March 1967)

54. ACCURATE CALCULATION OF THE REACTION MATRIX IN LIGHT NUCLEI
A. Kallio and B. D. Day
Phys. Letters 25B(2), 72-74 (7 August 1967)

55. ELEMENTS OF THE BRUECKNER-GOLDSTONE THEORY OF NUCLEAR MATTER
B. D. Day
Rev. Mod. Phys. 39(4), 719-744 (October 1967)

56. INFINITE SYSTEMS OF CLASSICAL PARTICLES
Amnon Katz
J. Math. Phys. 8, 2451-2459 (December 1967)

57. THE ΛΛ-HYPERNUCLEUS $^{6}He_{\Lambda\Lambda}$
S. Ali* and A. R. Bodmer
Nuovo Cimento 50, 511-534 (1 August 1967)

58. THE ΛΛ HYPERNUCLEI $_{\Lambda\Lambda}^{6}He$ AND $_{\Lambda\Lambda}^{10}Be$ AND THE Λ-Λ AND Λ-N INTERACTIONS
Shamsher Ali* and A. R. Bodmer
Phys. Letters 24B(7), 343-346 (3 April 1967)

59. THE TENSOR VIRIAL-THEOREM INCLUDING VISCOUS STRESS AND THE OSCILLATIONS OF A MACLAURIN SPHEROID
Carl E. Rosenkilde
Astrophys. J. 148, 825-832 (June 1967)

60. BASIS FOR THE DEPARTURE FROM EXPONENTIAL DECAY
M. N. Hack
Nuovo Cimento 47, 301-302 (11 February 1967)

61. BOUNDARY CONDITIONS THAT ENFORCE MACH'S PRINCIPLE IN GENERAL RELATIVITY
A. Katz
Nuovo Cimento B51(2), 502-513 (11 October 1967)

62. FORMULATION OF NEWTON'S SECOND LAW
Amnon Katz
Am. J. Phys. 35(9), 882-883 (September 1967)

63. LINEWIDTH OF MÖSSBAUER ABSORPTION
Juergen Heberle
Nucl. Instr. Methods 58, 90-92 (1968)

64. MAGNETIC MOMENT OF THE FIRST EXCITED STATE IN ^{133}Cs BY THE MÖSSBAUER EFFECT
L. E. Campbell and G. J. Perlow
Nucl. Phys. A109(1), 59-61 (1968)

---

*International Centre for Theoretical Physics, Trieste, Italy.

65. INTERNAL MAGNETIC FIELD AT AN ANTIMONY IMPURITY IN IRON OR NICKEL
S. L. Ruby and C. E. Johnson*
Phys. Letters 26A(2), 60-61 (18 December 1967)

66. INTERPRETATION OF MÖSSBAUER MEASUREMENTS IN TIN AND ANTIMONY
S. L. Ruby, G. M. Kalvius (Solid State Science), G. B. Beard,† and R. E. Snyder†
Phys. Rev. 159, 239-245 (10 July 1967)

67. MAGNETIC HYPERFINE INTERACTIONS IN Sb^{121} USING THE MÖSSBAUER EFFECT
S. L. Ruby and G. M. Kalvius (Solid State Science Division)
Phys. Rev. 155, 353-355 (10 March 1967)

68. FERROMAGNESIAN SILICATE ABUNDANCES IN BRONZITE CHONDRITES AS DETERMINED BY THE MÖSSBAUER EFFECT
E. L. Sprenkel-Segel and G. J. Perlow
Icarus 8, 66-74 (January 1968)

69. HYPERFINE STRUCTURE OF NINE LEVELS IN TWO CONFIGURATIONS OF V^{51}. I. EXPERIMENTAL
W. J. Childs and L. S. Goodman
Phys. Rev. 156, 64-70 (5 April 1967)

70. HYPERFINE STRUCTURE OF NINE LEVELS IN TWO CONFIGURATIONS OF V^{51}. II. THEORETICAL
William J. Childs
Phys. Rev. 156, 71-82 (5 April 1967)

71. CONTACT MAGNETIC-DIPOLE HYPERFINE STRUCTURE IN $3d^N4s^2$ ATOMS
W. J. Childs
Phys. Rev. 160, 9-10 (5 August 1967)

---

*A.E.R.E., Harwell, Didcot, Berkshire, England.

†Wayne State University, Detroit, Michigan.

72. INDUCTANCE-VARIATION METHOD OF MEASURING CHARACTERISTICS OF ELECTROMAGNETIC LEVITATION SYSTEMS
Albert J. Hatch and W. E. Smith*
J. Appl. Phys. 38, 742-745 (February 1967)

73. VIBRATIONS AND THERMODYNAMIC PROPERTIES OF HEXASULFUR
Joseph Berkowitz, W. A. Chupka, Edward Bromels,† and R. Linn Belford†
J. Chem. Phys. 47, 4320-4324 (1 December 1967)

74. PHOTOIONIZATION OF ETHANE, PROPANE, and n-BUTANE WITH MASS ANALYSIS
William A. Chupka and Joseph Berkowitz
J. Chem. Phys. 47, 2921-2933 (15 October 1967)

75. PHOTOIONIZATION OF THE CF_3 FREE RADICAL
Chava Lifshitz and William A. Chupka
J. Chem. Phys. 47, 3439-3443 (1 November 1967)

76. SPEKTREN UND WINKELVERTEILUNGEN DER PHOTOELEKTRONEN VON ATOMEN UND MOLEKÜLEN
J. Berkowitz, H. Ehrhardt,‡ and T. Tekaat‡
Z. Physik 200, 69-83 (1967)

77. ATOMNYE I IONNYE STOLKNOVENIYA NA POVERKHNOSTI METALLA
M. Kaminskii
Publishing House "Mir," Moscow, 1967 [Russian translation of ATOMIC AND IONIC IMPACT PHENOMENA ON METAL SURFACES by Dr. Manfred Kaminsky (Springer-Verlag, Berlin, 1965), edited by Academician L. A. Artsimovich]

---

* The University of New South Wales, Sydney, Australia.

† University of Illinois, Urbana, Illinois.

‡ Physikalisches Institut der Universität Freiburg, Germany.

B. PUBLISHED REPORTS AT MEETINGS

Symposium on the Use of Computers in Analysis of Experimental Data and the Control of Nuclear Facilities, Argonne National Laboratory, Argonne, Illinois, 4—6 May 1966

1. CONTRIBUTIONS TO PANEL PRESENTATION: FUTURE TRENDS IN DATA ANALYSIS, AUTOMATIC CONTROL, DISPLAY, AND PATTERN RECOGNITION
   D. S. Gemmell
   Use of Computers in Analysis of Experimental Data and the Control of Nuclear Facilities, Proceedings of a Symposium, No. 10 in the AEC Symposium Series, edited by Bernard I. Spinrad. Available as CONF-660527 from Clearinghouse for Federal Scientific and Technical Information, National Bureau of Standards, U.S. Department of Commerce, Springfield, Virginia 22151, pp. 270-272, 278-279.

International Symposium on Organic Scintillators, Argonne National Laboratory, 20-22 June 1966

2. TIMING WITH ORGANIC SCINTILLATORS
   Frank J. Lynch
   Mol. Cryst. 3, 168-169 (August 1967)

International Nuclear Physics Conference, Gatlinburg, Tennessee, 12-17 September 1966, edited by R. L. Becker and A. Zucker (Academic Press Inc., New York, 1967)

3. ENERGY DEPENDENCE AND SPIN DEPENDENCE OF THE NEUTRON STRENGTH FUNCTION
   S. De Barros,* P. L. Chevillon,* H. Jackson, J. Julien,* G. Le Poittevin,* J. Morgenstern,* F. Netter,* and C. Samour*
   p. 283

4. AN INVESTIGATION OF NEUTRON PICKUP FROM B^{11}
   D. Dehnhard, G. C. Morrison, and Z. Vager
   pp. 112-115

---

*Centre d'Etudes Nucleaires de Saclay, Saclay, France.

International Nuclear Physics Conference, Gatlinburg, Sept. '66 (cont'd)

5. INTERMEDIATE STRUCTURE OBSERVED IN NEUTRON CROSS SECTIONS
   A. J. Elwyn, J. E. Monahan, and F. P. Mooring
   p. 282

6. PROPERTIES OF PARTIAL RADIATION WIDTHS IN ^{196}Pt
   H. E. Jackson, J. Julien,* C. Samour,* A. Bloch,* C. Lopata,* and J. Morgenstern*
   p. 829

7. SPECTROSCOPIC FACTORS FOR FORBIDDEN TRANSITIONS
   Dieter Kurath
   pp. 861-864

8. MEASUREMENTS OF MIXED $p_{1/2}$-$p_{3/2}$ (d, p) TRANSITIONS IN LIGHT NUCLEI
   D. Kurath, G. C. Morrison, J. P. Schiffer, R. H. Siemssen, and B. Zeidman
   p. 169

9. SHELL-MODEL CALCULATIONS
   R. D. Lawson and J. M. Soper
   pp. 511-525

10. NUCLEAR PHYSICS CONCEPTS RELATED TO ELEMENTARY PARTICLE PHYSICS
    H. J. Lipkin
    pp. 450-459

11. THE GIANT DIPOLE RESONANCE IN SOME SELF-CONJUGATE NUCLEI IN THE 1s-2d SHELL
    L. Meyer-Schützmeister
    p. 404

---

*Centre d'Etudes Nucleaires de Saclay, Saclay, France.

12. FREQUENCY OF SPURIOUS "INTERMEDIATE RESONANCES" IN RANDOMLY GENERATED CROSS SECTIONS
P. P. Singh,* P. Hoffman-Pinther,* and D. W. Lang
pp. 249-251

Intense Neutron Sources, Proceedings of a USAEC/ENEA Seminar, Santa Fe, New Mexico, 19—23 September 1966, USAEC Report CONF-660925 (Clearinghouse for Federal Scientific and Technical Information, National Bureau of Standards, U.S. Department of Commerce, Springfield, Virginia, 1966)

13. CONTRIBUTIONS TO PANEL DISCUSSION ON NEUTRON AND FISSION PHYSICS
L. M. Bollinger
pp. 803, 804, 811-814, 815, 816, 830

14. NUCLEAR PHYSICS EXPERIMENTS PERFORMED WITH NEUTRONS
L. M. Bollinger
pp. 47-88

15. CONTRIBUTION TO PANEL DISCUSSION ON NUCLEAR PHYSICS
G. R. Ringo
pp. 820-821

Abstracts of Papers to be Read at the International Conference on Hyperfine Nuclear Spectroscopy at Victoria University of Wellington, Wellington, New Zealand, 17—21 October 1966. (The Royal Society of New Zealand, Wellington, New Zealand, 1966)

16. THE MÖSSBAUER EFFECT IN METALLIC CESIUM
Gilbert J. Perlow and A. J. F. Boyle†
pp. 20-21

17. INTERPRETATION OF QUADRUPOLE SPLITTINGS AND ISOMER SHIFTS IN ANTIMONY AND TIN
S. L. Ruby, G. M. Kalvius (Solid State Science), R. E. Snyder,‡ and G. B. Beard‡
pp. 6-7

---

*Indiana University, Bloomington, Indiana.

†University of Western Australia, Nedland, Western Australia.

‡Wayne State University, Detroit, Michigan.

American Physical Society, 8th Annual Meeting of the Division of Plasma Physics, Boston, Massachusetts, 2—5 November 1966

18. SLAB-MODEL THEORY OF ADMITTANCE OF HIGH-FREQUENCY PLASMOIDS
M. Hasan, Albert J. Hatch, and J. Taillet*
Bull. Am. Phys. Soc. 12, 769 (May 1967)

19. APPARATUS FOR STUDYING PLASMA CONFINEMENT IN HIGH-FREQUENCY FIELDS
Albert J. Hatch
Bull. Am. Phys. Soc. 12, 759 (May 1967)

Annual Meeting of the Meteoritical Society, Smithsonian Institution, Washington, D.C., 3—5 November 1966

20. MÖSSBAUER DETERMINATION OF THE RATIO OF OLIVINE IRON TO PYROXENE IRON IN THE HIGH-IRON AND LOW-IRON GROUPS OF STONE METEORITES
E. L. Sprenkel-Segel and G. J. Perlow
Meteoritics 3, 126-127 (April 1967)

Mössbauer Effect Methodology (Proceedings of the Third Symposium, New York, 29 January 1967), edited by I. J. Gruverman (Plenum Press, New York, 1967), Vol. 3

21. THE MÖSSBAUER EFFECT IN Cs^{133}
G. J. Perlow
pp. 191-201

22. PRESENT STATUS OF EXPERIMENTS WITH Sb^{121}
S. L. Ruby
pp. 203-215

in High Energy Physics and Nuclear Structure, Proceedings of the Second International Conference, Weizmann Institute of Science, Rehovoth, 27 February-3March 1967, edited by Gideon Alexander (North-Holland Publishing Company, Amsterdam, 1967)

23. HYPERNUCLEAR SPECTROSCOPY
A. R. Bodmer
pp. 60-87

---

*Centre d'Etudes Nucleaires, Saclay, France.

1967 U. S. National Particle Accelerator Conference, Washington, D.C., 1—3 March 1967

24. DECADE OF PROGRESS IN CYCLOTRONS—FREQUENCY-MODULATED AND ISOCHRONOUS
T. K. Khoe (Particle Accelerator Division) and J. J. Livingood
Bull. Am. Phys. Soc. 12, 939 (August 1967)
IEEE Trans. NS-14(3), 23-28 (June 1967)

25. SIMPLE IMPROVEMENTS IN SMALL HIGH-VOLTAGE DC POWER SUPPLIES
Alexander Langsdorf, Jr.
Bull. Am. Phys. Soc. 12, 942 (August 1967)
IEEE Trans. NS-14(3), 143-144 (June 1967)

American Physical Society Meeting, Washington, D.C., 24—27 April 1967

26. LIFETIMES OF THE SECOND, THIRD, AND FOURTH EXCITED STATES IN Si^{29}
S. I. Baker and R. E. Segel
Bull. Am. Phys. Soc. 12, 570 (April 1967)

27. COULOMB EXCITATION OF LOW-LYING EXCITED STATES IN Sc^{45}
A. E. Blaugrund, R. E. Holland, and F. J. Lynch
Bull. Am. Phys. Soc. 12, 587 (April 1967)

28. ENERGY DEPENDENCE OF HIGH-ENERGY RADIATIVE TRANSITIONS
L. M. Bollinger and G. E. Thomas
Bull. Am. Phys. Soc. 12, 597-598 (April 1967)

29. HFS STUDIES OF LOW-LYING LEVELS IN Pt^{195} BY ATOMIC-BEAM MAGNETIC RESONANCE
W. J. Childs and L. S. Goodman
Bull. Am. Phys. Soc. 12, 509 (April 1967)

APS, Washington, D. C. 24—27 April 1967 (cont'd)

30. HYPERFINE MUONIC SPECTRA OF SEPARATED ISOTOPES OF EUROPIUM
R. E. Coté, W. V. Prestwich, R. A. Carrigan, Jr.,* P. D. Gupta,* R. B. Sutton,* M. N. Suzuki,* A. Gaigalas,† and S. Raboy†
Bull. Am. Phys. Soc. 12, 581 (April 1967)

31. $Si^{30}(d, t)Si^{29}$ AND $Si^{30}(He^3, \alpha)Si^{29}$ REACTIONS
D. Dehnhard and J. L. Yntema
Bull. Am. Phys. Soc. 12, 571 (April 1967)

32. POSSIBLE INTERMEDIATE RESONANCE STRUCTURE IN THE SCATTERING OF NEUTRONS BY Cr
A. J. Elwyn, J. E. Monahan, R. O. Lane, A. Langsdorf, Jr., and F. P. Mooring
Bull. Am. Phys. Soc. 12, 473 (April 1967)

33. THEORY OF NUCLEAR LEVEL DENSITY—MODIFICATIONS OF THE PERIODIC SINGLE-PARTICLE SPECTRUM
P. B. Kahn and N. Rosenzweig
Bull. Am. Phys. Soc. 12, 497 (April 1967)

34. ANGULAR DISTRIBUTIONS FROM $Na^{23}(p, \gamma)Mg^{24}$
L. Meyer-Schützmeister, R. C. Bearse, and R. E. Segel
Bull. Am. Phys. Soc. 12, 553 (April 1967)

35. (d, p) REACTION IN THE 1p SHELL
G. C. Morrison, J. P. Schiffer, R. H. Siemssen, and B. Zeidman
Bull. Am. Phys. Soc. 12, 501 (April 1967)

36. EXCITATION FUNCTIONS OF (p, p) SCATTERING OVER THE "QUASIELASTIC" (p, n) THRESHOLD
J. A. Nolen, Jr., G. C. Morrison, J. P. Schiffer, and N. Williams
Bull. Am. Phys. Soc. 12, 526 (April 1967)

---

*Carnegie Institute of Technology, Pittsburgh, Pennsylvania.

†State University of New York at Binghamton, Binghamton, New York.

APS, Washington, D.C. 24—27 April 1967 (cont'd.)

37. DYNAMIC QUADRUPOLE EFFECTS IN MUONIC ATOMS OF EVEN NUCLEI
S. Raboy,* A. K. Gaigalas,* R. E. Coté, W. V. Prestwich, R. A. Carrigan, Jr.,† R. B. Sutton,† and C. C. Trail‡
Bull. Am. Phys. Soc. 12, 522 (April 1967)

38. ELASTIC SCATTERING OF ALPHA PARTICLES FROM CALCIUM-44
P. P. Singh,§ J. J. Kroepfl,§ B. A. Watson,§ T. P. Marvin,§ A. H. Sauter,§ D. W. Devins,§ A. J. Elwyn, and J. P. Schiffer
Bull. Am. Phys. Soc. 12, 586 (April 1967)

39. CONCERNING THE PARENT FERROMAGNESIAN SILICATE RESERVOIR OF THE BRONZITE CHONDRITE METEORITES
E. L. Sprenkel-Segel and G. J. Perlow
Bull. Am. Phys. Soc. 12, 593 (April 1967)

40. $Mg^{25}(He^3, d)Al^{26}$ REACTION AT 12 MEV
A. Weidinger,‖ G. C. Morrison, R. H. Siemssen, and B. Zeidman
Bull. Am. Phys. Soc. 12, 555 (April 1967)

41. NUCLEON TRANSFER REACTIONS ON Mo ISOTOPES
J. L. Yntema and H. Ohnuma
Bull. Am. Phys. Soc. 12, 526 (April 1967)

---

*State University of New York at Binghamton, Binghamton, New York.

†Carnegie Institute of Technology, Pittsburgh, Pennsylvania.

‡Brooklyn College, Brooklyn, New York.

§Indiana University, Bloomington, Indiana.

‖Yale University, New Haven, Connecticut.

Fifteenth Annual Conference on Mass Spectrometry and Allied Topics, 14-19 May 1967, Denver, Colorado (ASTM Committee E-14)

42. KINETIC ENERGY SPECTRUM AND ANGULAR DISTRIBUTION OF PHOTOELECTRONS FROM SOME ATOMS AND MOLECULES
J. Berkowitz, H. Ehrhardt,* and T. Tekaat*
pp. 124-128

43. REACTIONS OF IONS PRODUCED IN SELECTED STATES BY PHOTOIONIZATION
W. A. Chupka
p. 63

44. LATTICE EFFECTS ON THE EMISSION OF SECONDARY PARTICLES FROM METAL MONOCRYSTALS UNDER HIGH-ENERGY ION BOMBARDMENT
Manfred Kaminsky
p. 246

Nuclear Research with Low Energy Accelerators, Proceedings of the Symposium, University of Maryland, 19-24 June 1967, edited by J. B. Marion and D. M. Van Patter (Academic Press Inc., New York, 1967)

45. ANALOG-STATE EXPERIMENTS
George C. Morrison
pp. 275-309

American Physical Society Meeting, Toronto, 21—23 June 1967

46. ATOMIC-BEAM MAGNETIC-RESONANCE MEASUREMENTS OF Rh^{103}
Y. W. Chan and L. S. Goodman
Bull. Am. Phys. Soc. 12, 653 (May 1967)

47. PROGRESS REPORT ON THE ARGONNE POLARIZED ION SOURCE
D. C. Hess, C. W. Schmidt, and D. von Ehrenstein
Bull. Am. Phys. Soc. 12, 634-635 (May 1967)

---

*Physikalisches Institut der Universität, Freiburg, Germany.

American Physical Society, Toronto, 21-23 June 1967 (cont'd)

48. ANOMALOUS ENERGY LOSSES OF ENERGETIC PROTONS (0.75—1.75 MEV) IN COPPER MONOCRYSTALS OF VARIOUS CRYSTALLOGRAPHIC ORIENTATIONS
M. Kaminsky
Bull. Am. Phys. Soc. 12, 635 (May 1967)

49. ENERGY LEVELS OF Si^{30}
N. G. Puttaswamy, D. S. Gemmell, L. Meyer-Schützmeister, and H. Ohnuma
Bull. Am. Phys. Soc. 12, 665 (May 1967)

50. (d, p) STRIPPING REACTIONS ON THE BARIUM ISOTOPES
D. von Ehrenstein, G. C. Morrison, J. A. Nolen, Jr., and N. Williams
Bull. Am. Phys. Soc. 12, 714 (May 1967)

51. ISOBARIC ANALOG STATES IN THE BARIUM ISOTOPES
N. Williams, G. C. Morrison, J. A. Nolen, Jr., and D. von Ehrenstein
Bull. Am. Phys. Soc. 12, 714 (May 1967)

Fifth International Conference on the Physics of Electronic and Atomic Collisions, Leningrad, USSR, 17-23 July 1967; Abstracts of Papers, edited by I. P. Flaks and E. S. Solovyov (Publishing House "Nauka," Leningrad, 1967)

52. HIGH-RESOLUTION PHOTOIONIZATION AND MASS ANALYSIS OF SMALL MOLECULES
J. Berkowitz and W. A. Chupka
pp. 608-610

Phenomena in Ionized Gases 1967: Contributed Papers, Eighth International Conference, Vienna, 27 August-2 September 1967 (Springer-Verlag, Mölkerbastei 5, A-1010 Vienna)

53. SLAB-MODEL THEORY OF ADMITTANCE OF HIGH-FREQUENCY PLASMOIDS
M. Hasan, A. J. Hatch, and J. Taillet*
p. 167

---

*Office National d'Etudes et de Recherches Aerospatiales Chatillon-sous-Bagneux, France.

Phenomena in Ionized Gases, 1967 (cont'd.)

54. ADMITTANCE OF LOW-PRESSURE HIGH-FREQUENCY DISCHARGES
A. J. Hatch, R. J. Freiberg, S. V. Paranjape, and B. A. Tryba-Wolterbeek
p. 166

American Physical Society meeting, Seattle, 31 August—2 September 1967

55. PERTURBATION OF THE PORTER-THOMAS DISTRIBUTION BY INTERACTIONS WHICH ARE ODD UNDER TIME REVERSAL
Norbert Rosenzweig
Bull. Am. Phys. Soc. 12, 894-895 (August 1967)

Contributions, International Conference on Nuclear Structure, Institute for Nuclear Study, University of Tokyo, 7—13 September 1967

56. PERTURBATIVE METHODS IN THE THEORY OF NUCLEAR LEVEL DENSITIES
P. B. Kahn* and N. Rosenzweig
p. 353

57. EXTENSION OF M3 MATRIX ELEMENTS
Dieter Kurath
p. 371

58. GIANT DIPOLE RESONANCE IN Ar^{36}
L. Meyer-Schützmeister, D. S. Gemmell, R. C. Bearse, N. G. Puttaswamy, and R. E. Segel
p. 385

59. AN ATTEMPT TO TEST THE RANDOM-MATRIX MODEL
J. E. Monahan and Norbert Rosenzweig
p. 354

60. STUDY OF THE (d, p) REACTION IN THE 1p SHELL
G. C. Morrison, J. P. Schiffer, R. H. Siemssen, and B. Zeidman
p. 259

---

*State University of New York, Stony Brook, New York.

International Conference on Nuclear Structure, Tokyo, 7—13 Sept. 1967 (cont'd.)

61. GAMMA DECAY OF THE TWO LOWEST T = $\frac{3}{2}$ STATES IN Al^{25}
G. C. Morrison, D. Youngblood, R. C. Bearse, and R. E. Segel
p. 143

62. PRECISE COULOMB ENERGIES OF ISOBARIC PAIRS FROM THE (He^3, p) REACTION
J. A. Nolen, Jr., J. P. Schiffer, and N. Williams
p. 118

63. THE LEVEL STRUCTURE OF Sc^{48}
H. Ohnuma, J. R. Erskine, J. A. Nolen, Jr., J. P. Schiffer, and N. Williams
p. 119

64. PERTURBATION OF THE PORTER-THOMAS DISTRIBUTION BY INTERACTIONS WHICH ARE ODD UNDER TIME REVERSAL
Norbert Rosenzweig
p. 340

65. LIFETIME OF THE 1.059-MeV STATE IN Al^{28}
R. E. Segel, D. H. Youngblood, R. C. Bearse, A. E. Blaugrund, and N. Williams
p. 197

66. NUCLEON-TRANSFER REACTIONS ON Mo ISOTOPES
J. L. Yntema and H. Ohnuma
p. 307

Proceedings of the International Congress on Magnetism, Boston-Cambridge, Massachusetts, 11—15 September 1967

67. TEMPERATURE DEPENDENCE OF ISOMER SHIFT AND HYPERFINE FIELD NEAR THE CURIE POINT IN IRON
R. S. Preston
J. Appl. Phys. 39(2), 1231 (1 February 1968)

Nuclear Physics Division of the American Physical Society, Madison, Wisconsin, 23-25 October 1967

68. GAMMA-RAY SPECTRA FROM $Si^{28,29,30}(n,\gamma)Si^{29,30,31}$ REACTIONS
G. B. Beard and G. E. Thomas
Bull. Am. Phys. Soc. 12, 1199 (December 1967)

69. DETERMINATION OF SPINS AND PARITIES OF LOW-ENERGY STATES FROM AVERAGE NEUTRON-RESONANCE CAPTURE SPECTRA
L. M. Bollinger and G. E. Thomas
Bull. Am. Phys. Soc. 12, 1200 (December 1967)

70. EVIDENCE FOR INTERMEDIATE RESONANCE STRUCTURE IN THE SCATTERING OF NEUTRONS BY Fe
A. J. Elwyn and J. E. Monahan
Bull. Am. Phys. Soc. 12, 1186 (December 1967)

71. $K^{39}(He^3,p\gamma)Ca^{41}$ REACTION
D. S. Gemmell, L. Meyer-Schützmeister, H. Ohnuma, and N. G. Puttaswamy
Bull. Am. Phys. Soc. 12, 1183 (December 1967)

72. SMALL-ANGLE SCATTERING OF NEUTRONS BY HEAVY NUCLEI
F. T. Kuchnir, A. J. Elwyn, A. Langsdorf, Jr., and F. P. Mooring
Bull. Am. Phys. Soc. 12, 1187 (December 1967)

73. POLARIZATION AND DIFFERENTIAL CROSS SECTION FOR NEUTRONS SCATTERED FROM ^{12}C
R. O. Lane, A. J. Elwyn, F. P. Mooring, J. E. Monahan, and A. Langsdorf, Jr.
Bull. Am. Phys. Soc. 12, 1185-1186 (December 1967)

74. APPLICATION OF A SELF-INDICATION METHOD TO THE MEASUREMENT OF NEUTRON ABSORPTION, TOTAL CROSS SECTION, AND THE VARIANCE OF THE TOTAL CROSS SECTION
F. P. Mooring and J. E. Monahan
Bull. Am. Phys. Soc. 12, 1187 (December 1967)

APS, Madison, Wisconsin, 23—25 October 1967 (cont'd.)

75. THE J DEPENDENCE OBSERVED AT SMALL ANGLES IN THE (d, He^3) REACTION
H. Ohnuma and J. L. Yntema
Bull. Am. Phys. Soc. 12, 1188 (December 1967)

76. ENERGY LEVELS OF S^{36} AND S^{34}
N. G. Puttaswamy and J. L. Yntema
Bull. Am. Phys. Soc. 12, 1182 (December 1967)

77. LEVEL STRUCTURE OF Al^{29}
D. H. Youngblood, J. L. Yntema, and R. C. Bearse
Bull. Am. Phys. Soc. 12, 1181 (December 1967)

American Physical Society, Division of Plasma Physics, Austin, Texas 8-11 November 1967

78. PERSEVERANCE OF NORMAL MODES IN A PLASMA-LOADED RESONANT CAVITY
A. J. Hatch, S. L. Halverson (Electronics), and
A. E. Froehlich
Bull. Am. Phys. Soc. 13, 301 (February 1968)

American Physical Society, New York, 16-18 November 1967

79. CAPTURE-GAMMA-RAY SPECTRUM OF $Te^{123}(n, \gamma)Te^{124}$ AND THE ASSOCIATED ENERGY LEVELS IN Te^{124}
R. P. Chaturvedi, D. Bushnell, and R.K. Smither
Bull. Am. Phys. Soc. 12, 1064 (November 1967)

80. HFS OF THE SEVEN LOWEST ATOMIC LEVELS OF Co^{59}, AND THE NUCLEAR GROUND-STATE ELECTRIC QUADRUPOLE MOMENT
W. J. Childs and L. S. Goodman
Bull. Am. Phys. Soc. 12, 1046 (November 1967)

81. LEVEL SCHEME OF Sm^{153} BASED ON (n, γ), (n, e^-), AND (β, γ) EXPERIMENTS
R. K. Smither, E. Bieber, T. v. Egidy,*
W. Kaiser,* and K. Wien†
Bull. Am. Phys. Soc. 12, 1065 (November 1967)

---

*Technischen Hochschule München, Germany.

†Technischen Hochschule Darmstadt, Germany.

APS New York meeting, 16-18 November 1967 (cont'd.)

82. (He^3, d) REACTION ON THE LEAD ISOTOPES
Nelson Stein,* R. H. Siemssen,* and B. Zeidman
Bull. Am. Phys. Soc. 12, 1066 (November 1967)

American Physical Society, Pasadena, 18-20 December 1967

83. LEVEL STRUCTURE OF THE LOW-LYING EXCITED STATES OF Sc^{46}
H. H. Bolotin
Bull. Am. Phys. Soc. 12, 1123-1124 (December 1967)

84. Cl^{37}(d, t)Cl^{36} REACTION
N. G. Puttaswamy and J. L. Yntema
Bull. Am. Phys. Soc. 12, 1123 (December 1967)

85. MÖSSBAUER STUDIES OF K AND ITS COMPOUNDS
S. L. Ruby, P. K. Tseng, and D. H. Vincent†
Bull. Am. Phys. Soc. 12, 1149 (December 1967)

Colloque International sur l'Interaction des Champs H. F. (Appliques ou Auto Engendres) Associes a un Champ Magnetique Statique avec un Plasma (L'Institut National des Sciences et Techniques Nucleaires et la Direction de la Physique, Saclay, France, 15-18 January 1968)

86. FREQUENCY-SHIFTING METHOD OF EXCITING PLASMAS IN FUNDAMENTAL-MODE RESONANT CAVITIES
Albert J. Hatch, S. L. Halverson (Electronics), and A. E. Froehlich
Session VII

87. POTENTIAL-WELL THEORY OF CONFINEMENT OF PLASMAS IN NONUNIFORM RADIOFREQUENCY FIELDS
Albert J. Hatch, M. Hasan, and W. E. Smith (Applied Mathematics)
Session VII

*Yale University, New Haven, Connecticut.

†University of Michigan, Ann Arbor, Michigan.

American Physical Society, Chicago, 29 January—1 February 1968

88. HYPERFINE EFFECTS IN MUONIC x RAYS OF BISMUTH
R. A. Carrigan, Jr.,* P. D. Gupta,* R. B. Sutton,* M. N. Suzuki,* A. C. Thompson,* R. E. Coté, W. V. Prestwich, A. K. Gaigalas,† and S. Raboy†
Bull. Am. Phys. Soc. 13, 65 (January 1968)

89. HYPERFINE STRUCTURE OF LOW ATOMIC LEVELS OF La^{139}
W. J. Childs and L. S. Goodman
Bull. Am. Phys. Soc. 13, 20 (January 1968)

90. ISOMER SHIFTS OF Sb AND Sn IN SOLID SOLUTIONS OF THE Sb + Sn SYSTEM
C. W. Kimball (Solid State Science), Hugh Montgomery (Metallurgy), and S. L. Ruby
Bull. Am. Phys. Soc. 13, 123-124 (January 1968)

91. SIMPLIFICATION OF Ge(Li) SPECTRA BY CALCULATION
J. P. Marion, L. M. Bollinger, and G. E. Thomas
Bull. Am. Phys. Soc. 13, 51 (January 1968)

92. EXCITED STATES OF As^{77} POPULATED IN THE 11-h DECAY OF Ge^{77}
D. A. McClure and H. H. Bolotin
Bull. Am. Phys. Soc. 13, 118 (January 1968)

93. NEUTRON PARTICLE-HOLE STATES IN THE EVEN-A BARIUM ISOTOPES
G. C. Morrison, N. Williams, J. A. Nolen, Jr., and D. von Ehrenstein
Bull. Am. Phys. Soc. 13, 70 (January 1968)

94. NEUTRON RADIUS OF Pb^{208}
J. A. Nolen, Jr., J. P. Schiffer, and N. Williams
Bull. Am. Phys. Soc. 13, 65 (January 1968)

---

*Carnegie-Mellon University, Pittsburgh, Pennsylvania.

†State University of New York, Binghamton, New York.

APS Chicago, 29 January—1 February 1968 (cont'd.)

95. PROTON-HOLE STATES IN Ar^{40} FROM THE $K^{41}(d, He^3)Ar^{40}$ REACTION
N. G. Puttaswamy and J. L. Yntema
Bull. Am. Phys. Soc. 13, 87 (January 1968)

96. ENERGY DEPENDENCE OF OPTICAL-MODEL PARAMETERS IN THE ELASTIC SCATTERING OF He^3 PARTICLES BY Ca^{40} AND Ni^{58}
B. W. Ridley,* T. W. Conlon,* and T. H. Braid
Bull. Am. Phys. Soc. 13, 117 (January 1968)

97. UNIMPORTANCE OF d ELECTRONS ON TIN ISOMER SHIFTS
S. L. Ruby, M. Wilson (Chemistry), and Hwa-Sheng Cheng†
Bull. Am. Phys. Soc. 13, 30 (January 1968)

98. OPTICAL-MODEL ANALYSIS OF PROTON ELASTIC SCATTERING FROM BORON AND BERYLLIUM
R. E. Segel, B. A. Watson, and P. P. Singh‡
Bull. Am. Phys. Soc. 13, 115 (January 1968)

99. ELASTIC SCATTERING OF ALPHA PARTICLES BY Si^{28}
P. P. Singh,‡ R. K. Li,‡ D. W. Devins,‡ J. W. Smith,‡ J. J. Kroepfl,‡ T. P. Marvin,‡ and A. J. Elwyn
Bull. Am. Phys. Soc. 13, 117-118 (January 1968)

100. ISOMER SHIFTS OF TIN IONS IN ICE
P. K. Tseng, S. L. Ruby, and Hwa-Sheng Cheng†
Bull. Am. Phys. Soc. 13, 30 (January 1968)

101. INELASTIC SCATTERING OF PROTONS BY B^{10}
B. A. Watson, P. P. Singh,‡ J. J. Kroepfl,‡ and R. E. Segel
Bull. Am. Phys. Soc. 13, 115 (January 1968)

---

*A. E. R. E., Harwell, Didcot, Berkshire, England.

†Tsing-Hua University, Taiwan, China.

‡Indiana University, Bloomington, Indiana.

APS Chicago, 29 January—1 February 1968 (cont'd.)

102. COULOMB DISPLACEMENT ENERGIES OF THE NICKEL ISOTOPES
N. Williams, J. A. Nolen, Jr., J. P. Schiffer, and G. C. Morrison
Bull. Am. Phys. Soc. 13, 105 (January 1968)

103. GAMMA DECAY OF $T = \frac{3}{2}$ STATES IN Al^{25} AND P^{29}
D. H. Youngblood, G. C. Morrison, R. C. Bearse, and R. E. Segel
Bull. Am. Phys. Soc. 13, 85-86 (January 1968)

104. $Zn^{64,66,68,70}$(d, He^3) REACTIONS AT 23.3 MEV
B. Zeidman and J. A. Nolen, Jr.
Bull. Am. Phys. Soc. 13, 105 (January 1968)

C. LECTURE SERIES

SHELL MODEL THEORY OF IDENTICAL NUCLEONS
M. H. Macfarlane
Lectures in Theoretical Physics (University of Colorado Press, Boulder, 1966), Vol. VIII-C, pp. 583-677

D. PHYSICS DIVISION INFORMAL REPORTS

MEASUREMENT OF THE POLARIZATION OF THERMAL NEUTRONS BY USE OF DEPOLARIZING STEEL SHEETS
M. T. Burgy and G. R. Ringo
Physics Division Informal Report PHY-1967B (January 1967)

THE REACTION MATRIX IN NUCLEAR SHELL THEORY
Malcolm H. Macfarlane
Physics Division Informal Report PHY-1967C (September 1967)

POLARIZATION AND NUCLEAR REACTIONS
J. E. Monahan
Physics Division Informal Report PHY-1968A (March 1968)

E. THESES

TOTAL CROSS SECTIONS FOR 14-MEV NEUTRONS
Jack Haugsnes
Ph. D. Thesis, Northwestern University, Evanston, Illinois (June 1967)

LIFETIME MEASUREMENTS IN Ca^{41} AND Si^{29}
Samuel I. Baker
Ph. D. Thesis, Illinois Institute of Technology, Chicago (June 1967)

($^3He, \alpha$) REACTIONS ON INTERMEDIATE-MASS NUCLEI
David D. Borlin
Ph. D. Thesis, Washington University, St. Louis, Missouri (June 1967)

MÖSSBAUER EFFECT IN K^{40}
P. K. Tseng
Ph. D. Thesis, University of Michigan (1968)

THE $Ge^{73}(n, \gamma)Ge^{74}$ GAMMA-RAY SPECTRUM AND ENERGY LEVELS OF Ge^{74}
Allen Paul Magruder
M. S. Thesis, Illinois Institute of Technology (January 1968)

VI. STAFF MEMBERS OF THE PHYSICS DIVISION

The Physics Division staff for the year ending 31 March 1968 is listed below. Although the members are classified by programs, it must be understood that many of them work in two or more of the areas. In such cases, the classification indicates only the current primary interest.

In the period from 1 April 1967 through 31 March 1968, there were 35 temporary staff members (16 staff members from universities and other laboratories and 19 postdoctoral fellows), 7 graduate students doing thesis research, and 41 undergraduates (5 in the Argonne Semester program of the Associated Colleges of the Midwest, 11 co-op technicians, 14 CSUI-ANL Honor Students, 10 on summer appointments, and 1 other).

SLOW-NEUTRON PHYSICS

Permanent Staff

*Lowell M. Bollinger, Ph. D., Cornell University, 1951

Herbert H. Bolotin, Ph. D., Indiana University, 1955

Harold E. Jackson, Jr., Ph. D., Cornell University, 1959

Victor E. Krohn, Ph. D., Case-Western Reserve University, 1952

Allen P. Magruder, B. S., University of Chicago, 1959

J. P. Marion, M. S., DePaul University, 1959

G. R. Ringo, Ph. D., University of Chicago, 1940

Robert K. Smither, Ph. D., Yale University, 1956

George E. Thomas, Jr., B. A., Illinois Wesleyan University, 1943

---

*Director of Physics Division.

Temporary Staff

†Erhard Bieber, Dr. rer. nat. in Physics, Technische Hochschule, 1965

†Donald Blatchley, Ph. D., Indiana University, 1964

†David L. Bushnell, Ph. D., Virginia Polytechnic Institute, 1961
(On leave from Northern Illinois University)

Duane J. Buss, Ph. D., University of Notre Dame, 1966

†Ram Chaturvedi, Ph. D., University of British Columbia, 1963
(On leave from State University of New York, Cortland)

Carl J. Christensen, M. S., Danish Technical University, Copenhagen, 1957
(On leave from Danish AEC, Research Establishment, Risø)

†William V. Prestwich, Ph. D., McMaster University, 1963

†M. Hla Shwe, Ph. D., University of California, Berkeley, 1962
(On leave from Ripon College)

Karl J. Wetzel, Ph. D., Yale University, 1965

FAST-NEUTRON REACTIONS

Permanent Staff

Alexander J. Elwyn, Ph. D., Washington University, 1956

Carl T. Hibdon, Ph. D., Ohio State University, 1944

Alexander Langsdorf, Jr., Ph. D., Massachusetts Institute of Technology, 1937

F. P. Mooring, Ph. D., University of Wisconsin, 1951

Temporary Staff

†Karl K. Ilgen, Ph. D., Technical University, Stuttgart, Germany, 1966
(On leave from Technical University, Stuttgart, Germany)

Franca T. Kuchnir, Ph. D., University of Illinois, 1965

---

†No longer at Argonne as of 31 March 1968.

CHARGED-PARTICLE REACTIONS

Permanent Staff

Thomas H. Braid, Ph. D., Edinburgh University, 1950

John R. Erskine, Ph. D., University of Notre Dame, 1960

Donald S. Gemmell, Ph. D., Australian National University, 1960

Robert E. Holland, Ph. D., University of Iowa, 1950

Frank J. Lynch, B. S., University of Chicago, 1944

Luise Meyer-Schützmeister, Ph. D., Technical University of Berlin, 1943

George C. Morrison, Ph. D., University of Glasgow, 1957

*John P. Schiffer, Ph. D., Yale University, 1954

Ralph E. Segel, Ph. D., Johns Hopkins University, 1955

J. L. Yntema, Ph. D., Free University of Amsterdam, 1952

Benjamin Zeidman, Ph. D., Washington University, 1957

Temporary Staff

David L. Auton (SA, thesis, University of Chicago)

Robert C. Bearse, Ph. D., Rice University, 1964

†David D. Borlin (AMU-ANL Predoctoral Fellow, Washington University)

H. T. Fortune, Ph. D., Florida State University, 1967

†Paul Kienle, Ph. D., Technische Hochschule München, 1962
(On leave from Technische Hochschule München, Germany)

Richard A. Morrison (SA, thesis, University of Chicago)

J. A. Nolen, Jr., Ph. D., Princeton University, 1965

Hajime Ohnuma, Ph. D., University of Tokyo, 1966

N. G. Puttaswamy, Ph. D., Stanford University, 1966

---

*Associate Director of Physics Division.

†No longer at Argonne as of 31 March 1968.

Bruce A. Watson (AMU-ANL Predoctoral Fellow, Indiana University)

Norman Williams, Ph. D., Manchester University, 1965

[†] Dave Youngblood, Ph. D., Rice University, 1965

DEVELOPMENT OF EQUIPMENT AND ACCELERATORS

Permanent Staff

David C. Hess, Ph. D., University of Chicago, 1949

John J. Livingood, Ph. D., Princeton University, 1929

Dieter von Ehrenstein, Ph. D., University of Heidelberg, 1960

Jack R. Wallace, B. A., College of Wooster, 1942

GAMMA- AND BETA-RAY SPECTROSCOPY

Permanent Staff

S. B. Burson, Ph. D., University of Illinois, 1946

G. T. Wood, Ph. D., Washington University, 1956

Temporary Staff

Pieter F. Goudsmit (RSA, thesis, University of Amsterdam, Netherlands)

Donald A. McClure (AMU-ANL Predoctoral Fellow, University of Missouri at Rolla, Missouri)

[†] No longer at Argonne as of 31 March 1968.

ATOMIC-BEAM STUDIES

Permanent Staff

William J. Childs, Ph. D., University of Michigan, 1956

John A. Dalman

Leonard S. Goodman, Ph. D., University of Chicago, 1952

Henry Stanton, Ph. D., University of Chicago, 1944

MÖSSBAUER STUDIES

Permanent Staff

Gilbert J. Perlow, Ph. D., University of Chicago, 1940

Richard S. Preston, Ph. D., Yale University, 1954

Stanley Ruby, B. A., Columbia University, 1947

Temporary Staff

L. E. Campbell, Ph. D., Carnegie-Mellon University, 1966

†Michael A. Grace, Ph. D., Oxford University, 1950
(On leave from Oxford University)

Duane N. Olson, Ph. D., Cornell University, 1960
(On leave from St. Olaf College, Northfield, Minnesota)

Esther L. Segel, Ph. D., University of Rochester, 1959
(On leave from Illinois Institute of Technology)

†Poh-Kun Tseng (RSA, thesis, University of Michigan)

†Hiroyuki Yoshida, Ph. D., Tohoku University, 1964
(On leave from Rutgers, The State University)

---

†No longer at Argonne as of 31 March 1968.

MUONIC x RAYS

Permanent Staff

*Robert E. Coté, Ph. D., Columbia University, 1953

THEORETICAL PHYSICS

Permanent Staff

Arnold R. Bodmer, Ph. D., Manchester University, 1953
Fritz Coester, Ph. D., University of Zurich, 1944
Stanley Cohen, Ph. D., Cornell University, 1955
Hans Ekstein, Ph. D., University of Berlin, 1934
Melvin Hack, Ph. D., Princeton University, 1956
David R. Inglis, Ph. D., University of Michigan, 1931
Dieter Kurath, Ph. D., University of Chicago, 1951
Robert D. Lawson, Ph. D., Stanford University, 1953
Malcolm H. Macfarlane, Ph. D., University of Rochester, 1959
James E. Monahan, Ph. D., St. Louis University, 1953
†Murray Peshkin, Ph. D., Cornell University, 1951
Norbert Rosenzweig, Ph. D., Cornell University, 1951

Temporary Staff

‡Benjamin Day, Ph. D., Cornell University, 1963

*Deceased.

†Associate Director of Physics Division.

‡Became permanent 1 September 1967.

†Alpo J. Kallio, Ph. D., University of Helsinki, 1964

†Amnon Katz, Ph. D., Weizmann Institute of Science, 1961
(On leave from Weizmann Institute of Science)

†Harry J. Lipkin, Ph. D., Princeton University, 1950
(On leave from Weizmann Institute of Science)

James MacKenzie, Ph. D., University of Minnesota, 1966

†Madan L. Mehta, Docteur-ès-Sc. Physique, Université de Paris, 1961

Carl Rosenkilde, Ph. D., University of Chicago, 1966

†Lindsay J. Tassie, Ph. D., University of Melbourne, 1957
(On leave from Australian National University, Canberra)

Christopher M. Vincent, Ph. D., University of the Witwatersrand, 1966

CHEMICAL PHYSICS

Permanent Staff

Joseph Berkowitz, Ph. D., Harvard University, 1955

William A. Chupka, Ph. D., University of Chicago, 1951

Temporary Staff

Theodore A. Walter, Ph. D., Harvard University, 1967

†Peter Williams, Ph. D., King's College, London, 1966

SURFACE PHYSICS

Permanent Staff

Manfred S. Kaminsky, Ph. D., University of Marburg, Germany, 1957

†No longer at Argonne as of 31 March 1968.

PLASMA PHYSICS

Permanent Staff

Albert J. Hatch, M.S., University of Illinois, 1947

ADMINISTRATIVE

Permanent Staff

Charles Eggler, B.S., Virginia Polytechnic Institute, 1944

Francis E. Throw, Ph.D., University of Michigan, 1940